

# **Analysis of Asymmetric Division of Hematopoietic Stem Cells by Continuous Single Cell Observation**

Dissertation  
der Fakultät für Biologie  
der Ludwig-Maximilian-Universität  
München

Prepared at the  
Institute of Stem Cell Research  
Helmholtz Zentrum München

Submitted by  
**Andrea Hermann**

23 July, 2009

Erster Gutachter: Prof. Dr. Benedikt Grothe

Zweiter Gutachter: Prof. Dr. Peter Becker

Tag der mündlichen Prüfung: 15.3. 2010

**Part of this work is published as follows:**

Hermann AC, Drew E, Shigeta M, Schroeder T (2010) **Intrinsic control of HSC asymmetric fate decisions**. Manuscript in preparation.

Eilken HM, Rieger, MA, Hoppe PS, Hermann AC, Smejkal BM, Drew EC, Thum T, Ninkovic J, Beckervordersandforth RM and Schroeder T (2010) **Continuous long-term detection of live cell surface markers by 'in culture' antibody staining**. Manuscript submitted.

Rastelli J, Hömig-Hölzel C, Seagal J, Müller W, Hermann AC, Rajewsky K, Zimmer-Strobl U. (2008) **LMP1 signaling can replace CD40 signaling in B cells in vivo and has unique features of inducing class-switch recombination to IgG1**. *Blood* **111**(3):1448-55.

Klier M, Anastasov N, Hermann A, Meindl T, Angermeier D, Raffeld M, Fend F, Quintanilla-Martinez L. (2008) **Specific lentiviral shRNA-mediated knockdown of cyclin D1 in mantle cell lymphoma has minimal effects on cell survival and reveals a regulatory circuit with cyclin D2**. *Leukemia* **22**(11):2097-105



---

## 1. Table of Content

1. Table of Content	1
2. Abstract	7
3. Introduction	9
3.1. The Hematopoietic System	9
3.2. Expression of Surface Markers by Blood Cells	12
3.3. Elucidating the Mechanism of Asymmetric Cell Division	15
3.4. Requirement for Time Lapse Microscopy and Single Cell Tracking	17
3.5. HSC Properties	18
3.6. Assays for HSC and Progenitor Cells	20
3.7. Using in vitro Markers to Label Stem Cells and Differentiated Cells	21
3.8. Environment for Blood Cells: The Niche	22
3.8.1. Artificial Environment: Stromal Cell Lines	23
3.8.2. Artificial Environment: Stroma Free Suspension Culture	24
3.9. Mechanism Influencing Asymmetric Fate Decisions: Protein Segregation	26
3.10. Candidate Genes for Protein Segregation	26
3.10.1. Candidate Gene Stauf1	26
3.10.2. Candidate Gene Pumilio	28
3.10.3. Candidate Gene Quaking1	29
3.10.4. Candidate Gene Prominin1	30
3.11. Experimental Approach	31

<b>3.11.1. Overexpression of Candidates with a Lentivirus</b>	<b>33</b>
<b>3.12. Conclusion</b>	<b>34</b>
<b>4. Goals of the Thesis</b>	<b>35</b>
<b>5. Results</b>	<b>37</b>
<b>5.1. Asymmetric Fates of HSC Daughters</b>	<b>37</b>
<b>5.1.1. Experimental Setup for Analysis of Asymmetric Fates</b>	<b>37</b>
<b>5.1.2. Divisional Kinetics of HSC and MPP</b>	<b>38</b>
<b>5.1.3. Searching for Markers of Intrinsic Control of HSC Asymmetric Daughter Cell Fates</b>	<b>44</b>
<b>5.1.3.1. Quantification of Daughter Generation Time Reveals Environmentally Controlled Asymmetric Fates</b>	<b>44</b>
<b>5.1.3.2. Quantification of Apoptotic Cells Reveals no Conclusion about Asymmetric Fates</b>	<b>47</b>
<b>5.1.3.3. Quantification of Megakaryocyte Fates Reveals no Conclusion about Asymmetric Fates</b>	<b>50</b>
<b>5.1.4. Evaluation of HSC Daughter Fates by 'Loss of Stemness Marker' CD48</b>	<b>53</b>
<b>5.1.4.1. Establishing CD48 as a Live Marker of Loss of Stemness</b>	<b>55</b>
<b>5.1.4.1.1. CD48 Antibody Titration in FACS and Expression in Freshly Isolated Cells</b>	<b>55</b>
<b>5.1.4.1.2. CD48 Expression in Cultured Cells</b>	<b>57</b>
<b>5.1.4.1.3. Confirmation that CD48<sup>-</sup> but not CD48<sup>+</sup> Cells Possess Reconstitution Potential</b>	<b>59</b>

---

5.1.4.2.	Type of CD48 Expression Onset in HSC and MPP Pedigrees	63
5.1.4.3.	Time of CD48 Expression Onset in HSC and MPP Pedigrees	69
5.1.4.4.	Asymmetric CD48 Expression Onset Reveals Intrinsic Control of Asymmetric Fates of HSC Daughters	71
5.2.	Examining Candidate Protein Segregation as a Potential Mechanism Controlling Asymmetric Fate Decisions of HSC	76
5.2.1.	Expression of Candidate Genes in Bone Marrow Populations	76
5.2.2.	Cloning of Candidate Expression Constructs	78
5.2.3.	Optimization of Lentivirus Infection	79
5.2.4.	Segregation of Candidate Proteins during HSC Divisions	82
5.2.4.1.	Experimental Setup for Analysis of Protein Segregation	82
5.2.4.2.	Staufen1 and Staufen <sup>i</sup> Are Not Segregated during HSC Divisions	84
5.2.4.3.	Evaluating the Number of Analyzed Divisions	88
5.2.4.4.	Pumilio1 Is Not Segregated during HSC Divisions	90
5.2.5.	Influence of Candidate Genes on Fate Decisions	93
5.2.5.1.	No Influence of Staufen1 and Staufen <sup>i</sup> on Proliferation and Lineage Choice of Progenitor Cells <i>In Vitro</i>	97
5.2.5.2.	Negative Influence of Pumilio1 on <i>In Vitro</i> Progenitor Potential	99
5.2.5.3.	Quaking1 Influences GM Lineage Decisions	101
5.2.6.	Influence of Candidate Genes on <i>In Vivo</i> HSC Potential	104
5.2.6.1.	Reconstitution Potential of Candidate Transduced HSC Reveals Influence of Candidates during Expansion Conditions	104
5.2.6.1.1.	Contribution to Peripheral Blood of Recipient Mice	104

5.2.6.1.2.	Contribution to Bone Marrow Populations of Recipient Mice	108
5.2.6.2.	Candidate Transgenic Mice Allow Analysis of Candidate Influence on Hematopoiesis during Homeostasis Conditions	116
5.2.6.2.1.	Testing Functionality of Transgenes: Expression in the Skin	116
5.2.6.2.2.	Testing Functionality of Transgenes: Expression in Bone Marrow Cells	119
5.2.6.3.	Tie2 Controlled Homeostatic Pumilio2 Overexpression Allows Maintenance of Cells with HSC Phenotype	121
5.3.	Conclusion	123
6.	Discussion	125
6.1.	Asymmetric Fate Potential of HSC	125
6.2.	Choice of Culture Conditions	127
6.3.	Divisional Kinetics of HSC and MPP	128
6.4.	Asymmetries in Generation Time Length of Daughter Cells	129
6.5.	Intrinsic Control of Asymmetric Fate Decisions	130
6.6.	Exploring the Mechanism Controlling Asymmetric Fate Choice	132
6.7.	Candidate Segregation in HSC Divisions	133
6.8.	Candidate Influence on Fate Decisions	135
6.8.1.	Effect of Stauf1 on Fate Decisions	135
6.8.2.	Effect of Pumilio on Fate Decisions	136
6.8.3.	Effect of Quaking1 on Fate Decisions	138
6.9.	Conclusion	140

---

<b>7. Experimental Procedure</b>	<b>141</b>
7.1. Isolation of Stem and Progenitor Populations	141
7.2. Antibody Staining	141
7.2.1. Labelling of CD48 Antibody	143
7.2.2. Titration of CD48 Antibody	143
7.3. Flow Cytometry	143
7.4. Cell Culture Conditions	144
7.4.1. Colony Formation Assay	144
7.4.2. Cell Lines	146
7.4.2.1. PA6 Cell Culture	146
7.4.2.2. Freezing and Thawing of Cells	146
7.4.2.3. Transient transfections	147
7.4.3. Primary Cells	147
7.4.3.1. HSC Cocultures on PA6	147
7.4.3.2. Stroma Free Suspension Culture	148
7.4.3.3. Fibroblast Isolation from Mouse Tail Clips	148
7.5. Virus Production	148
7.5.1. Virus Titration	150
7.5.2. Virus Infection	150
7.6. Transplantation Experiments	151
7.7. Plasmid Vector Cloning	152
7.7.1. Purification of Plasmid DNA	152
7.7.2. Construction of Plasmid DNA	152
7.7.3. Transformation of Bacteria	153

<b>7.7.4. Restriction Digestions and Ligations</b>	<b>153</b>
<b>7.7.5. Agarose Gels</b>	<b>153</b>
<b>7.7.6. Purification of DNA Fragments</b>	<b>154</b>
<b>7.7.7. Sequencing</b>	<b>154</b>
<b>7.8. Reverse Transcriptase-PCR of Stem and Progenitor Cells</b>	<b>154</b>
<b>7.8.1. Primer design</b>	<b>155</b>
<b>7.9. Time Lapse Microscopy</b>	<b>155</b>
<b>7.9.1. Preparation of Specimen</b>	<b>155</b>
<b>7.9.2. Acquisition of Time Lapse Images</b>	<b>155</b>
<b>7.10. Data Analysis</b>	<b>156</b>
<b>7.10.1. Image Processing</b>	<b>157</b>
<b>7.10.2. Statistical Analysis</b>	<b>157</b>
<b>8. References</b>	<b>159</b>
<b>9. Legends to Time Lapse Movies</b>	<b>179</b>
<b>10. Abbreviations</b>	<b>183</b>

## 2. Abstract

Every second, millions of blood cells are generated and destroyed by a mammalian organism. At the same time, a constant pool of hematopoietic stem cells that are able to self renew and reconstitute the entire blood system is maintained. The question of how HSC can achieve self renewal and differentiation at the same time remains unsolved. Asymmetric cell division has been proposed as a mechanism of asymmetric fate choice in HSC. Employing a new imaging and single cell tracking technology we address the question if HSC undergo asymmetric cell division. We observed divisional kinetics and marker expression of HSC and closely related MPP to elucidate if HSC produce asymmetrically fated daughter cells. We found that HSC show later cell cycle entry and also longer generation time in subsequent divisions compared to MPP and that this is an intrinsic property of HSC. However, HSC specific asymmetric generation time length of daughter cells is environmentally controlled and not intrinsic. The use of a live marker in our movies, CD48, which identifies cells that have lost the ability to reconstitute the bone marrow of a mouse for its lifetime, allows *in vitro* identification of asymmetric fate decisions between self renewal and differentiation. Quantification of cells with asymmetrically fated daughter cells, according to CD48 expression onset, reveals that most HSC produce asymmetric daughter cells, while most MPP do not. This behaviour is independent of the environment. This indicates that HSC intrinsically control asymmetric fates of daughter cells.

Trying to elucidate the mechanism controlling these asymmetric fate decisions in HSC we chose candidates that are known to play a role in asymmetric fate decisions in other species or tissues. We examined if these candidates are segregated during HSC division and found no asymmetrically segregated protein when overexpressing Staufen1, Staufen<sup>i</sup> and Pumilio1 as fusions to VENUS protein. Furthermore, we analyzed if candidates had an influence on HSC and progenitor fate decisions *in vitro* and *in vivo*. We found that Staufen1 isoforms did not influence colony potential and lineage decision *in vitro*, Quaking1 isoforms influenced GM lineage decisions of progenitors *in vitro* and Pumilio1 overexpression led to reduced colony formation as well as altered GM lineage decisions. In HSC expansion

conditions as assayed by reconstitution experiments, we found, that *Staufen1* isoforms, *Pumilio1* as well as *Quaking1* isoforms did not allow HSC maintenance in recipient mice for 18 weeks. In HSC homeostatic conditions, as assayed in a transgenic mouse line, we found that *Pumilio2* when expressed under *Tie2* regulatory elements allows HSC maintenance in adult mice. Thus, we provide evidence that these genes, that were not implicated in hematopoiesis so far, could play a role in maintenance of HSC.

In summary we show evidence that HSC produce asymmetric fates and that they control asymmetric fate choices between self renewal and differentiation intrinsically. We could exclude involvement of several candidate molecules in molecular control of asymmetric cell division. In addition, we provide a method to screen candidate genes for their role in asymmetric protein segregation.

### 3. Introduction

#### 3.1. The Hematopoietic System

Blood is a very complex organ system encompassing many different cell types that are produced in the bone marrow, mature in tissues like the lymph nodes and the thymus and fill arteries and veins. Blood is needed to transport oxygen and to close wounds, to ward off bacteria and clear viral infections. Every second, millions of blood cells are produced and destroyed in the body. The precursors of all blood cells are the hematopoietic stem cells (HSC) which maintain a constant pool of themselves throughout the lifetime of the organism and at the same time proliferate and differentiate into all mature blood cell lineages.

In the case of loss of a large proportion of mature and progenitor blood cells, for example during irradiation to treat leukemia, HSC are needed to replenish the lost cells. Given to an irradiated patient through a bone marrow transplant, they expand their numbers and also produce progenitor and mature cells. Human bone marrow and peripheral blood cells have been studied closely to identify HSC and to try to expand these cells to be able to transplant bone marrow from one donor into several hosts. However, the difficulty to perform *in vivo* experiments, have prevented the isolation of cell population with a high percentage of true HSC. The use of immunocompromised SCID mice as recipients of human bone marrow grafts allowed the purification of progenitor populations with 3% HSC purity (McKenzie, Takenaka et al. 2007). However, it is not known if cells that are able to engraft in these murine hosts are the same cells that can engraft in humans and replenish the human bone marrow. These limitations in HSC purity and of *in vivo* experiments have prompted us to conduct our experiments on murine HSC, as they can be isolated with much higher purity (47%) (Kiel, Yilmaz et al. 2005) than their human counterpart. In addition, *in vivo* experiments analyzing long term HSC potential have a greater validity than engraftment across species. Finally, there are more tools available for mice than for humans, including unlimited samples (e.g. mice) and transgenic mice, and more knowledge about differentiation along blood cell lineages and identity of progenitors.

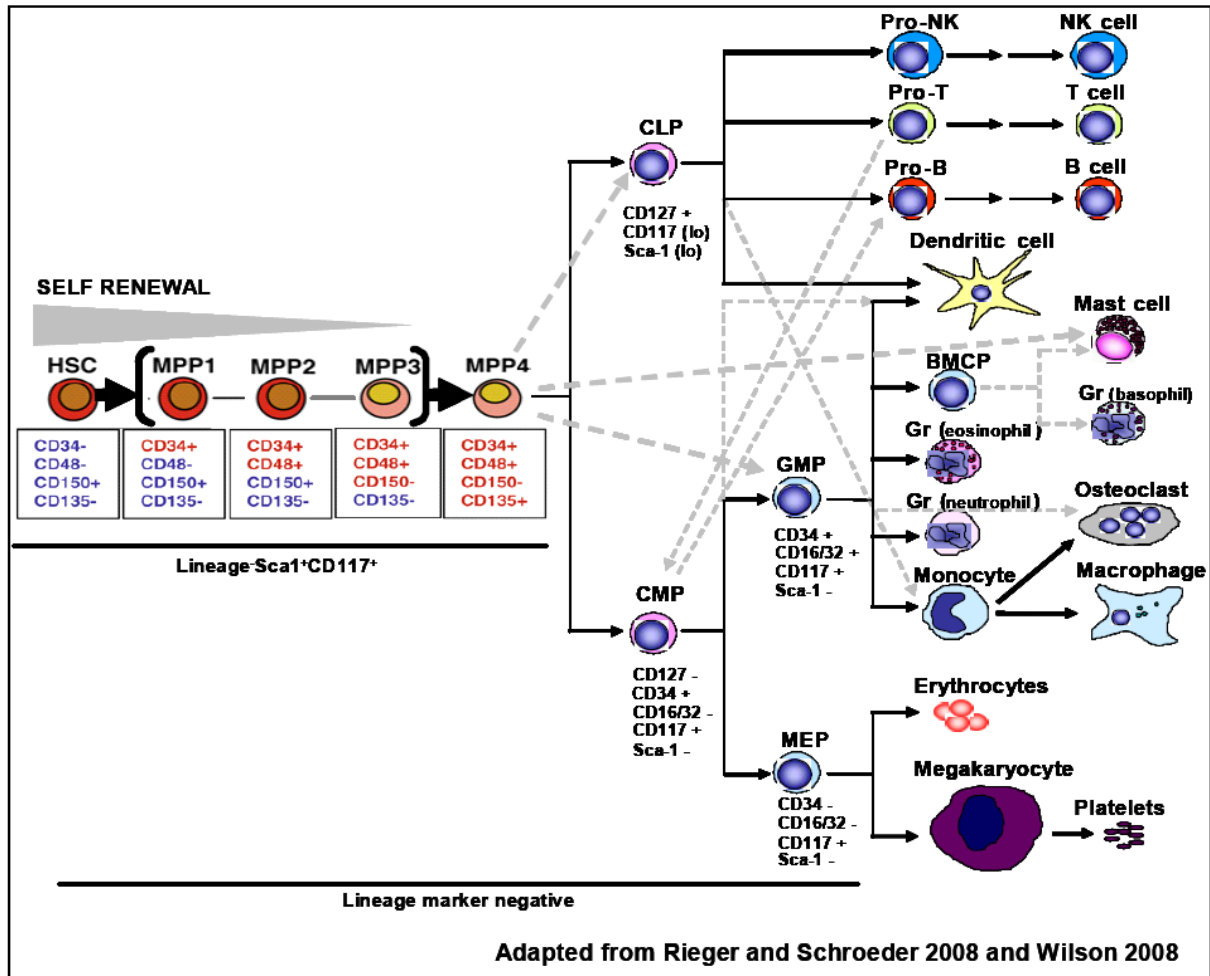


**Figure 3.1: Differentiation of hematopoietic stem cells (HSC) into the lineages of the blood system.** HSC are able to self renew for life and give rise to all myeloid and lymphoid blood lineages. The different MPP stages self renew only for a short time (weeks), but are still multipotent. Figure adapted from Rieger and Schroeder, 2008 and Wilson, Laurenti et al. 2008.

A model of the hierarchy of murine blood development from the HSC down to mature blood cells is depicted in Figure 3.1. It is believed, that blood cell differentiation can only start at the HSC on the left side and irreversibly follows one direction towards mature blood cells. Differentiation means the decision to change one cell type into a different cell type with different potential (e.g. cell lineage potential). Typically, differentiation is accompanied by a loss in potential. For example, HSC are able to self renew and reconstitute all the blood cells of an organism for its lifetime. When they give rise to MPP, HSC differentiate and lose lifelong reconstitution potential and their self renewal ability decreases. Self renewal is the capacity to produce progeny which are identical to the mother cell thus allowing maintenance of a certain cell type even during proliferation. It is not known

---

until what stage in the blood cell hierarchy cells still possess self renewal capacity however it is generally assumed that further differentiated cells possess less self renewal capacity than their more immature progenitors.

MPP have lost their potential to reconstitute the full hematopoietic system life-long (Yang, Bryder et al. 2005). However, just like HSC they are still multipotent, that means that they can give rise to all mature blood cell types. Blood cells that have differentiated from MPP and are not anymore multipotent are assigned to either the myeloid or lymphoid lineage. Cells of the myeloid lineage include erythroid cells, megakaryocytic, granulocytic and monocytic cells. They are produced by bipotent progenitor cells, the megakaryocyte-erythrocyte progenitor (MEP) and the granulocyte-monocyte progenitor (GMP), which are derived from MPP.

MEP differentiate into erythrocytes, which make up the majority of blood cells found in the blood stream and are necessary for transport of oxygen, as well as megakaryocytes, which are large cells that when fully matured produce platelets necessary for blood clotting. GMP give rise to granulocytes as well as monocytic cells which both play an important role in the first line of defence against pathogens and constitute the innate part of the immune system. They impede infections by producing substances detrimental to pathogens, phagocytose bacteria, and alert cells of the adaptive immune system.

Cells of the lymphoid lineage include B-, T- and Nk-cells, which provide the adaptive immune system. The common lymphoid progenitor (CLP) gives rise to these three blood cell types (Kondo, Weissman et al. 1997). B-cells produce antibodies specific to surface proteins on pathogens and constitute the humoral immunity. T-cells as well as Nk-cells constitute the cellular immunity. They recognize processed antigen presented by antigen presenting cells of the innate immune system.

All of these blood cell types need specific environments that sustain either the maintenance of a certain maturation stage or provide cues for maturation towards mature cells. Maturation refers to a change in morphology and/or surface marker expression by cells that are already committed to a certain lineage. The environments supporting maturation or sustaining arrest in a maturation stage are called niches and each cell type needs a different niche that is constituted of various cell types providing surface bound as well as secreted signals to the blood cells. HSC

self renewal niches, for example can be found in the bone marrow and it is thought that they are supported by stromal cells (Moore and Lemischka 2006), osteoblasts (Calvi, Adams et al. 2003) and endothelial cells (Kiel, Yilmaz et al. 2005). Only signals from this niche are able to sustain HSC potential, the ability to reconstitute the bone marrow for life, indefinitely. Ex vivo culture attempts to imitate this niche, but usually a constant decline of HSC potential per culture time illustrates the insufficient capacity of the artificial niche to support HSC maintenance. Other blood cell types require niches to complete maturation. For example, T-cells have to migrate to the thymus, where they learn to distinguish self from non-self to produce functional T-cells, and B-cells need maturation steps in spleen and lymph nodes to produce antigen specific antibodies.

### **3.2. Expression of Surface Markers by Blood Cells**

The different blood cell types found in the murine bone marrow can be easily distinguished by their expression of surface markers specific to certain maturation stages. Starting at the bottom of the hierarchy, the commitment to the erythroid lineage from MEP is characterized by the upregulation of the transferrin receptor CD71 (Rieger, Smejkal et al. 2009). Cells of the erythroid lineage are additionally also negative for myeloid as well as lymphoid markers. Further maturation of these erythroid progenitors is accompanied by a decrease in size and increase in haemoglobin concentration, which can be visualized by microscopic approaches. The maturation stages leading to fully mature erythrocytes have been defined from these snapshots in differentiation. They are also accompanied by a subsequent loss of CD71 expression and gain of Ter119 expression (reviewed in Testa 2004). The last step in erythrocyte maturation includes expelling the nucleus and the progressive loss of all organelles and yields reticulocytes.

Cells committed to the megakaryocyte lineage that eventually give rise to platelets have lost erythroid potential of their MEP progenitors and can be identified by the expression of CD41 (Pronk, Rossi et al. 2007). Megakaryocyte maturation is accompanied by an increase in size reflecting several rounds of endomitotic divisions,

which encompass DNA replication and nuclear segmentation but lack nuclear and cytoplasmic divisions (Cramer 1999). The maturation into proplatelets involves the formation of pseudopodial projections by fragmentation of megakaryocyte membranes. These proplatelets are subsequently filled with organelles and granules and upon detachment from the core form platelets (Kaushansky 2008).

Cells of the granulocytic and monocytic lineage have to undergo several maturation steps to arrive at mature macrophages and granulocytes (reviewed in Metcalf 2005). Both mature cell types express high levels of the integrin CD11b, also called Mac-1 (reviewed in Mazzone and Ricevuti 1995), but only mature granulocytes express the Ly6G antigen (Fleming, Fleming et al. 1993). Therefore, a combinatorial staining with antibodies directed against these two surface proteins can distinguish granulocytes from macrophages in fluorescent activated cell sorting (FACS) approaches.

The progenitors of the four described mature blood cell types, MEP, GMP and a population known as the common myeloid progenitor (CMP), which contains both GM and ME progenitor cells, are all characterized by the lack of lineage marker specific surface markers. They further have in common a lack of stem cell antigen (Sca)-1 expression, but express high levels of the receptor tyrosine kinase c-kit that serves as the receptor for stem cell factor (SCF). The three progenitors can be distinguished by their expression of the sialomucin CD34 and Fc $\gamma$  receptor. MEP are low for Fc $\gamma$ R and are low for CD34, CMP express CD34 but lack Fc $\gamma$ R and GMP express high levels of both antigens.

Like myeloid cells, lymphoid cells can be identified by the expression of specific surface receptors as well. The maturation of B-cells is accompanied by a change in surface marker expression (reviewed in Hardy and Hayakawa 2001). For example, B220, the receptor of the pan hematopoietic marker CD45, as well as CD19 are both expressed early in B-cell maturation and are thus utilized to identify bone marrow cells committed to the B-cell lineage. T-lymphocytes can be distinguished by FACS from other bone marrow cells by the expression of CD3, which is part of the T-cell receptor (TCR) complex (reviewed in Kuby 1997). Natural killer cells share many characteristics with T-cells, but their maturation is thymus independent and they do not express TCR and CD3, but express Fc $\gamma$  receptor and CD56 (reviewed in Jobim

and Jobim 2008).

CLP, the immediate precursors of all lymphoid cells, can be distinguished from myeloid progenitors as well as earlier multipotent progenitors by the expression of the IL7R. Antibodies against its  $\alpha$ -chain allow specific isolation of early lymphoid cells (Kondo, Weissman et al. 1997). In addition, CLP express low levels of both sca-1 and c-kit.

CLP are derived from MPP that still have the potential to give rise to blood cells of both the myeloid and lymphoid lineages. MPP can self renew for a limited time and have been recently very thoroughly classified and subdivided according to their expression of surface markers (Wilson, Laurenti et al. 2008). All MPP are lineage marker negative, express high levels of both sca-1 and c-kit (KSL phenotype) and are positive for CD34 but can be subdivided by their expression of CD135. In addition, they differentially express the SLAM family receptors CD150 and CD48, which were recently found to be differentially expressed on stem and progenitor populations of the hematopoietic system (Kiel, Yilmaz et al. 2005). Their discovery as HSC markers have improved and facilitated the isolation of purer HSC populations.

In this thesis, MPP that are positive for CD34, but negative for CD135 are employed in various experiments. These MPP were not analyzed for the expression of CD150 and CD48 and therefore encompass MPP stages 1 through 3 from Wilson (Figure 3.1), but for simplification will be termed MPP. In addition, in some experiments Flt3<sup>+</sup> MPP are utilized which represent MPP4 from Wilson and are identified as such.

HSC are at the top of the hierarchy of the hematopoietic system. HSC are the only blood cells that are able to self renew and reconstitute the bone marrow of an organism for life. In addition, they are able to proliferate and differentiate into all the mature blood cell lineages and progenitors including the MPP. How HSC manage to self renew and to differentiate at the same time remains an enigma. In recent years researcher have been able to study the properties of HSC closely through the advancement in isolating populations with a high percentage of HSC (Uchida and Weissman 1992). Like their MPP progeny, HSC display the KSL phenotype. However, when freshly isolated and quiescent, HSC are negative for CD34, but upregulate its expression when they become activated upon cytokine stimulation or mobilization

(Brown, Greaves et al. 1991). When isolating this population as CD34<sup>+</sup>KSL not all of these cells have HSC properties. Of freshly isolated CD34<sup>+</sup>KSL, 21%-40% are able to reconstitute lethally irradiated mice (Osawa, Hanada et al. 1996; Ema, Takano et al. 2000). The addition of antibodies against SLAM receptors to the isolation scheme allows isolation of cell population that contain HSC with reconstitution potential higher than 47%. Freshly isolated HSC are positive for CD150 and negative for CD48 in addition to their CD34<sup>+</sup>KSL phenotype (Kiel, Yilmaz et al. 2005; Wilson, Laurenti et al. 2008). As a further advantage of the SLAM code, it is possible to purify with the same marker combination adult as well as fetal HSC and HSC from mice of different strains as well as aged and reconstituted mice as this was previously not possible (Kiel, Yilmaz et al. 2005; Kim, He et al. 2006; Yilmaz, Kiel et al. 2006). The improvement in HSC purity in recent years enables researchers to tackle long standing questions concerning self renewal and differentiation of HSC.

### 3.3. Elucidating the Mechanism of Asymmetric Cell Division

It is not known how precisely the stem cell pool of an organism stays constant during the course of its life and how at the same time short-lived mature cells are generated regularly. To reach this goal, the stem cell has to either produce two identical fated daughter cells whose fates are subsequently altered by extrinsic signals like cytokines or surface molecules on surrounding cells. Another possibility involves intrinsically controlled generation of differently fated daughter cells. The fate decision is made either in the mother cell prior to mitosis or directly during the division. This mechanism called asymmetric cell division (ACD) is widely used in cell specification during invertebrate development, however it is not known if this mechanism is utilized by mammalian HSC (Figure 3.2).

Several scenarios of mechanisms controlling ACD have been reported in invertebrates. In the *Drosophila* germ line only one of the prospective daughters of the germ line stem cell receives maintenance signals from the surrounding niche (Xie and Spradling 2000). While the daughter lying adjacent to the niche remains a stem cell, the other daughter differentiates. In *Drosophila* eye development, lateral

inhibition causes two identical precursor daughter cells to induce different cell fates amongst each other (Baker, Mlodzik et al. 1990). The third example of cell specification during division involves the asymmetric segregation of a factor in the mother cell and its subsequent inheritance by only one daughter, which leads to asymmetric fate specification in the daughter cells (reviewed in Schroeder 2007).

From invertebrates like *Drosophila* we know that asymmetric protein segregation is employed for cell specification during embryonic development. In the hematopoietic system the only example of ACD was shown in T-cells which display factor segregation upon stimulation by an antigen presenting cell and subsequent asymmetric cell fate specification in their daughters (Chang, Palanivel et al. 2007). However, whether ACD occurs in mammalian HSC is unclear at the moment.

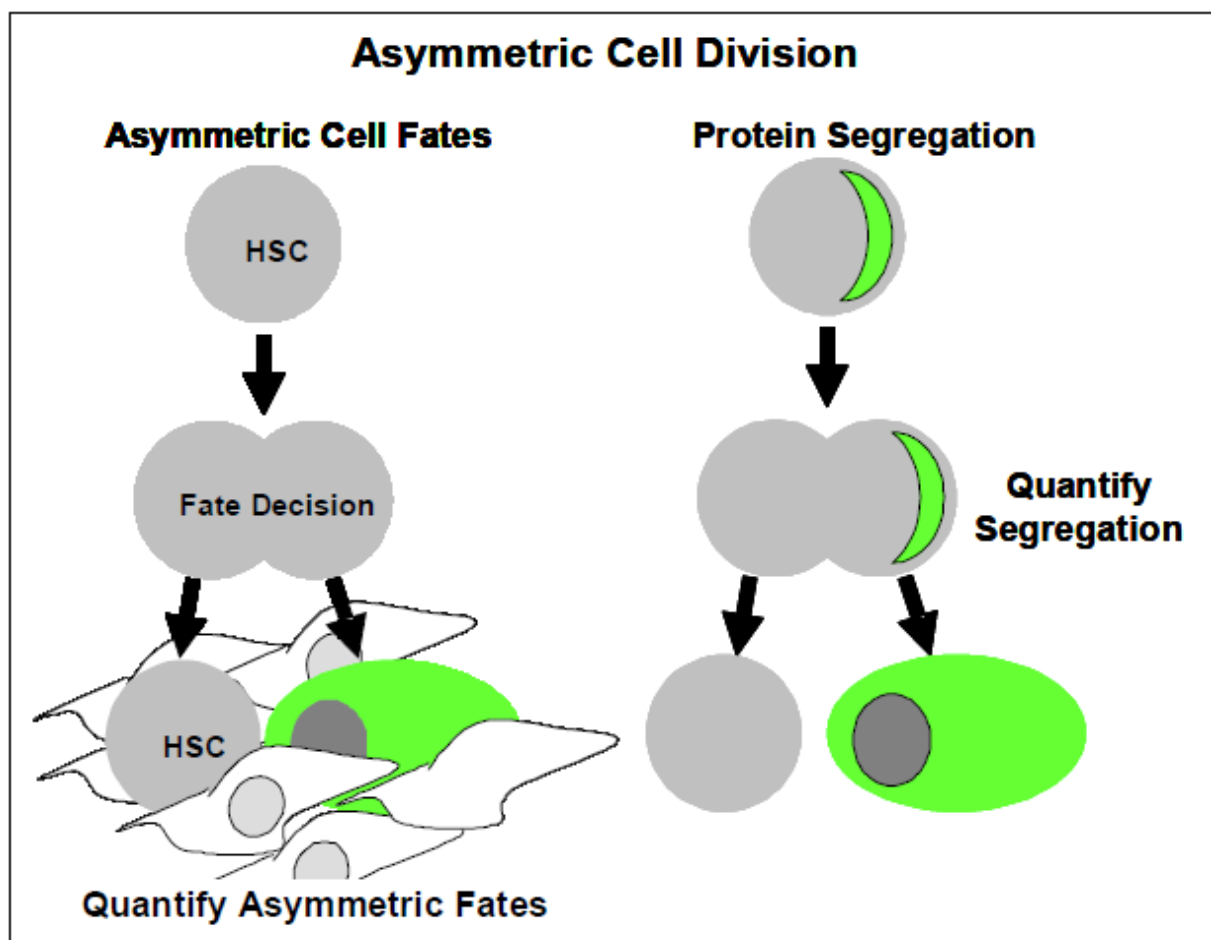


**Figure 3.2: Asymmetric cell division (ACD) of HSC.** ACD describes a hypothesis that links asymmetric HSC daughter cell fates to intrinsic decisions taking place during HSC mitosis. Fate decisions take place during division and influence asymmetric fates of daughter cells (**A**). One possibility involves segregation of self renewing or differentiation promoting factors during division (**B**).

### 3.4. Requirement for Time Lapse Microscopy and Single Cell Tracking

It is conceivable that HSC employ asymmetric cell division by segregating determinants that ensure self renewal or lead to differentiation in one daughter cell to meet the needs of long lived mammalian organisms with a constant need of short lived mature blood cells. Many studies have tried to tackle this long standing question. However, so far it has proven too challenging to connect events taking place during HSC division with fate choices of their progeny.

In order to study the mechanism of ACD that controls cell specification it is necessary to connect divisions of individual HSC to the fates of their daughters. Events taking place during division, like protein segregation, have to be observed and their effect on fate specification has to be analyzed. Asymmetric protein segregation during division is a process which can be captured only when monitored constantly. Snapshots of mitotic cells are difficult to obtain without manipulating cells to arrest them during mitosis. It is furthermore difficult to ensure from a still image if two adjacent cells are sister cells, and if a protein is segregated during division or if it is just silenced in one daughter.

To identify HSC daughter cell fates, fluorescent markers and morphological criteria can be employed that identify cells committed to a certain lineage. However, these fates of HSC become apparent only after days or weeks have passed and the cells have undergone several divisions. Even when starting with a single cell per well, after two divisions, the identity of each cell is not apparent anymore in still images. To overcome this problem, researchers have used micromanipulation to separate cells after their division and used reconstitution experiments and colony assays as a fate readout (Ema, Takano et al. 2000; Takano, Ema et al. 2004). With this method they could identify daughter and granddaughter fates of HSC. However, it was not possible to observe divisions directly and it is not known if manipulation of the cells might have altered their fates.

Consequently, to study protein segregation and fate choice in HSC it is indispensable to monitor cells constantly over several days. Thus, we have developed

a novel imaging and tracking system in our lab, that allows continuous observation using time lapse microscopy (Rieger and Schroeder 2008; Eilken, Nishikawa et al. 2009; Rieger, Hoppe et al. 2009). In our time lapse setup we can culture cells for at least two weeks, while phase contrast images with a high resolution are taken in 2 minute intervals. A motorized stage moves the culture vessels to allow monitoring of several positions which allows the continuous observation of large areas in a culture dish including migrating cells and expanding colonies. Fluorescence images are taken to identify fluorescent marker expression by cells that have reached certain maturation stages and to monitor segregation of fluorescently tagged proteins during division.

The collected time lapse videos are then analyzed frame by frame with the help of a self-programmed tracking software that allows manually tracking of individual cells and their progeny (Eilken, Nishikawa et al. 2009). Their ancestral relationship is recorded in pedigrees that contain information regarding cell division, generation time, migration, adherence, speed, cell death, morphological changes and marker expression of the analyzed cells. In addition, it is possible to quantify fluorescence intensities of labelled proteins that vary in expression strength. The information obtained from the individual pedigrees can then be statistically analyzed by the same program, yielding continuous population data with single cell resolution.

The combined use of high resolution time lapse imaging and single cell tracking allows us to elucidate longstanding hypotheses, for example if HSC undergo ACD, by examining protein segregation during division and evaluation of its effect on fate choices of HSC daughters.

### **3.5. HSC Properties**

Researchers have not been able to clarify if HSC use ACD as a mechanism of cell specification. However, many other properties of HSC have been elucidated in recent years. A hallmark of HSC is that they stay quiescent in their bone marrow niches during homeostasis conditions in an adult mammalian organism. When no expansion of HSC is needed, they divide very rarely (only every 36 to 145 days) and

are kept mostly in G0 and G1 phase of the cell cycle (Wilson, Laurenti et al. 2008). In this quiescent state, HSC have been shown to possess a more potent reconstitution capacity than activated HSC that are in S/G2/M phase (Nygren, Bryder et al. 2006). Many studies examining HSC properties however use cytotoxic drugs like 5-FU or BrdU to eliminate mature cells or to directly label HSC *in vivo* (Boswell, Wade et al. 1984). However, these agents induce stress and so HSC leave their dormant state and enter the cell cycle to replace the damaged or lost cells (Wilson, Laurenti et al. 2008). Therefore, many properties of HSC found by studies using agents that cause stress are properties that HSC display in artificial expansion conditions and not during normal homeostasis. When activated by stress or mobilizing agents, HSC change their surface marker expression. They for example upregulate CD34 which is absent in quiescent HSC (Sato, Laver et al. 1999) and activate various signalling cascades, like the FoxO3/Akt pathway (Yamazaki, Iwama et al. 2006). In addition, activated HSC divide more frequently and therefore spend an increased time in S/G2/M cell cycle phase (Kiel, Yilmaz et al. 2005; Nygren, Bryder et al. 2006; Wilson, Laurenti et al. 2008). In these characteristics, activated HSC resemble their immediate progeny the MPP more closely than their quiescent HSC sisters. MPP contain fewer cells in G0/G1 than HSC, have much shorter cell cycle transit times and do not contain as many long term label retaining cells within their population as true HSC (Nygren, Bryder et al. 2006; Wilson, Laurenti et al. 2008)

As the *in vivo* observation of HSC at the single cell level over time is impossible at the moment, it is indispensable to culture these cells *in vitro* in order to examine ACD of HSC. In addition, expansion of HSC is an important goal for clinical applications. The analysis of *in vitro* HSC maintenance and control of self renewal are important steps towards this goal. When culturing HSC *in vitro*, through cytokine stimulation they become activated, gaining therefore many properties of MPP. Therefore, we decided to compare the behavioural differences of HSC and MPP regarding their fate decisions *in vitro* to identify intrinsically controlled properties of HSC that are retained in culture.

### 3.6. Assays for HSC and Progenitor Cells

Examining the behaviour and fate potential of HSC and MPP, assays to measure these properties are needed. The only assay that identifies HSC as such involves the evaluation of their reconstitution potential of bone marrow cells *in vivo*. Cells are injected into the tail vein of a mouse from where they are homing via the blood stream to the bone marrow. In order to avoid elimination of the introduced stem cells by the immune system of the recipient, it is necessary to utilize immune compromised or irradiated wildtype mice as recipients. To analyze the reconstitution ability of the injected cells, donor mice with a different blood cell surface allele or a fluorescent marker are utilized. The peripheral blood of the recipient mice is then analyzed for at least 16 weeks for the presence of donor type blood cells, at which time only true donor HSC are still able to give rise to differentiated cells in the periphery. However, by definition, to prove self-renewal potential it is necessary to transplant bone marrow from these mice into secondary recipients. To assess exact numbers of HSC potential within a population of cells, they can be transplanted in limiting dilution. By coinjection of the cells of interest with competitor cells the exact number of competitive repopulation units (CRUs) present in the initial population can be measured (Szilvassy, Humphries et al. 1990).

In contrast to true stem cell potential, proliferation and multilineage potential can also be evaluated by *in vitro* assays. For example, myeloid as well as B-cell colony forming potential can be assayed by plating the cells in semisolid media containing cytokines that allow the formation of all myeloid and B-lymphoid lineages, respectively (Bradley and Metcalf 1966; Metcalf, Nossal et al. 1975). In this assay cells are seeded into semisolid media containing various growth factors and are allowed to proliferate and differentiate. After a certain amount of time colonies produced by the seeded cells are scored and identified according to colony morphology and blood cell types they contain. With this assay it is possible to read out the proliferation potential (size of colonies), colony formation potential (number of colonies) as well as lineage choice (types of colonies) of any blood cell progenitor population.

In summary we can only identify HSC by their ability to reconstitute the bone marrow of a mouse and it is not possible to use any *in vitro* assays to identify HSC.

---

The two described assays provide us with means to evaluate stem cell and *in vitro* proliferation and multilineage potential of freshly isolated, cultured as well as manipulated HSC and their progenies.

### 3.7. Using *in vitro* Markers to Label Stem Cells and Differentiated Cells

When examining stem cell fate choices *in vitro* and identifying self renewal as well as differentiation behaviour, it is important to be able to distinguish cultured cells that have retained or lost their HSC potential. As cultured HSC can only retrospectively be identified by transplanting single cells into lethally irradiated hosts, we have to rely on marker expression which correlates with reconstitution potential. Unfortunately HSC cannot be isolated by a single marker, but require several antibodies labelled by different colours for identification. In addition, several of the markers that distinguish freshly isolated HSC from their more differentiated progeny, are actually markers that recognize cell activation and mobilization rather than reconstitution potential. These markers, for instance CD34, are not present in dormant HSC, but are upregulated upon activation of HSC by cytokine stimulation *in vitro* (Sato, Laver et al. 1999).

In contrast, there are many markers available for labelling mature blood cells. Especially cells derived from transgenic mice that express a fluorescent protein under the control of lineage specific markers, therefore, identifying specific lineages, have been useful in a great number of studies. For example, cells committed to either the granulocyte or macrophage lineage can be identified by the expression of EGFP that is knocked into the Lysozyme M locus (Faust, Varas et al. 2000). Lysozyme M is contained in neutrophil granules (Cramer and Breton-Gorius 1987) and is secreted by macrophages (Gordon, Todd et al. 1974) and is utilized by these cells to cleave components in the cell wall of bacteria and thus serves as a pathogen defence mechanism. In these transgenic mice, EGFP expression identifies cells that have lost the bipotentiality of GMP and are committed to either the granulocytic or monocytic lineage (Rieger, Hoppe et al. 2009).

Cells committed to the megakaryocyte lineage can be identified either by antibody detection of CD41 surface expression or by utilizing cells from CD41

membraneYFP Knockin mice (Zhang, Varas et al. 2007). Cells of the erythroid lineage can be identified using cells of transgenic mice expressing ECFP under regulatory elements of the  $\beta$ -globin gene (Heck, Ermakova et al. 2003). Cells of the lymphoid lineage can be identified by utilizing cells derived from mice heterozygously expressing GFP knocked into the Rag1 gene identifying early lymphoid progenitors (Kuwata, Igarashi et al. 1999) as well as taking cells derived from mice expressing Pax5 controlled GFP identifying committed B-cell progenitors (Fuxa and Busslinger 2007). In few cases phase contrast microscopy can help to identify the identity of cells. Developing megakaryocytes undergo endomitosis and increase in size during their maturation, which can be easily followed by time lapse microscopy.

With the described markers it is possible to identify all the mature cell types of the blood system in culture. Therefore, retrospectively the lineage commitment of progenitor cells can be concluded. However when examining fate decisions of HSC, it takes several days or even weeks to differentiate an HSC into a mature cell that can be recognized by these markers. Thus, *in vitro* differentiation of HSC cannot be monitored easily at the single cell level. In order to overcome this problem, a marker identifying early differentiation or loss of stemness is required. Recently, the SLAM code marker CD48 that is not expressed on freshly isolated HSC, but on progenitors that have lost stem cell potential was shown to also identify the loss of reconstitution potential in cultured cells (Noda, Horiguchi et al. 2008).

In summary although many markers are known that label maturation stages of mature blood cells, no single marker exists that can identify HSC in culture. CD48 however can be used indirectly to identify HSC in culture, as it reveals loss of stemness events during HSC differentiation.

### **3.8. Environment for Blood Cells: The Niche**

The natural environment for HSC *in vivo* is constituted by the stem cell niche which provides HSC with cues for self renewal and differentiation (Moore and Lemischka 2006). The identity of the niche cells is not fully elucidated yet, but it is speculated that a mixture of osteoblasts (Calvi, Adams et al. 2003), endothelial cells

(Heissig, Hattori et al. 2002), stromal cells (Dexter, Wright et al. 1977), as well as blood cells provide self renewal and differentiation signals to HSC. *In vitro* this niche can be recapitulated by the use of stromal cells, either derived directly from primary bone marrow or by using immortalized stromal cell lines. A wide variety of stromal cell lines have been generated for various purposes, but only few of them support maintenance of hematopoietic stem cells. Some of the stromal cell lines that can maintain at least some HSC potential in culture over a few days to several weeks are summarized below.

In order to examine protein segregation and asymmetric fate decisions in HSC it is necessary to provide an environment that supports HSC maintenance. At the same time, the differentiation into and survival of progenitor cells that can be identified by the expression of loss of stemness or lineage restricted markers has to be possible. For the quantification of asymmetric fates of stem cell progeny, it is important to ensure that the chosen environment supports the generation of asymmetric fates

### 3.8.1. Artificial Environment: Stromal Cell Lines

PA6, which are a pre-adipose stromal cell line derived from the calvaria of newborn mice (Kodama, Amagai et al. 1982), have been utilized to provide a stem cell maintaining environment for HSC. PA6 have been shown to be able to sustain at least some HSC potential for two to six weeks (Kodama, Nose et al. 1992; Szilvassy, Weller et al. 1996; Shimizu, Noda et al. 2008). The addition of cytokines, which induce survival signals increased the percentage of HSC maintained (Szilvassy, Weller et al. 1996). PA6 are also able to support the growth of MPP-like spleen colony forming units and their differentiation into mature myeloid lineages and can support long term hematopoiesis *in vitro* for several weeks (Kodama, Amagai et al. 1982; Kodama, Sudo et al. 1984). With the addition of IL-7 to PA6 cocultures, PA6 stromal cells are also able to support B lymphopoiesis (Sudo, Ito et al. 1989).

Another widely used stromal cell line, AFT024, are derived from the fetal liver and support the maintenance of adult bone marrow as well as fetal liver HSC for

up to 7 weeks (Moore, Ema et al. 1997). In addition to HSC maintenance, AFT024 also support the generation of progenitors as well as mature blood cell types.

A third stromal cell line, OP9 cells, are derived from newborn B6C3F1-op/op mouse calvaria lacking a functional M-CSF receptor (Kodama, Nose et al. 1994). OP9 are widely known to support hematopoiesis and are commonly used to differentiate ES-cells into mature blood cell lineages (Nakano, Kodama et al. 1994; Nakano, Kodama et al. 1996) as well as for the study of lymphocyte development from bone marrow progenitors (Wang, Pierce et al. 2005; Wang, Pierce et al. 2006). However, OP9 have not been sufficiently proven to support the maintenance of HSC.

Other stromal cell lines with varying degrees of HSC supporting capacity have been described (Szilvassy, Weller et al. 1996; Wu, Kwon et al. 2007), however these cell lines are not widely used and therefore not useful for our purpose.

Confronted with the challenge to choose an appropriate stromal cell line, we decided that OP9 are not appropriate to provide an HSC supporting environment. AFT024 do maintain HSC, however they are not contact inhibited and need to be irradiated for HSC co-culture. This results in a less uniform cell layer that makes identification of HSC on these stroma cells difficult which is a disadvantage for imaging purposes. Finally, PA6 are contact inhibited and optically clear, they support HSC over a timeframe interesting for imaging purposes and several researchers have used this cell line to study hematopoiesis. Therefore, we decided to use PA6 to provide an *in vitro* niche to study HSC fate decisions.

### **3.8.2. Artificial Environment: Stroma Free Suspension Culture**

Stromal cell lines provide supporting and differentiation signals through direct cell - cell contact as well as by secreting cytokines. In addition, the cultivation of HSC on stromal cells requires the use of serum. The variety of signals from cytokines, surface proteins and serum components are not well defined and characterized and therefore make it difficult to assess the cause of a behavioural change in the blood cells. In order to distinguish intrinsic properties and decisions of HSC from behavioural changes that are the result of extrinsic cues it is necessary to compare HSC behaviour in different environments. Therefore, we decided in addition

---

to an environment that closely resembles the *in vivo* niche, to use a clearly defined culture system where HSC are kept in stroma free, serum free medium with the addition of specified growth factors.

Assessing self-renewal divisions of HSC, just like on stromal cells, conditions are needed that maintain stem cells over several days, and allow the generation of progenitor as well as mature blood cell types. As we want to study ACD, that by definition should keep HSC numbers constant, it is important to choose culture conditions that maintain HSC numbers, but do not expand them, as this would point towards symmetric self renewal divisions rather than asymmetric maintenance divisions.

A cytokine known for its activity to support stem cell survival is SCF, which is the ligand for c-kit. SCF was shown to maintain stem cells in culture for at least 3 days (Seita, Ema et al. 2007). However, SCF alone does not support proliferation or multi-lineage differentiation *in vitro* (Kato, Iwama et al. 2005) which excludes it as a condition to monitor asymmetric fates of HSC.

In contrast, single HSC suspension culture with the addition of both SCF and thrombopoietin (TPO) as well as SCF together with Interleukin 3 (IL3) maintained stem cell potential for several days, without expanding the number of stem cells (Ema, Takano et al. 2000). Further, these conditions allow for the differentiation of HSC into mature lineages and do so by generating asymmetric fates of HSC daughters and granddaughters (Takano, Ema et al. 2004).

Although asymmetric fates have been previously studied under these conditions we wanted to elucidate on the single cell level and under constant observation how asymmetric fates are generated. Therefore, we decided to use these two conditions that support limited stem cell maintenance of HSC to study their fate decisions. In addition, we decided to compare this data of HSC behaviour in supporting suspension conditions to non supporting conditions provided by SCF and Interleukin 6 (IL6) (Ema, Takano et al. 2000) and to HSC behaviour on PA6.

### **3.9. Mechanism Influencing Asymmetric Fate Decisions: Protein Segregation**

Trying to elucidate the influence of protein segregation on HSC fate decisions, we decided to use a candidate approach and test if selected proteins play a role in this process. We selected candidate genes according to two criteria: Firstly, genes were chosen that are known to play a role in ACD in organ systems of invertebrates like *Drosophila* or *C. elegans*, or in other mammalian tissues. We also were interested in genes that regulate other genes on the RNA level, as it was hypothesized that this may be a mechanism important in stem cell fate specification. Determinants important for cell specification are often found already to be present in the undifferentiated stem cell as RNAs waiting to execute decisions by translation into proteins once a differentiation cue has been received. Finally it was of course important to test if the selected genes are expressed in mouse HSC.

### **3.10. Candidate Genes for Protein Segregation**

#### **3.10.1. Candidate Gene Staufen**

As the first candidate for experiments elucidating ACD in HSC we chose Staufen. Staufen was first identified in a genetic screen of embryonic patterning determinants in *Drosophila* (Schupbach and Wieschaus 1986). Staufen protein contains dsRNA binding domains (dsRBD) with which it binds target mRNAs sequence independently within the 3'UTR (St Johnston, Brown et al. 1992; Ferrandon, Elphick et al. 1994; Li, Yang et al. 1997; Wickham, Duchaine et al. 1999). By employing separate domains, Staufen links target mRNAs to actin and microtubule filaments and transports them to the rough endoplasmatic reticulum (rER) for translation (Wickham, Duchaine et al. 1999; Micklem, Adams et al. 2000). By localizing target mRNAs, Staufen generates mRNA gradients within a mother cell that are subsequently segregated into only one of the daughter cells. This happens in the *Drosophila* germline (St Johnston, Beuchle et al. 1991) where Staufen plays an important role in determining already in the oocyte anterior-posterior axis formation of the developing embryo. By asymmetrically localizing homeobox mRNAs within the

*Drosophila* oocyte, Staufen sets the stage for early embryonic patterning after fertilization (St Johnston, Driever et al. 1989; Ephrussi, Dickinson et al. 1991; Kim-Ha, Smith et al. 1991; Ferrandon, Elphick et al. 1994; Kim-Ha, Kerr et al. 1995).

Staufen also plays a role in ACD in cell specification in the developing nervous system of *Drosophila* (St Johnston, Beuchle et al. 1991). There, Staufen is responsible for the basal localization of the mRNA of the homeobox gene Prospero (Li, Yang et al. 1997; Broadus, Fuerstenberg et al. 1998). Prospero and Staufen are then segregated into only one daughter of a dividing neuroblast which leads to the specification of the ganglion mother cell.

In mammals, two homologues of *Drosophila* Staufen exist. Nothing is known about a role of either protein in ACD or cell specification. However Staufen1 and Staufen2 both play important roles in several cellular processes, like dendritic transport (Kiebler, Hemraj et al. 1999; Kohrmann, Luo et al. 1999; Tang, Meulemans et al. 2001; Duchaine, Hemraj et al. 2002) and translational initiation (Dugre-Brisson, Elvira et al. 2005). Mammalian Staufen also regulates nonsense mediated mRNA decay (Kim, Furic et al. 2005), binds to human Telomerase RNA (Le, Sternglanz et al. 2000) and plays a role in genomic RNA encapsidation in Lentivirus assembly (Mouland, Mercier et al. 2000). There is no known function for Staufen1 in the blood system, but expression data reveals expression of human Staufen2 in hematopoietic progenitor as well as leukemic cells (Faubert, Lessard et al. 2004).

We decided to use Staufen as a candidate gene since it plays an important role in ACD in invertebrates. We decided to concentrate on Staufen1, rather than Staufen2 as a candidate gene, since its reading frame was easily accessible. Staufen1 gene produces two alternative splice forms, Staufen1 and Staufen<sup>i</sup>. Both are expressed in all major tissues and we tested expression in bone marrow progenitor populations and HSC (see Results). Staufen1 and Staufen<sup>i</sup> localize within the rER and found together in the same RNA-protein complexes. Staufen<sup>i</sup> contains an amino acid insertion into the dsRBD3 which results in a reduced dsRNA binding affinity of Staufen<sup>i</sup>. It has been suggested that Staufen<sup>i</sup> regulates the amount of mRNA present within Staufen mRNA complexes (Wickham, Duchaine et al. 1999; Duchaine, Wang et al. 2000).

In summary, Staufen plays a role in asymmetric cell division in *Drosophila*

development, regulates cellular processes on the RNA level and is expressed in HSC. This renders *Staufen* an ideal candidate gene to examine ACD in HSC. In addition, the existence of a natural mutant, *Staufen<sup>i</sup>* provides us with an ideal functional control.

### 3.10.2. Candidate Gene *Pumilio*

As a second candidate gene, we chose *Pumilio*, which was first identified in *Drosophila* and is the founding member of the PUF proteins consisting of six domains containing a 36 amino acid repeat (Lehmann and Nusslein-Volhard 1991; Macdonald 1992). *Pumilio* plays an important role in ACD in *Drosophila* as well as in *C. elegans* germ line stem cells (Lin and Spradling 1997; Forbes and Lehmann 1998; Crittenden, Bernstein et al. 2002). *Pumilio* executes its function by binding sequence specifically to the 3'UTR of target mRNAs and represses their translation (Murata and Wharton 1995). In *Drosophila* for example, *Pumilio* represses translation of the mRNA of the anterior determinant Hunchback at the posterior end of the embryo, leading to formation of the abdominal segments (Barker, Wang et al. 1992).

In mammals two separate *Pumilio* genes exist, that play an important role in mammalian stem cells and in differentiation processes and act on the RNA as well as protein level. As in *Drosophila*, mammalian *Pumilio2* is expressed in female and male germ cells as well where it interacts with proteins and mRNAs with a function in fertility and maintenance of germ cells (Moore, Jaruzelska et al. 2003; Spik, Oczkowski et al. 2006). In addition to its function in germ cells, *Pumilio* also plays a role in further differentiated cells of the nervous system. It regulates neuronal excitability through controlling Na<sup>+</sup> channel mRNAs (Schweers, Walters et al. 2002; Mee, Pym et al. 2004; Muraro, Weston et al. 2008) and modulates synaptic function and morphology in developing neurons (Menon, Sanyal et al. 2004; Ye, Petritsch et al. 2004; Vessey, Vaccani et al. 2006).

*Pumilio* expression in germ cells and the early embryo points towards a general role in stem cell regulation. Also, *C.elegans* *Pumilio* proteins have been shown to regulate mRNAs encoding MAP kinase proteins, which are implicated in

stem cell maintenance and tumor progression (Lee, Hook et al. 2007). Pumilio's putative role in stem cell regulation is further corroborated by the fact that Pumilio1 and 2 are expressed in stem cell enriched populations of mouse fetal liver and adult bone marrow (Spasov and Jurecic 2003).

The described expression of Pumilio1 and 2 in early bone marrow progenitors as well as their function as translational repressors and their role in asymmetric cell division in invertebrates have led us to choose these genes as further candidates for asymmetric cell division in mouse hematopoietic stem cells.

### 3.10.3. Candidate Gene Quaking1

As a third candidate gene we chose a member of the signal transduction and activator of RNA (STAR) family of proteins. The STAR domain is composed of a KH homology (hnRNP K homology) domain, responsible for RNA binding, flanked by two QUA domains that manage signal transduction (Vernet and Artzt 1997). The *C.elegans* gene Gld1 (Jones and Schedl 1995) as well as the closely related mouse gene Quaking1, are both members of this family. This protein family was interesting to us, because in *C.elegans* Gld1 is a target of the Pumilio homologue Fbf. Fbf represses the translation of Gld1 mRNA to prevent germ line stem cells to enter meiosis (Crittenden, Bernstein et al. 2002; Suh, Jedamzik et al. 2006). Gld-1 protein itself acts as a translational repressor and controls mitosis promoting genes such as the Notch receptor Glp1, thereby favouring entry of germ line stem cells into the meiotic pathway (Francis, Barton et al. 1995; Marin and Evans 2003).

The mammalian homologue of Gld1, Quaking1, is the gene found partially to be responsible for the quaking mutant phenotype, described in mice that display a myelination defect and shaking behaviour (Sidman, Dickie et al. 1964). Quaking1, like its homologue, is regulated at the RNA level and itself regulates, for instance, myelin basic protein, by binding to its RNA. This interaction is necessary for correct myelination of Schwann cells in the developing brain (Ebersole, Chen et al. 1996; Hardy, Loushin et al. 1996; Li, Zhang et al. 2000).

Quaking1 produces 3 major transcripts, which apart from their expression in

the brain, are also expressed in a variety of other tissues. Quaking1 isoforms are expressed in the visceral endoderm of the yolk sac in mouse and control endothelial cell proliferation as well as vascular remodelling during development (Noveroske, Lai et al. 2002; Bohnsack, Lai et al. 2006) Also in *Xenopus* embryogenesis a Quaking1 homologue is found in the organizer region and the notochord during gastrulation (Zorn and Krieg 1997). In chicken the transcripts of an orthologue of Quaking1 show differential expression in spermatogenesis (Mezquita, Pau et al. 1998).

The control of a STAR protein by a PUF family member in *C.elegans* makes mouse Quaking1 an interesting protein to study together with Pumilio in HSC. So far, nothing is known about a connection of Quaking1 and Pumilio in the mouse, however, we found both genes to be expressed in HSC. Therefore, Quaking1 is an interesting candidate gene to try to study fate decisions in these cells. Also Quaking1, like Pumilio, regulates its targets on the RNA level and is found in various stem cell types. As Quaking1 produces three known natural splice variants, we decided to incorporate all of them to study HSC fate choice.

#### **3.10.4. Candidate Gene Prominin1**

Our last candidate gene, Prominin1, is a five transmembrane glycoprotein that localizes to cholesterol binding lipid rafts present in plasma membrane protrusions. (Weigmann, Corbeil et al. 1997; Roper, Corbeil et al. 2000). Prominin1 is the first gene that has been implicated to play a role in ACD in mammals. In dividing neuroepithelial cells, Prominin1 concentrates at the midbody apical surface. Upon division, the midbody is released and, if the cells are undergoing asymmetric divisions, the apical surface containing Prominin1 is retained by one of the daughters. In symmetric divisions, the released midbodies are called prominosomes and include apical membrane containing Prominin1. They can be found in the lumen of the neural tube as well as in all bodily fluids (Marzesco, Janich et al. 2005; Dubreuil, Marzesco et al. 2007).

A similar mechanism has been suggested but not been proven to occur in human hematopoietic progenitor cells (Bauer, Fonseca et al. 2008). In these cells,

Prominin1 shows a polarized distribution during migration and can be asymmetrically distributed during mitosis (Giebel, Corbeil et al. 2004; Fargeas, Fonseca et al. 2006; Bauer, Fonseca et al. 2008). It is not known however, if this asymmetric localization influences fate decisions in the daughter cells, as these studies were done in fixed cells.

Human Prominin1, also known as CD133, has led to the isolation of purer stem and progenitor cells from various tissues, including neuronal and hematopoietic stem cells and is now regarded as a pan adult stem cell marker (Yin, Miraglia et al. 1997; Richardson, Robson et al. 2004; Lee, Kessler et al. 2005). However, nothing is known so far about the expression of Prominin1 in mouse HSC and progenitor cells and there is no information about the function of Prominin1 in any cell type. Nevertheless, I found Prominin1 an interesting candidate for protein segregation and influence on HSC fate decisions and decided to analyze its expression in mouse HSC.

All of the discussed genes are involved in ACD or fate decisions of stem cells of various cell types and species. Because such basic and ancient mechanisms such as protein segregation and ACD are often conserved across species and cell types, it is possible that these genes also play a role in HSC asymmetric fate decisions of mammals. Three of the candidates also influence their target genes on the RNA level. It is known, that in stem cells of all tissues, many of the genes necessary for the differentiation into mature cells are already present as RNAs but not as proteins in the stem cell compartment. Translational repressors, like Pumilio, are needed to prevent translation of these RNAs into proteins and therefore could provide a checkpoint control for differentiation into progenitors and loss of stemness. Therefore, RNA regulation could be a common characteristic of genes regulating stem cell fate decisions.

### 3.11. Experimental Approach

There are several possibilities to screen for candidate genes that play a role in ACD in HSC. The most physiological method would be to knock in a fluorescent reporter protein fused to the reading frame of the candidate gene into the natural

locus of the gene. With this system, the kinetics of unmanipulated wildtype gene expression can be observed in all cell types and during every developmental stage. A disadvantage to this approach is that it is not useful for screening candidates because of the great effort and time that is needed to generate Knock-in lines.

Another commonly employed approach to examine physiological protein segregation *in vitro* uses antibody detection of endogenous candidate proteins in fixed cells. Although it is possible to observe wildtype expression and distribution of candidate proteins with this method, it has severe disadvantages. In order to capture a large number of cells during mitosis, agents to arrest cells during division have to be employed and can influence protein segregation. More importantly, observing the segregation of proteins in fixed cells does not allow following the fates of the two daughter cells, which cannot be read out until several days after the division took place. Without a fate-readout of the daughter cells, it is impossible to make a statement about the influence of a candidate protein that is segregated during division on fate choices of HSC daughters.

The third avenue to elucidate the mechanism of ACD is to exogenously introduce a fusion of the candidate gene with a fluorescent protein into the cell and to visualize the segregation of this protein chimera during division, proliferation and differentiation towards various cell fates. The disadvantage to this approach is that it introduces non-physiological levels of the transgene since its expression is controlled not by its endogenous, but by an exogenous promoter. This could lead to overloading of the protein segregation machinery and proteins that are segregated asymmetrically when expressed endogenously could be missed using this approach. This method however, allows following the fate of both daughters by using our movie system combined with single cell tracking and provides a fast approach to screen several candidate genes.

In addition to examining the role of candidate genes in protein segregation, the effect of candidate overexpression on HSC maintenance and lineage choice can be evaluated with this method as well. For this purpose the candidate gene and the fluorescent protein are separated by an internal ribosome entry site (IRES). In contrast to the fusion gene approach, this ensures that the wild type candidate protein is not altered by the fusion with a fluorescent protein and therefore, the

effect of the non-manipulated protein on stem cell function can be assessed. We chose to employ this method as it allows for fast screening of several candidate genes for their ability to segregate during stem cell divisions and to elucidate their role in fate determination.

### 3.11.1. Overexpression of Candidates with a Lentivirus

For overexpression of the candidate genes in HSC a transfection system is needed. Since plasmid transfection using lipofectamine or similar reagents does not work well in primary cells, we chose to use a viral vector for gene transfer.  $\gamma$ -retroviral vectors are widely used for gene transfer into hematopoietic cells, however, they are able to infect only dividing cells since they lack nuclear localization signals and the polypurine tract that are needed to cross an intact nuclear membrane (Uchida, Sutton et al. 1998; Chang and Sadelain 2007).

When introducing candidate genes by overexpression into HSC, it is important to consider that only 30-50% of starting cells will be true HSC (Osawa, Hanada et al. 1996; Ema, Takano et al. 2000; Kiel, Yilmaz et al. 2005). In addition, as HSC in maintenance conditions will undergo ACD as well as symmetric differentiation divisions, an even lower percentage of HSC within the total population will be present after the first division. The lower the number of true HSC within an evaluated population, the more difficult it will be to identify cells that show protein segregation and asymmetric fate choice in daughters as this is thought to be a mechanism highly specific to HSC. Therefore, it is important to introduce the candidate gene into cells that have not yet divided and monitor transgene segregation during the first division. As  $\gamma$ -retroviral vectors cannot infect quiescent cells, they are not useful for our purposes.

Lentiviral vectors, derived from the human immunodeficiency virus (HIV) can infect non dividing cells and are therefore the vector of choice to monitor protein segregation during first divisions (Naldini, Blomer et al. 1996). Lentiviral vectors of the 4<sup>th</sup> generation have been used widely to transduce bone marrow and specifically hematopoietic stem cells (Dull, Zufferey et al. 1998; Schambach, Galla et al. 2006). These lentiviral vectors are replication incompetent and lack virulence genes not

necessary for viral packaging and DNA integration. For added security, viral components are divided between four separate plasmids, ensuring that virus recombination cannot occur.

Lentiviral vectors can be made specific for various species as well as cell types by using different envelop proteins. Ecotropic pseudotyped lentiviral vectors can only infect rodents but not humans or other primates (Schambach, Galla et al. 2006). Therefore, these viruses do not pose a risk to the researcher. In contrast, lentiviral vectors using an envelop protein from the Vesicular Stomatitis virus, the VSVG protein, can bind to all cells expressing the receptor for this protein, including rodent as well as human cells (Chang, Urlacher et al. 1999). Handling of these lentiviruses does pose a potential risk to the researcher. However, it is known that VSVG protein renders the Lentivirus more stable in ultracentrifugation and we found infection efficiencies of HSC to be higher with this virus. In experiments contributing to this thesis both virus types were used.

### **3.12. Conclusion**

In summary, the work presented in this thesis, explores the mechanism of asymmetric cell division as a means to control HSC self renewal. Towards this goal it was first examined if HSC produce daughters with asymmetric fates. The behaviour of cultured HSC regarding divisional kinetics and marker expression indicating loss of reconstitution potential was quantified using time lapse microscopy and single cell tracking and compared to the behaviour of closely related cells. It was further investigated if HSC specific behaviour is caused by certain environmental cues or if this behaviour is intrinsically controlled by HSC themselves. To this end behaviour of HSC and MPP was analyzed using several different culture conditions.

To gain insight into the molecular mechanism controlling potential ACD in HSC, candidate proteins were screened for their ability to segregate asymmetrically during HSC divisions. In addition, it was analyzed if the overexpression of candidates in HSC causes a change in fate choice and self renewal capacity.

## 4. Goals of the Thesis

Asymmetric cell division has been shown to be a mechanism of cell specification in invertebrate as well as few mammalian cell types. For the hematopoietic stem cell (HSC) this mechanism has been long postulated, but could not be proven so far.

The aim of my thesis is to employ time lapse imaging and single cell analysis to clarify if HSC undergo asymmetric cell division. First it has to be established if HSC produce asymmetric fates and whether they are controlled intrinsically by the HSC or extrinsically by the environment. Therefore, HSC behaviour on different environments needs to be compared. In addition, it is important to compare obtained data about marker expression as well as divisional kinetics and number of apoptotic events from HSC to closely related cells that have lost reconstitution potential, MPP, to be able to identify HSC specific characteristics. To identify asymmetric fates in daughter cells, a marker identifying either HSC or loss of HSC potential needs to be identified. With this marker, asymmetric fates of HSC and MPP daughters cultivated on different environments need to be quantified and compared to draw conclusions about the existence, the specificity to HSC, and the intrinsic or extrinsic control of asymmetric fates.

Furthermore, the mechanism controlling asymmetric cell division needs to be explored. Several candidate genes have to be evaluated for their role in fate specification of HSC. First, lentiviral infection of HSC with viral vectors containing candidate genes has to be optimized to yield a high infection efficiency of HSC. Second, it has to be examined if candidate genes are segregated asymmetrically into HSC daughter cells when overexpressed as a reporter gene fusion. And third, it has to be established if candidate overexpression in HSC influences fate decisions in vitro and in vivo.



## 5. Results

### 5.1. Asymmetric Fates of HSC Daughters

#### 5.1.1. Experimental Setup for Analysis of Asymmetric Fates

In order to determine if HSC undergo ACD, it was first analyzed if HSC produce asymmetric fates. This requires following individual cells during the course of their proliferation and differentiation and quantifying their daughter cell fates. Fates of HSC and their progeny were observed on PA6 stroma as well as in stroma free suspension culture by time lapse microscopy. To elucidate HSC specific behavior, we compared them to closely related cells, MPP, which share the multi-lineage potency of HSC but have lost their long term self renewal potential. This enables us to identify behavior that is specifically connected to self renewal of HSC.

To this end we isolated the bone marrow of 12 week old male C57Bl6/6J mice by crushing femur and tibia to dislodge bone marrow cells from the bone. Cells were stained with antibodies for the isolation of HSC populations. HSC and MPP were isolated by using CD48<sup>-</sup>CD34<sup>-</sup>Flt3<sup>-</sup>KSL and CD34<sup>+</sup>Flt3<sup>-</sup>KSL marker combinations respectively (Figure 5.1). In detail, cells with small size and low granularity containing immature cells were gated in the FSC/SSC plot. These cells were further purified by their lack of lineage marker expression and high expression of Sca-1 and c-kit. From this KSL population we then took on the one hand the CD34<sup>+</sup>Flt3<sup>-</sup> cells constituting the MPP population (Yang, Bryder et al. 2005) and on the other hand the CD48<sup>-</sup>CD34<sup>-</sup>Flt3<sup>-</sup> cells as the HSC population (Osawa, Hanada et al. 1996; Noda, Horiguchi et al. 2008). To validate the accuracy of our sorting gates for HSC and MPP we showed that 500 sorted HSC are sufficient to reconstitute W<sup>41</sup>/W<sup>41</sup> Gpi1a Ly5.1 mice for 16 weeks but not MPP (experiment performed by Angelika Roth, data not shown). In addition, we verified in colony assays that our freshly sorted HSC as well as MPP contained a high number of multipotent cells (data not shown). After sorting, cells were immediately plated either onto confluent layers of PA6 stromal cells or in stroma free suspension culture. As depicted in Figure 5.1, we then observed co-

cultured cells in time lapse movies for up to seven days, taking images in two minute intervals.

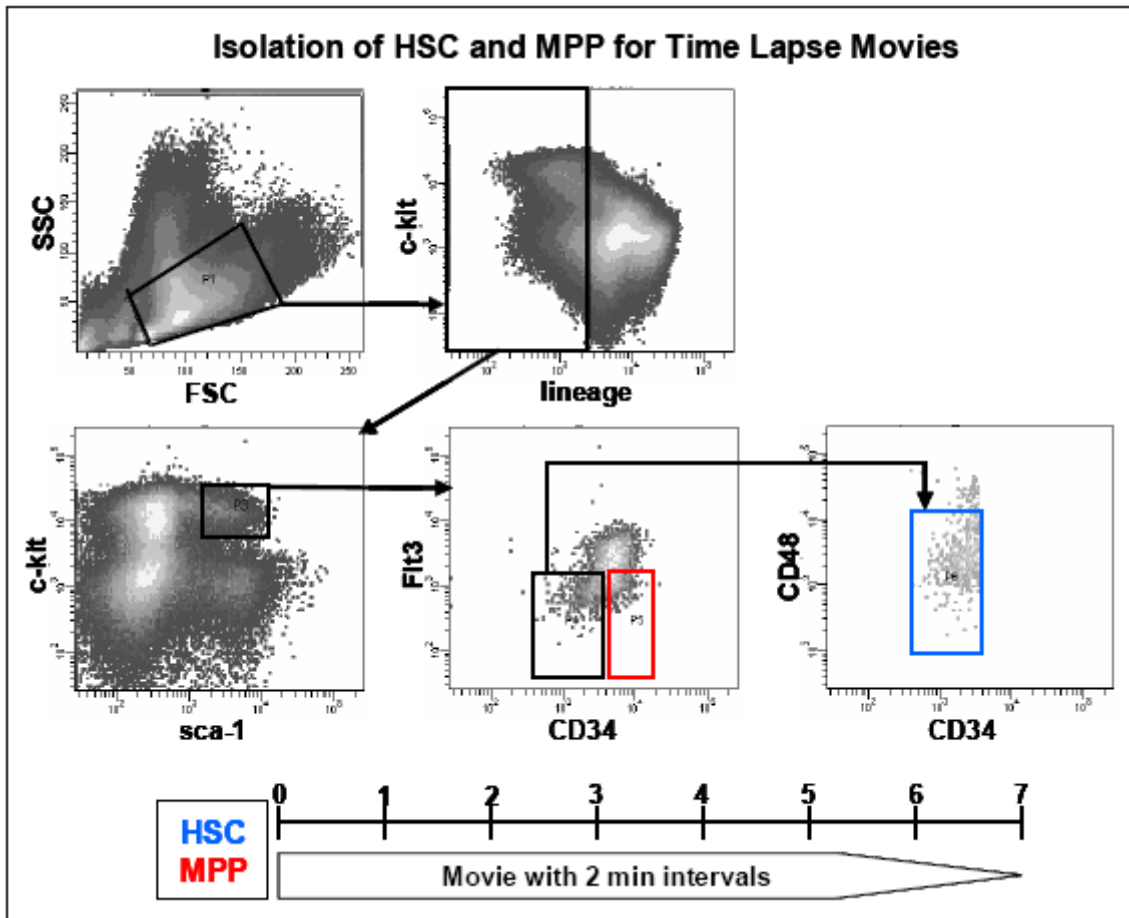


**Figure 5.1: Sorting scheme and imaging setup for time lapse movies recording HSC and MPP asymmetric fate.** For the HSC population  $CD34^+Flt3^-CD48^-c-kit^+sca-1^+lineage^-$  (KSL) cells were sorted. For the MPP population  $CD34^+Flt3^-KSL$  cells were sorted. Cells are imaged in time lapse movies with 2 minute intervals for up to 7 days.

### 5.1.2. Divisional Kinetics of HSC and MPP

We chose PA6 stroma as a niche for HSC and MPP, since PA6 provide an environment that allows self renewal of HSC. PA6 support HSC potential for at least 2 weeks with 14% reconstitution potential left at this time (Szilvassy, Weller et al. 1996). Our own data showed that HSC that were cultured for 4 days on PA6 still are able to contribute to the peripheral blood of recipient mice after 17 weeks, supporting the maintenance of HSC potential by PA6 stroma (Figure 13F). We conducted time lapse movies of HSC and MPP that were cultured on PA6 and analyzed them by tracking individual cells and recording their behavior in pedigrees. Supplemental Movie 5.1B shows an individual HSC that migrates underneath the PA6

---

stromal cells and divides to give rise to several generations of progeny. Supplemental Movie 5.1A shows in detail the second division of the HSC progeny. In Figure 5.2A this proliferation is depicted as a pedigree, displaying time of division, lifetime of the cells and hierarchical relationships graphically. The state of adherence of a cell over time (see also figure legend) is indicated by the color of the lines connecting one generation with the next. Cells migrating underneath stroma are called adherent whereas cells migrating above the stroma are in suspension. Initially we evaluated the first three divisions of individual HSC and MPP to determine if they differ in their divisional behavior. Figure 5.2B, C, and D show progeny after the first, second, and third division respectively that are migrating underneath the stroma.

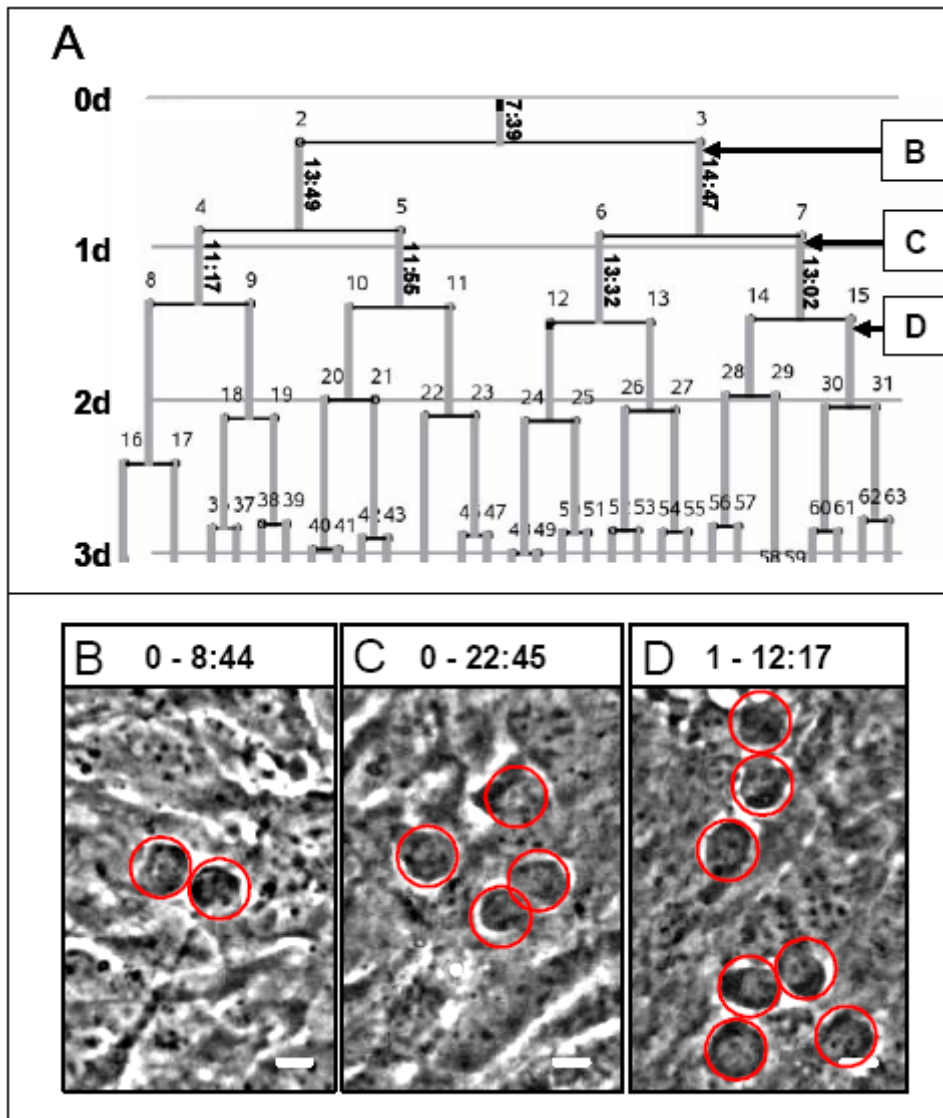


**Figure 5.2: Proliferation of HSC on PA6 stroma.** Pedigree shows the proliferation of a single HSC over the course of 3d. Arrows mark corresponding frames. Numbers next to cells 1 through 7 indicate generation time length (A). Panels show corresponding frames from movie1. Red circles show position of cells (B, C, and D). HSC daughter cells are shown shortly after their first (B), second (C), and third division (D). Scale bar: 10 $\mu$ m, time scale: days – hours:minutes

This data, together with data of the first 3 divisions from 120 HSC and 97 MPP trees from 4 separate movies is summarized in Figure 5.3A. Here the percentage of trees that have undergone their first, second and third division, respectively, is depicted for HSC and MPP over time. It is shown that after isolation, MPP go into cycle earlier than HSC. Also for the subsequent two divisions HSC on average have a

significantly longer generation time than MPP. This is depicted in Figure 5.3B, which shows the time point when 50% of cells have divided in HSC and MPP populations.

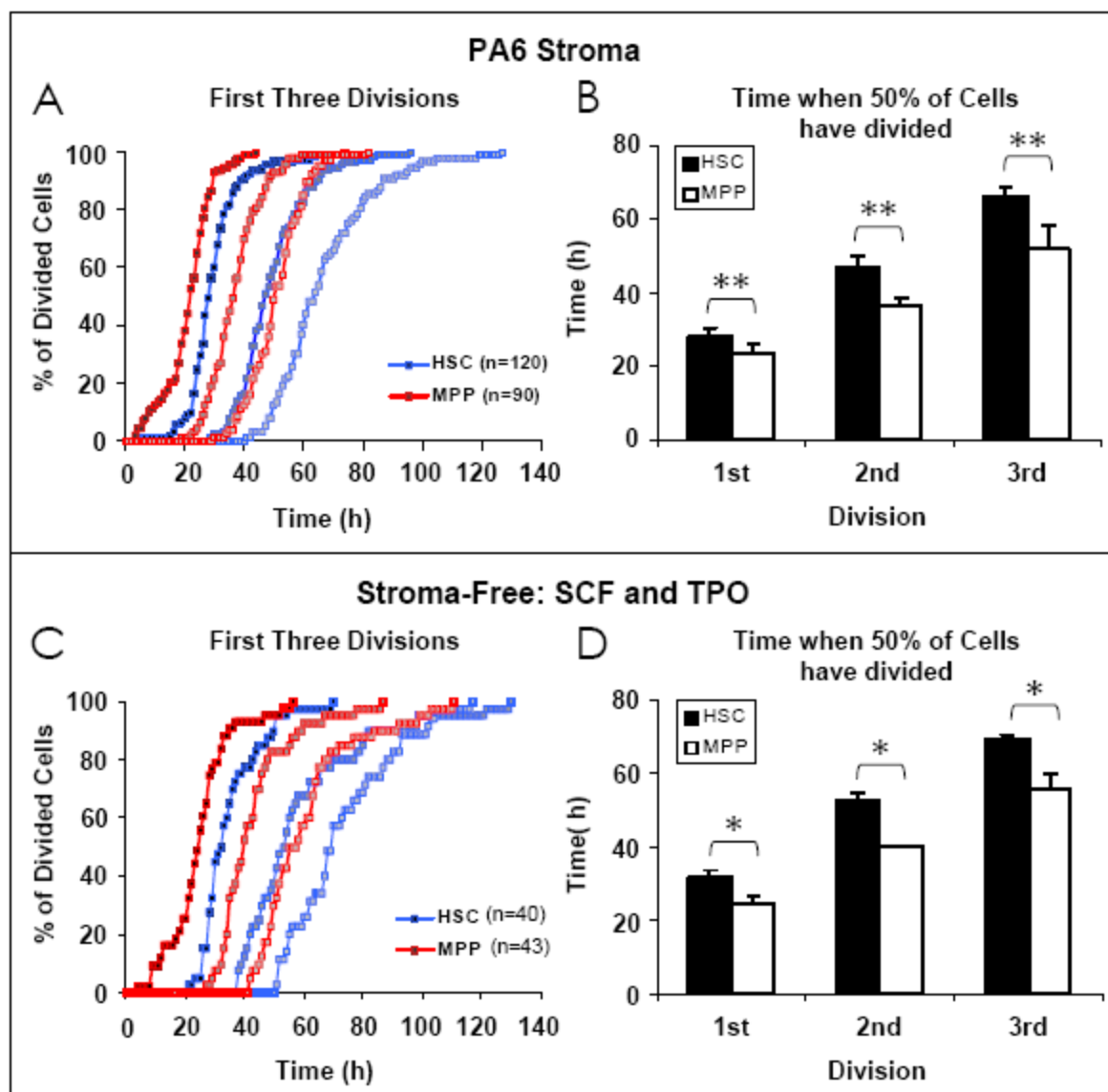


**Figure 5.2: Proliferation of HSC on PA6 stroma.** Pedigree shows the proliferation of a single HSC over the course of 3d. Arrows mark corresponding frames. Numbers next to cells 1 through 7 indicate generation time length (A). Panels show corresponding frames from movie1. Red circles show position of cells (B, C, and D). HSC daughter cells are shown shortly after their first (B), second (C), and third division (D). Scale bar: 10 $\mu$ m, time scale: days – hours:minutes

We asked if this difference in divisional kinetics was dependent on the PA6 environment itself or unknown effectors in the serum-containing media, or if the observed delay in cell cycle entry and longer generation time was an intrinsic property of HSC. Therefore, we also conducted experiments in stroma free and

serum free suspension culture, adding cytokines that allow for HSC self renewal. The addition of SCF and TPO allows maintenance of HSC for at least six days with 66% of initial HSC number left at this time (Ema, Takano et al. 2000). When comparing HSC and MPP divisional behavior in these self renewal conditions we found that the behavior of these two populations was similar as on PA6 and when containing serum. Initial cycle entry and subsequent generation times were significantly later and longer for HSC than for MPP (Figure 5.3C and D). To assess whether this behavior was specific to HSC self-renewing conditions we also analyzed cell behavior in differentiating conditions. We cultured HSC in SCF and IL3, which reduce self renewing capacity to 26.5 % after 3d compared to 66.7 % after 3d and 25.5 % after 6d in SCF, or in TPO and SCF and IL6 which do not maintain any self renewal capacity for three days (Ema, Takano et al. 2000). In both differentiation conditions we found similar kinetics of HSC divisional kinetics within their first three generations as in self renewal conditions (Figure 5.4A, B, and C). This indicates that later entry into cycle and longer generation time is an intrinsic property of HSC that is independent of culture conditions and that is lost in closely related cells such as MPP.

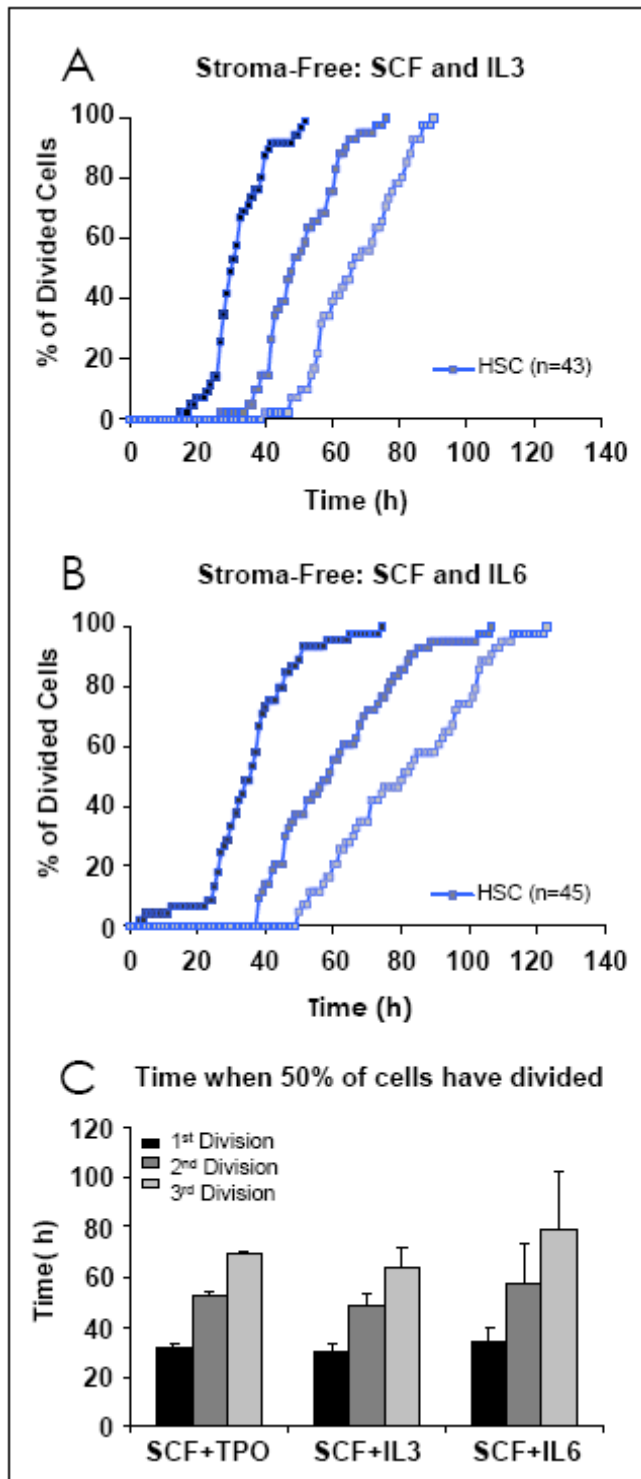


**Figure 5.4: Cell cycle entry and generation time length does not differ significantly between HSC cultured in stroma free self renewal and differentiation conditions.** First three divisions of HSC are shown as a percentage of divided cells over time in stroma free culture containing SCF and IL3. The data shown is the average of 2 independent experiments with a total of 43 pedigrees analyzed (**A**). First three divisions of HSC are shown as a percentage of divided cells over time in stroma free culture containing SCF and IL6. Data is the average of 2 independent experiments with a total of 45 HSC pedigrees analyzed (**B**). Time it takes for 50% of HSC to divide in stroma free culture containing differentiation cytokines. Data summarizes data from A and B as well as Figure 5.3D (**C**). Error bars show standard deviation.

### **5.1.3. Searching for Markers of Intrinsic Control of HSC Asymmetric Daughter Cell Fates**

#### **5.1.3.1. Quantification of Daughter Generation Time Reveals Environmentally Controlled Asymmetric Fates**

We were interested in asymmetric fates of HSC daughters and therefore, we had to find a marker that allowed us to read out asymmetric fate decisions of HSC. As we had already found a difference in cell cycle entry and divisional kinetics between HSC and MPP, we wondered whether we can use the generation time of HSC and MPP daughter cells to indicate asymmetric fates. Previous studies examining the daughter cell fates of human hematopoietic progenitors have used asymmetric generation time as an indicator for asymmetric fate potential as well (Brummendorf, Dragowska et al. 1998; Punzel, Zhang et al. 2002; Punzel, Liu et al. 2003). Therefore, we looked for differences of sister cell generation time (GT) lengths. This difference was calculated as the percentage difference between the longer lifetime and the shorter lifetime of sister cells in generation 1 (direct progeny from colony initiating cell) divided by the longer lifetime. An example of a pedigree with asymmetric GT in the HSC daughter cells is depicted in Figure 5.5A. This pedigree and corresponding Supplemental Movie 5.2 show a difference of 64% in the GT of daughter cells. It is shown that while cell 2 divides at 2d 3min 19sec after the start of the movie (Figure 5.5C), cell 3 almost takes another 2d until it divides at 4d 59sec after the movie had started (Figure 5.5D). Shortly thereafter, at 4 d 1 h 36 min, the daughter of cell 2, cell 5 divides again and produces granddaughter cells to cell 2. In summary, this pedigree shows asymmetric GT of the immediate daughter cells of the starting cell.

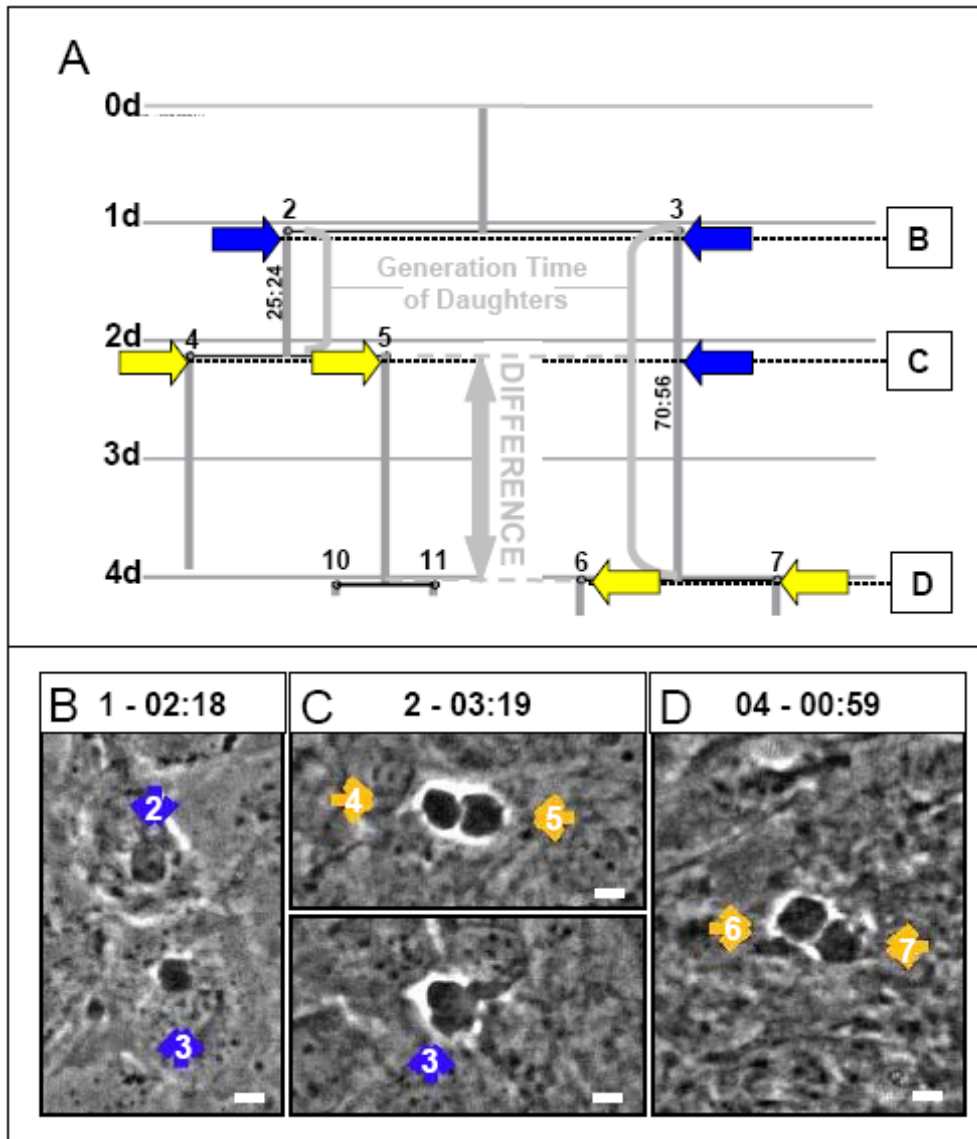


**Figure 5.5: Pedigree with asymmetric generation time of daughter cells.** Pedigree originates from an HSC that produces daughters with a different length of generation time (more than 20% difference). Arrows indicate corresponding cells in frames B, C, and D (A). Frames (B, C, D, and E) correspond to Movie 2. Cells after first division (B). Cells 4 and 5 shortly after second division while cell 3 has not divided yet (C). Two days later cell 3 has divided and produced cells 6 and 7 (D). Time scale: days – hours:minutes

We then quantified the number of trees with asymmetric GT that started from HSC and MPP and were cultured on PA6 stroma. We found that most of the analyzed trees showed a difference of generation time up to 30%. Therefore, we compared the number of trees from HSC and MPP with a generation time difference of at least 10%, 20% and 30% to evaluate which percentage of generation time difference of daughter cells indicated HSC specific behavior. We found that 58.3% ( $\pm 21.0$ ) of a

total of 125 analyzed HSC trees but only 21.1% ( $\pm 10.6$ ,  $p=0.04$ ) of a total of 87 MPP trees showed more than 10% generation time difference of daughter cells (Figure 5.6A). When 20% difference in generation time was used as a criteria of asymmetry, 21.4% ( $\pm 6.8$ ) of HSC and only 4.4% ( $\pm 5.9$ ) of MPP trees were asymmetric regarding their daughter cell generation time ( $p=0.001$ ), and a 30% difference in daughter generation time resulted in 11.6% ( $\pm 12.9$ ) and 2.3% ( $\pm 4.1$ ) of asymmetric HSC and MPP trees respectively ( $p=0.17$ ). These results show that significantly more HSC than MPP produce daughters with asymmetric generation time length suggesting that asymmetric daughter cell generation times are predetermined specifically in HSC.

To assess whether this asymmetric behavior was intrinsically controlled, we analyzed pedigrees of HSC and MPP that were cultured in stroma free HSC maintenance conditions containing SCF and TPO. However, we found that only 2.8% ( $\pm 3.9$ ) of 33 HSC showed asymmetric daughter cells GT, while 5.9% ( $\pm 8.3$ ) of 37 MPP were asymmetric regarding their daughter generation time, when quantifying trees with at least 20% GT length difference ( $p=0.7$ , Figure 5.6B). Also the number of trees with a difference of 10% or 30% in daughter cell GT length did not differ significantly between HSC and MPP (data not shown). This indicates that HSC, when cultured in stroma free self renewal conditions, do not produce daughters with asymmetric GT. Also, when we analyzed pedigrees of HSC cultured in differentiation conditions, we found a much lower number of asymmetric daughter generation times than when cultured on PA6. Only 2.5% ( $\pm 3.5$ ) of HSC cultured in SCF and IL3 ( $n=43$ ) and 9% ( $\pm 5.7$ ) of HSC cultured on SCF and IL6 produced daughters that differed in their generation time by at least 20% (Figure 5.6B). These results show that environment, such as PA6 stroma, can induce HSC to produce daughters with asymmetric GT. This induction can only be found for HSC, but not for MPP. However, the results also indicate that while cell cycle entry and average GT length of HSC daughters is intrinsically controlled, this does not hold true for asymmetric HSC daughter GT.

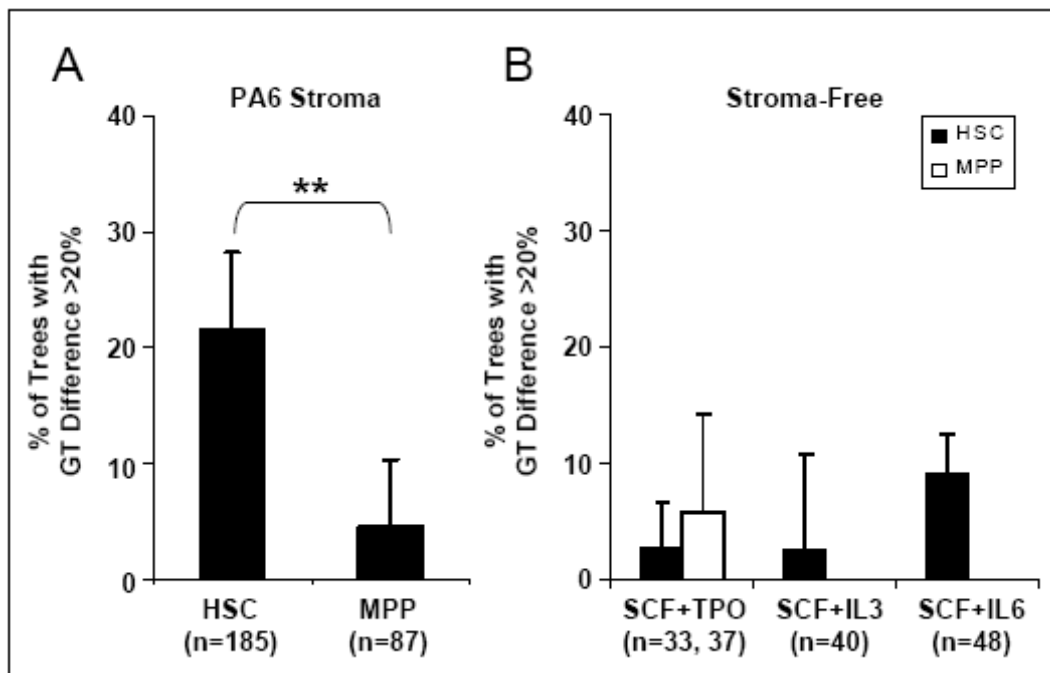


**Figure 5.6: PA6 dependent HSC specific asymmetric generation time of daughter cells.** Percentage of HSC and MPP that produce daughters with a difference in generation time of at least 20% when cultured on PA6 stroma. Data is the average of 5 independent experiments with a total of 185 HSC and 87 MPP pedigrees analyzed (A). Percentage of HSC and MPP that produce daughters with a difference in generation time of at least 20% when cultured in stroma free culture containing self renewing and differentiation cytokines. Data is the average of 2 independent experiments for each condition with 33 HSC and 37 MPP pedigrees analyzed for stroma free conditions containing SCF and TPO, and 40 and 48 HSC pedigrees analyzed for stroma free conditions containing SCF and IL3, and SCF and IL6, respectively (B). Error bars show standard deviation, \*\* =  $p < 0.01$

### 5.1.3.2. Quantification of Apoptotic Cells Reveals no Conclusion about Asymmetric Fates

Since we could only observe asymmetric GT of HSC daughters on PA6 stroma, but not in stromal free cultures also allowing HSC self renewal, asymmetric GT cannot serve as readout of asymmetric HSC self renewal. Therefore, we decided to look for other indicators of such decisions. It is known that apoptosis occurs in cultured cells. However, only snapshots of endpoint stainings have been evaluated for apoptotic cells so far. From these snapshots it cannot be assessed how many cells have died during the culture period and from which starting cell apoptotic cells have originated. By continuous observation and single cell tracking we can identify every apoptosis, know when it occurred, and know how the apoptotic cell is related

to the starting cell. Apoptosis on one hand indicates how well cultures are maintained and if cells for example were damaged during isolation. On the other hand, apoptosis can serve as a measure of fate decision. If cells have differentiated into a cell fate that requires certain survival signals and these signals are not provided by the environment, the cell will undergo apoptosis. In this respect, discrete apoptotic events can serve as an indicator of differentiation and lineage commitment. However, it is difficult to distinguish between these two possibilities as a mixture of both is likely to occur.

We quantified the number of apoptotic events in cells cultured on PA6 and in stroma free suspension culture. When cells were cultured on PA6, we found that 15.3% ( $\pm 8.2$ ) and 21.6% ( $\pm 9.4$ ) of HSC and MPP starting cells respectively had died before they could divide (Figure 5.7A). We found a similar number of apoptotic cells when HSC and MPP were cultured in stroma free culture. Of all analyzed starting cells we found 25.8% ( $\pm 3.9$ ), 28.8% ( $\pm 5.2$ ) and 19.6% ( $\pm 7.6$ ) of HSC cultured in SCF and TPO, SCF and IL3, and SCF and IL6 respectively to undergo apoptosis. For MPP cultured in conditions with SCF and TPO however this number was slightly smaller as we found only 6.6% ( $\pm 3.5$ ) of cells to die before their first division ( $p=0.02$ , Figure 5.7B). These initial apoptosis are likely due to stress caused by the isolation procedure. Overall, the number of apoptosis of HSC and MPP in suspension conditions decreased as the generation number increased for all the conditions used. In contrast, the percentage of apoptotic events for HSC and MPP cultured on PA6 remained the same or slightly increased. This seems to indicate that when cultured on PA6, a constant proportion of HSC and MPP are differentiating towards a lineage that is not supported by PA6. For example, PA6 do not support the formation of lymphoid cells without the addition of lymphoid cytokines. Therefore, it is possible that the observed apoptoses indicate differentiation of cells into the lymphoid lineage. To test this hypothesis we added cytokines necessary for lymphoid differentiation on PA6 (Flt3L and IL7) and asked if this would decrease the number of observed apoptosis. However, we could not observe any change in frequency or time of apoptotic events (data not shown) and therefore concluded that the observed apoptosis are not due to non supported lymphoid differentiation. Since PA6 cultures contain many different uncharacterized cell types and the utilized serum contains many unknown factors, a variety of explanations could account for the observed

apoptotic events. Moreover, as we did not observe similar kinetics for apoptosis of cells cultured with and without stroma, we decided that there might be a number of mechanisms contributing to the observed apoptotic events and that it was too difficult to attribute any to asymmetric fate decisions. Therefore, we could not utilize apoptotic events as an indicator of asymmetric fate decisions.

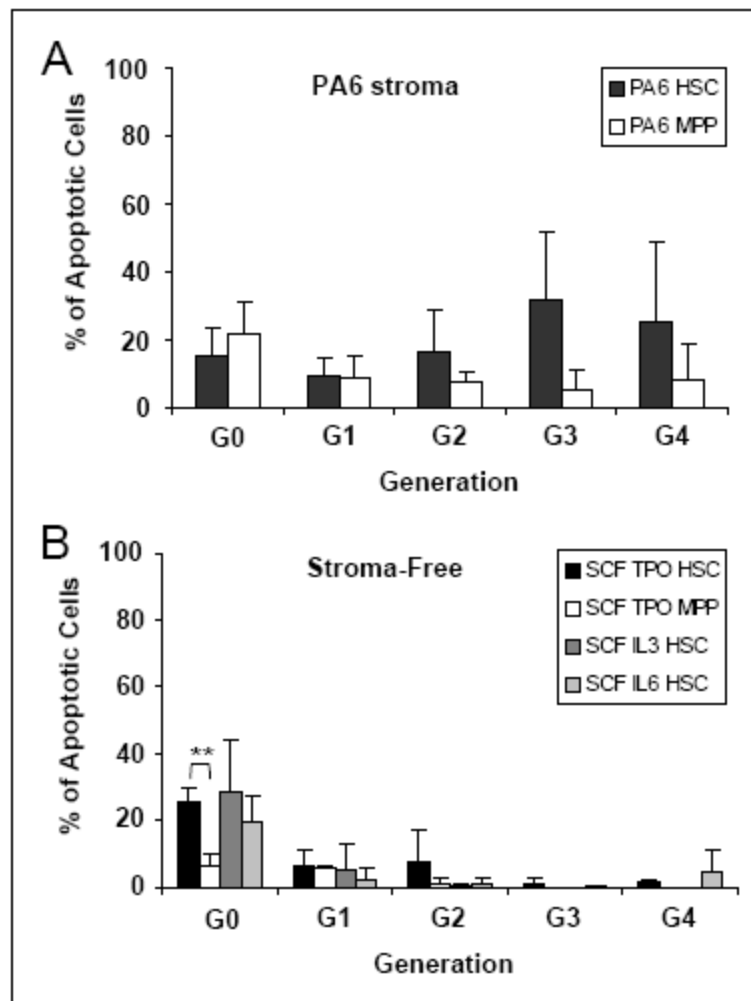


**Figure 5.7: Percentage of apoptotic cells in pedigrees of HSC and MPP.** Percentage of apoptotic cells per generation of all cells contained in that generation. Data of HSC and MPP cultured on PA6 is the average of 3 independent experiments with 69 HSC and 61 MPP trees analyzed (**A**). Data of HSC and MPP cultured in stroma free suspension culture is the average of 2 independent experiments for each condition. For data of cells cultured in SCF and TPO, 54 HSC and 46 MPP pedigrees were analyzed. For data of cells cultured in SCF and IL3, and SCF and IL6, 61 and 52 pedigrees were analyzed respectively (**B**). Error bars show standard deviation, \*\* =  $p < 0.01$

### **5.1.3.3. Quantification of Megakaryocyte Fates Reveals no Conclusion about Asymmetric Fates**

Since general characteristics of cells such as generation time and apoptosis were not useful as indicators of intrinsically controlled fate decisions, we wanted to quantify cell behavior indicating commitment towards a certain lineage and loss of HSC potential. When analyzing fates of HSC, it is necessary to identify lineage decisions using markers that indicate lineage commitment. However, most progenitors that have committed to a lineage do not upregulate markers of that lineage until a certain maturation stage is reached. Starting with an HSC, this can take several days or weeks in culture (personal communication with Dr. Michael Rieger). This makes identification of cell fates in short movies where cells are followed over few generations difficult. Running movies for several weeks is technically possible, but the more generations of a colony have to be tracked, the higher the chance of losing individual cells of the pedigree due to high cell density. We found however, that megakaryocytes can be easily identified by their size in time lapse movies and arise from HSC or MPP within days. These cells belong to the myeloid lineage and are the precursors of platelets which are necessary for blood clotting. Megakaryocytes undergo endomitoses, which involve DNA replication and nuclear segmentation without division of the nucleus and the cytoplasm. This process can be visualized as shown in Supplemental Movie 5.3 and in the pedigree in Figure 5.8A, where cells generated by an MPP develop into mature megakaryocytes. The movie shows cell 7 depicted in the pedigree and still images of Figure 5.8 dividing into two cells with normal size (Figure 5.8C). These cells then slowly increase in size by performing several rounds of endomitosis and are then identified as megakaryocytes (Figure 5.8D and E).

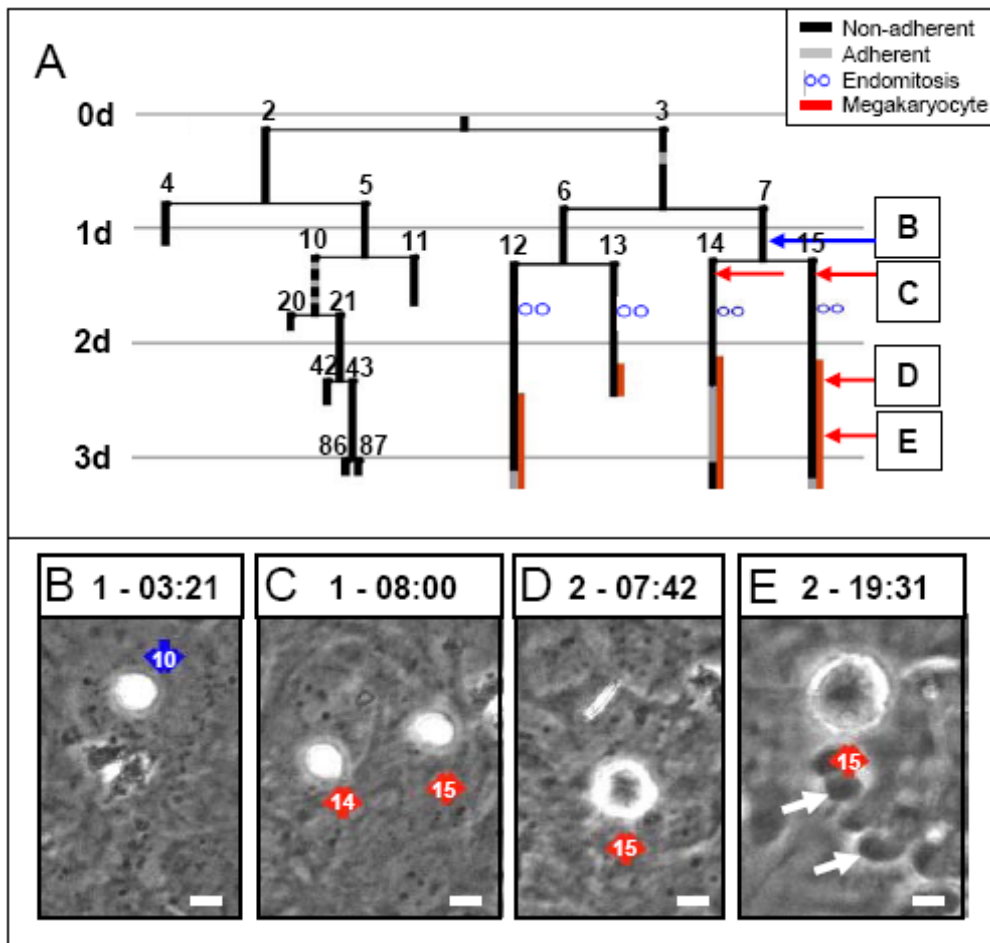


**Figure 5.8: Pedigree of a colony generating megakaryocytes.** Pedigree of an MPP differentiating into megakaryocytes and other cells. Some of the progeny cells of cell two were lost when they left the field of view. Arrows indicate corresponding movie panels (A). Frames corresponding to Movie 3. Cell 7 is marked by a blue arrow and is above the stroma and has not increased in size yet (B). Cell 14 and 15 are marked by red arrows. They will mature into megakaryocytes, but still are small in size (C). Cell 15 is marked by a red arrow and enlarged and now identified as a mature megakaryocyte (D). Cell 15 is marked by a red arrow and even larger and surrounded by progenitor cells that are from a different colony and underneath the stroma (E). Scale bars are 10 $\mu$ m, time scale: days – hours:minutes

We quantified the number of pedigrees producing megakaryocytes from HSC and MPP when cultured on PA6 (Figure 5.9A). We found similar numbers of pedigrees producing megakaryocytes from HSC (9.9%  $\pm$  7.2, n=159) and MPP (6.1%  $\pm$  5.8, p=0.38, n=128). In contrast, in stroma free cultures, hardly any cells developed into megakaryocytes in the tracked time. We did not find any trees containing megakaryocytes in SCF and TPO (n=40) and SCF and IL3 (n=43) conditions and only 3 trees containing megakaryocytes in stroma free conditions with

SCF and IL6 (n=45; data not shown). It appears that the first two cytokine conditions do not support either commitment to megakaryocyte fate or are not sufficient for maturation of megakaryocytes to stages that can be identified in time lapse microscopy.

We then analyzed the trees for asymmetries in megakaryocyte production. Trees where not all branches of the tree produce megakaryocytes at the same time could be indicators of lineage choice between self renewal and differentiation during division. An example is given in Figure 5.8A, where one of the daughters (cell 3) of the seeded MPP is committed to the megakaryocyte lineage since all its progeny produce megakaryocytes. At least one progeny of the other daughter (cell 2) however does not produce megakaryocytes within the same generation but continues to divide. The other progeny of cell 2 were lost in the tracking process and therefore, their fate cannot be determined.

We found that the number of asymmetric megakaryocyte trees was small and varied a lot between movies and so we could not see a difference in the frequency of asymmetric megakaryocyte trees between HSC and MPP (Figure 5.9B,  $59.5\% \pm 4.7$  and  $62.5\% \pm 41.5$  respectively). Since the percentage of pedigrees containing megakaryocytes as well as asymmetric onset of megakaryocytes was similar in pedigrees starting with HSC and MPP, we conclude that a population of cells that has already lost its HSC potential and that is present within both the sorted HSC and MPP population gives rise to megakaryocyte trees. Therefore, megakaryocytes cannot serve as an indicator of self renewal versus differentiation decisions in HSC.

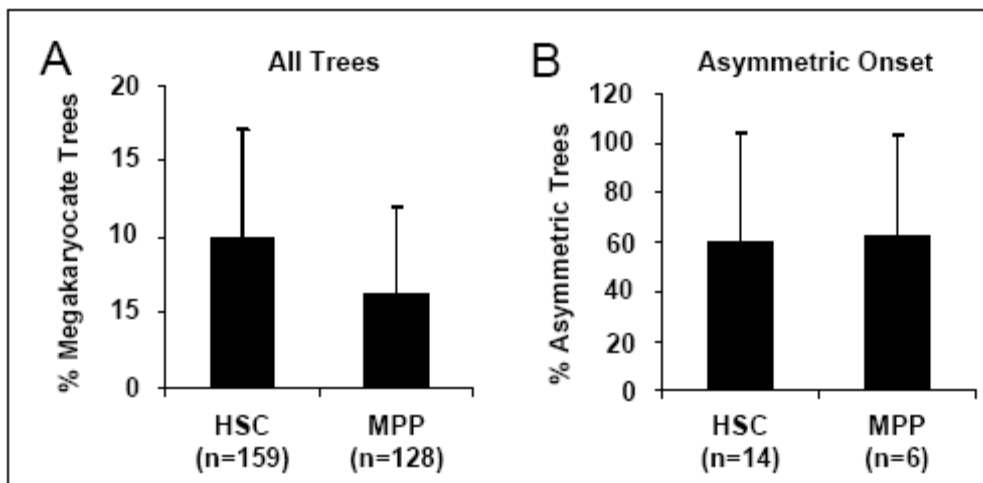


**Figure 5.9: Type and number of megakaryocyte containing pedigrees does not differ between HSC and MPP.** Percentage of megakaryocyte trees of all pedigrees derived from HSC and MPP cultured on PA6 stroma. Data is the average of 7 independent experiments with 159 HSC and 128 MPP analyzed trees (A). Number of trees with asymmetric onset of megakaryocytes as a percentage of all megakaryocyte containing trees derived from HSC and MPP cultured on PA6. Data shows the average of 7 independent experiments with 14 HSC and 6 MPP analyzed trees (B). Error bars show standard deviation.

#### 5.1.4. Evaluation of HSC Daughter Fates by 'Loss of Stemness Marker' CD48

Megakaryocyte differentiation did not prove to be a useful marker for asymmetric cell fate decisions, and therefore, a different marker indicating either true HSC themselves or marking cells that have lost their self renewal potential was needed. As mentioned in the introduction, markers reliably identifying cultured HSC are not available. Also, HSC that differentiate into progenitor cells and lose their self renewal capacity do not undergo morphological changes that can be visualized by phase contrast images. We therefore, needed a molecular marker that is expressed as soon as HSC have lost their repopulation capacity.

Recently, the SLAM markers CD150 and CD48 have been introduced for improved HSC sorting purities (Kiel, Yilmaz et al. 2005). Freshly sorted HSC, are positive for CD150 but negative for CD48. In addition, it was recently shown that HSC also stay negative for CD48 during *in vitro* culture. When reconstituting mice with cells from cultured HSC, only cells lacking CD48 expression were still able to reconstitute a lethally irradiated recipient, while large numbers of CD48<sup>+</sup> cells did not contain any cells with HSC potential (Noda, Horiguchi et al. 2008). Therefore, we

chose to employ CD48 in our time lapse movies to identify cells that have lost reconstitution potential.

It is possible to fix cultures after a movie is recorded, stain these fixed cultures with a labeled antibody and then deduct from this endpoint staining and the tracked pedigree which of the cells in the tree have switched on CD48. However, much more information can be drawn from a live staining where onset of CD48 expression can be visualized in real time. Therefore, we directly added a fluorochrome labeled antibody against CD48 in living cultures and observed its staining of cells by time lapse imaging. Eilken et al. have previously shown that this approach is applicable for several antibodies. Live staining however does not work with every antibody, which could be isotype or species specific. We chose Alexa647 as a direct label for CD48 antibody as this fluorochrome is detectable both in FACS as well as with our microscope filters (Figure 5.10) and can be spectrally combined with other typically used fluorochromes emitting green and red light.

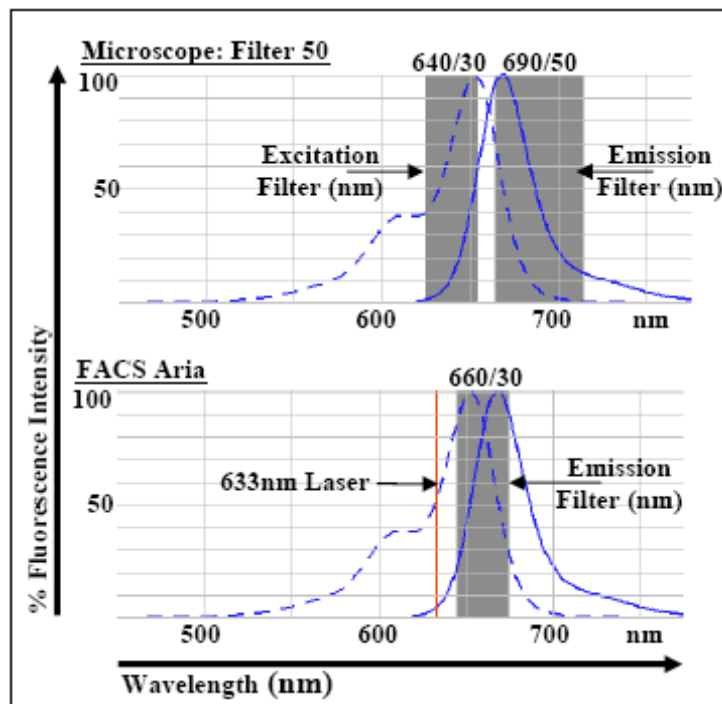


**Figure 5.10: Spectral properties of Alexa647 fluorochrome.** Alexa647 can be detected with Zeiss microscope filter 50 as well as with the FACS Aria using the 633nm laser and 660/30 emission filter.

#### 5.1.4.1. Establishing CD48 as a Live Marker of Loss of Stemness

##### 5.1.4.1.1. CD48 Antibody Titration in FACS and Expression in Freshly Isolated Cells

To evaluate the amount of self labeled antibody needed in a FACS stain, we utilized  $10^6$  lineage<sup>+</sup> cells per antibody concentration and stained them with 0.2, 0.5, 1 and 2  $\mu$ g of concentrated CD48 Alexa647 antibody in 50 $\mu$ l total staining volume (open squares Figure 5.11A). We compared this self labeled antibody with commercially available antibodies labeled with APC and with FITC. Cells stained with 0.2  $\mu$ g CD48 Alexa647 showed higher mean percentage of positive cells (46.9%) compared to cells stained with the same amount of FITC antibody (33.1%) and APC antibody (28.3%). An increase of CD48 Alexa647 concentration in the FACS staining solution did not yield a noticeable increase in positive cells. Therefore, we chose this concentration for all subsequent FACS stainings with CD48 Alexa647.

Using CD48 antibody as a real time marker in our movies, we wanted to determine what percentage of our sorted populations do express CD48 at the time of isolation. In CD34<sup>-</sup>Flt3<sup>-</sup>KSL cells we found 4% of CD48<sup>+</sup> cells. For all our analysis we have excluded this CD48<sup>+</sup> population by including CD48 in the sorting paradigm. For the Flt3<sup>-</sup>CD34<sup>+</sup>KSL MPP population we found 51% of cells to express CD48, whereas the Flt3<sup>+</sup>CD34<sup>+</sup>KSL population that identifies the MPP4 included 80% of cells with detectable CD48 expression (Figure 5.11B). These results are in accordance with published data and confirm that HSC do not express CD48, and that this marker is upregulated early during differentiation.

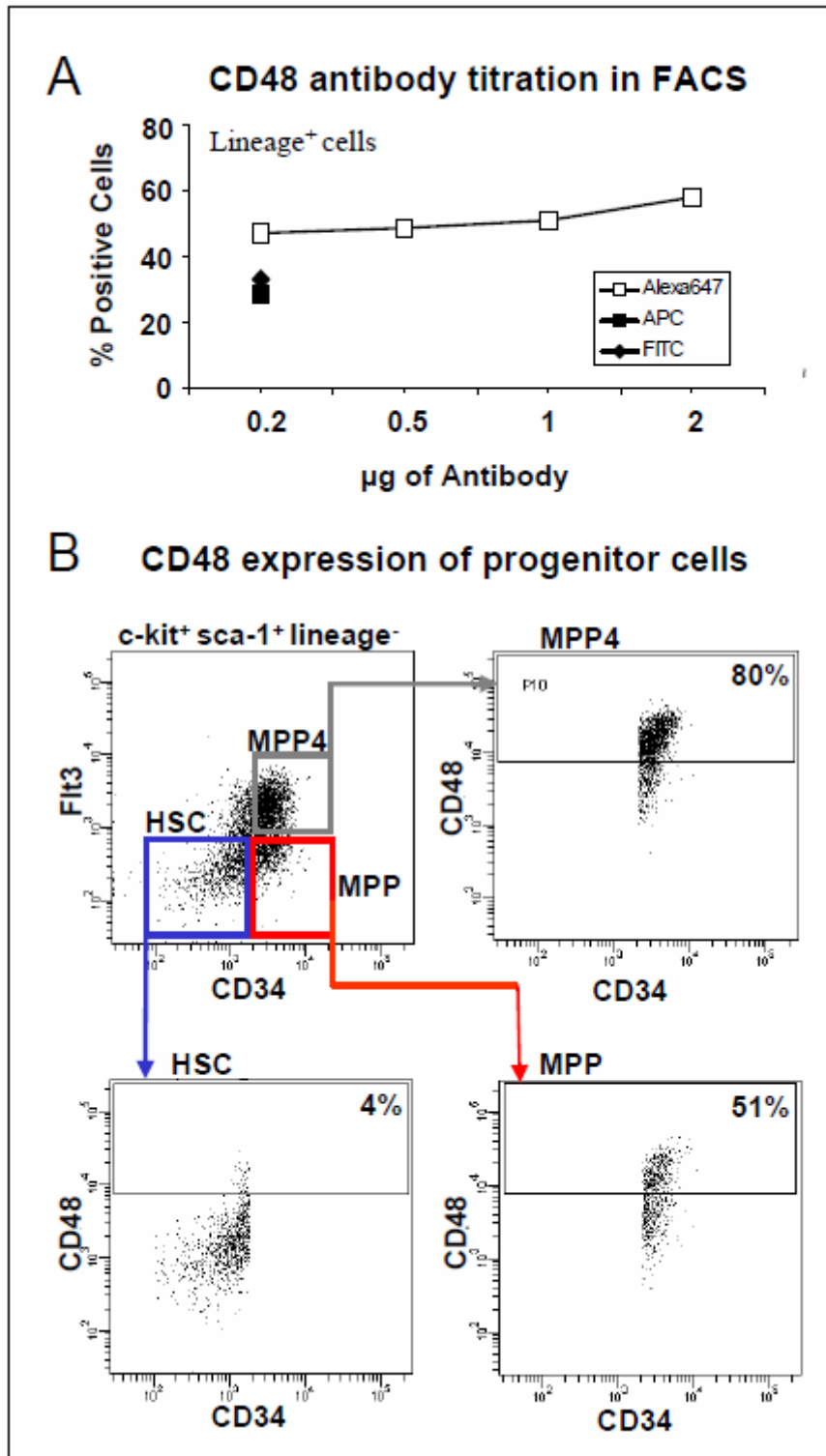


**Figure 5.11: FACS titration of Alexa647 labeled CD48 antibody and application in bone marrow staining.** Mean fluorescence of lineage<sup>+</sup> cells stained with CD48 antibody labeled with Alexa647, FITC and APC.  $10^6$  cells were labeled in 50 $\mu$ l staining solution (A). Percentage of CD48<sup>+</sup> cells in KSL populations stained with CD48 Alexa647 (B).

#### 5.1.4.1.2. CD48 Expression in Cultured Cells

To titrate our CD48 antibody in living cultures, we asked what concentration of antibody was sufficient to cover all CD48 epitopes on the cells and at what concentrations some of these epitopes would remain free for staining in a FACS stain with a differently conjugated antibody of the same clone. For this purpose we sorted KSL cells, which contain both HSC and MPP and cultured them with different concentrations of CD48 Alexa647 antibody for four days in stroma free culture in the presence of differentiation promoting cytokines (SCF, IL3, and IL6). We expected CD48 expression in at least some of the initial KSL cells, but in a larger proportion in the more differentiated cells that arise in culture after four days. After the four days of culture we washed the cells and stained them in a normal FACS stain with CD48 FITC antibody and analyzed them by FACS (Figure 5.12A). When using 2  $\mu\text{g/ml}$  and 1  $\mu\text{g/ml}$  concentrations of CD48 Alexa647 antibody in living cultures, all stained cells are only positive in the Alexa647 channel, but not the FITC channel when analyzed by FACS. However in these concentrations background fluorescence can be observed (not shown). No background fluorescence was visible when using antibody dilutions of 0.2  $\mu\text{g/ml}$  and 0.1  $\mu\text{g/ml}$ . When analyzing 0.2  $\mu\text{g/ml}$  dilution, 38 % of cells positive for CD48 Alexa647 were also positive for FACS staining with the FITC conjugated CD48 antibody (Figure 5.12B). This trend continued when a concentration of 0.1  $\mu\text{g/ml}$  of CD48 Alexa647 was utilized in culture staining. At this concentration, FACS staining with CD48 FITC rendered 75% of Alexa647 positive cells also positive for FITC signal. In none of these dilutions did the percentage of cells positive for in culture CD48 Alexa647 decrease, indicating that competitive binding of the two antibodies did not result in fewer cells being stained, but that only the percentage of epitopes per cell bound by in culture CD48 Alexa647 antibody was reduced. Indeed, the intensity of Alexa647 staining is slightly reduced with reduced amounts of CD48 Alexa647 antibody present in culture (Figure 5.12A). We decided to utilize 0.2  $\mu\text{g/ml}$  dilution of antibody in our cultures. Using this antibody dilution ensures that most of the epitopes recognized by CD48 antibody are covered in all cells expressing the antigen and additionally keeps background fluorescence to a minimum. The possibility of toxicity of antibody is also lower at lower concentrations.

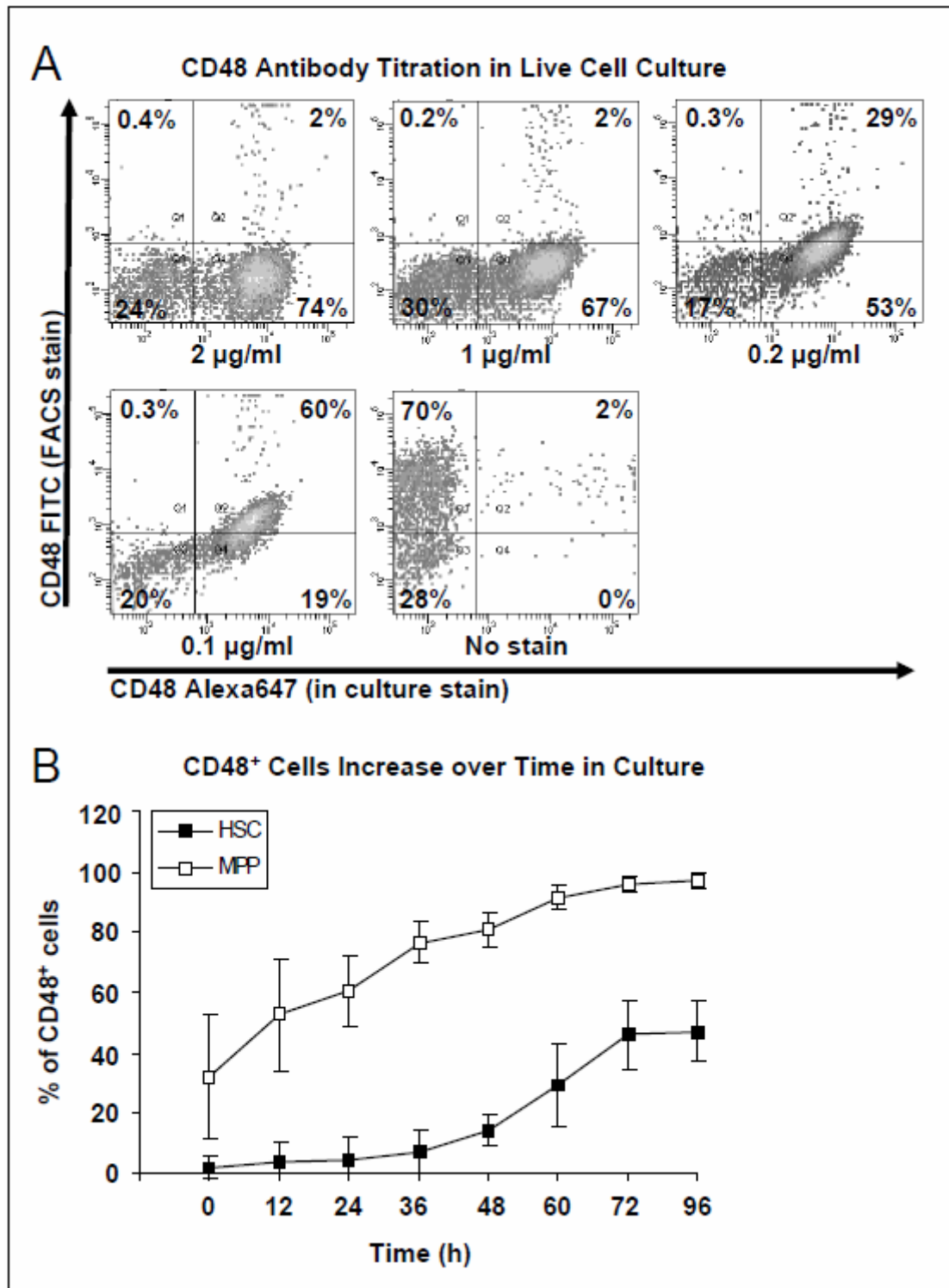


**Figure 5.12: In culture staining of progenitor cells with CD48 Alexa647.** CD48 Alexa647 titration in live cell culture. Decreasing concentrations of CD48 Alexa647 in culture staining compete for same epitopes on KSL cells with CD48 FITC FACS staining. CD48 Alexa647 in culture concentration shows final antibody concentration in culture medium. CD48 FITC is used in a FACS stain at 0.2µg/ml antibody in 50µl staining volume (A). Kinetics of CD48 expression onset in cells derived from MFP and HSC cultured on PA6 (B). Error bars show standard deviation

After showing that the self labeled CD48 antibody works in culture, we used it in movies as a live marker for loss of HSC potential of cultured cells. When we analyzed all trees starting from HSC and MPP cultured on PA6 and determined the percentage of cells that expressed CD48 over the course of the movie, we found that when analyzing HSC as a starting population, we observed less than 20% of all cells expressed CD48 by 60h from the start of the movie (Figure 5.12B). This percentage increased to 50% by 84h after movie start. In contrast, in cells arising from MPP, already 30% of cells were positive at 12h after movie start. The percentage of CD48<sup>+</sup> cells in trees with MPP as starting population increased over the next few days so that by 60h after movie start, 80% of cells were positive for CD48. This percentage increased to almost 100% by day 4. Therefore, the utilization of anti-CD48 in movies reveals increased differentiation of cells over time. As expected, in HSC, which remain in an undifferentiated state for longer, the percentage of CD48 expressing cells increases slower compared to MPP cells which show a sharp increase in the percentage of CD48<sup>+</sup> cells. MPP are already more differentiated from the start and reach CD48<sup>+</sup> maturation stages faster than HSC. It is established that MPP do not anymore possess long term reconstitution potential (Yang, Bryder et al. 2005). However, not all MPP are positive for CD48 when isolated. This indicates that anti-CD48 does not identify all cells immediately after losing their self renewal capacity, but at a slightly later stage. Nevertheless, the above data indicates that CD48 can be used as a marker to indicate asymmetric fate decisions. A difference in time of onset of CD48 expression between sibling cells can identify asymmetric fate decisions between self renewal and differentiation. In addition, CD48 expression started in many cells during the first four days, a time frame during which we can easily follow our cells by single cell tracking.

#### **5.1.4.1.3. Confirmation that CD48<sup>-</sup> but not CD48<sup>+</sup> Cells Possess Reconstitution Potential**

Our data concerning the difference in onset of CD48 expression in cultured HSC and MPP indicates that CD48 is a useful marker when analyzing loss of self

renewal potential in HSC. However, we wanted to confirm that CD48 expression in culture identifies cells that have lost their reconstitution potential. To analyze this, we sorted HSC (Figure 5.13A) and cultured them under the same conditions that we used for our PA6 co-culture movies. We cultured HSC for 90h, a time frame during which nearly 50% of the cells starting from HSC express CD48 (Figure 5.12B), but when CD48 has been expressed only for a short period of time in most positive cells. After culture on PA6 we purified hematopoietic cells according to their CD48 expression. Cells were also stained for CD45 to distinguish blood cells from PA6 cells (Figure 5.13B). In addition, we stained the cultured cells with KSL markers to assess their immaturity in relation to CD48 expression (Figure 5.13C, D and E). When analyzing CD45<sup>+</sup>CD48<sup>+</sup> cells for the presence of KSL markers, we found that of the CD48<sup>high</sup> cells only 7% were KSL cells after 90h (Figure 5.13E). In contrast, of the CD45<sup>+</sup>CD48<sup>-</sup> cells 61% were still KSL cells (Figure 5.13D). This indicated that CD48<sup>-</sup> cells contain a larger portion of immature cells than CD48<sup>+</sup> cells. We sorted CD48<sup>+</sup> and CD48<sup>-</sup> cells (Figure 5.13C) and transplanted them into recipient mice. For recipient mice we chose W<sup>41</sup>/W<sup>41</sup> Gpi1a Ly5.1 mice (kindly provided by Dr. Norman Iscove), that have a point mutation within the c-kit receptor. These mice contain a normal blood system and do have HSC however the mutation renders their HSC less competitive. Any congenic wild type HSC population that is transplanted into these mice can therefore expand in their bone marrow and slowly replace the host bone marrow without the need for irradiation of the recipients. W<sup>41</sup>/W<sup>41</sup> Gpi1a Ly5.1 mice are congenic to bl6 which were used for donor cells however donor type and recipient type cells can be distinguished by the expression of two different alleles of the pan hematopoietic marker CD45. Donor type cells from bl6 mice express CD45.2, whereas recipient type blood cells from the utilized W<sup>41</sup>/W<sup>41</sup> Gpi1a Ly5.1 mouse line express CD45.1. The presence of donor bone marrow cells is read out by analyzing the peripheral blood (PB) of the recipient. Donor derived bone marrow cells that produce lymphoid as well as myeloid PB cells for 16 weeks after transplantation are likely to be HSC, which should also have the ability to reconstitute secondary recipients. By analyzing the PB of recipient mice we can assess if the transplanted population contained any HSC. Analysis of peripheral blood of transplanted mice 17 weeks after transplantation of CD48<sup>+</sup> and CD48<sup>-</sup> cells indicated that indeed CD48<sup>+</sup> cells did not lead to any donor cell contribution within the peripheral blood (Figure

---

5.13F), whereas mice transplanted with low numbers of transplanted CD48<sup>-</sup> cells showed some contribution (2.9% ± 3.39) to the PB that was increased when higher numbers (equivalent of 500 CD48<sup>-</sup>KSL cells) of CD48<sup>-</sup> cells were transplanted into recipients (41.2%). This indicates that in cultured cells all HSC are contained within the CD48<sup>-</sup> fraction, while the CD48<sup>+</sup> fraction has completely lost all reconstitution potential. Transplantations of cells cultured on PA6 as well as FACS analysis of peripheral blood were performed by Angelika Roth.

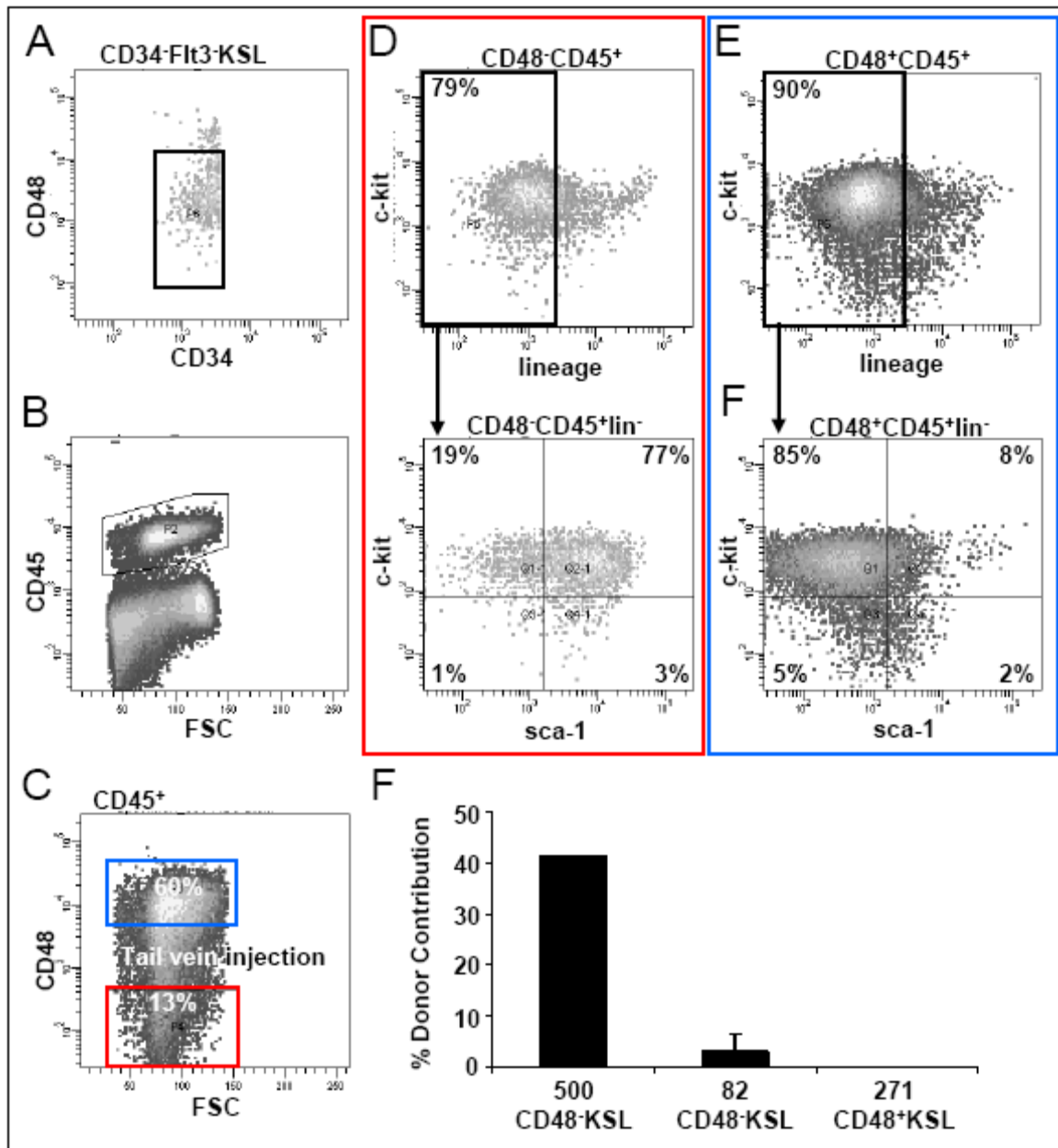


**Figure 5.13: Transplantation of HSC derived cultured cells with CD48<sup>-</sup> and CD48<sup>+</sup> phenotype into W<sup>41</sup>/W<sup>41</sup> Gpi1a Ly5.1 confirms retention of reconstitution potential in CD48<sup>-</sup> fraction.** CD48<sup>-</sup> HSC (A) were cultured on PA6 stroma for 3.75 days and CD45<sup>+</sup> cells (B) that are either CD48<sup>-</sup> or CD48<sup>+</sup> were transplanted (C). KSL marker expression of CD48<sup>-</sup> cells (D) and CD48<sup>+</sup> cells (E) after culture. (F) Percentage of donor contribution to peripheral blood of recipient mice 17 weeks after transplantation of CD48<sup>-</sup> and CD48<sup>+</sup> cells. Numbers of CD48<sup>-</sup>KSL and CD48<sup>+</sup>KSL cells are the equivalents of transplanted total CD48<sup>-</sup> and CD48<sup>+</sup> cells.

#### 5.1.4.2. Type of CD48 Expression Onset in HSC and MPP Pedigrees

As we now have shown that CD48 can be used as a live marker of loss of HSC potential, we set out to use this marker in movies to compare the differentiation behavior of HSC and MPP. As we used CD48 as a marker of loss of HSC potential, we defined every cell that had switched on CD48 as a differentiated cell that had lost HSC potential and would not regain that potential even upon loss of CD48 expression. We tracked pedigrees until the third division. In pedigrees that did not express CD48 by that time we decided to track cells and their progeny for at least 4d, after which cells are easily lost in the tracking process due to high cell density.

We observed different types of trees according to their expression of CD48. We saw CD48 negative trees that during a 4d time frame never switched on CD48 (Figure 5.5). We cannot say anything about the differentiation status of those cells, as the lack of CD48 expression does not necessary tell us if these cells still have HSC potential. Of the CD48 expressing pedigrees, some trees expressed CD48 in the starting cells. These cells were either already CD48<sup>+</sup> at the start of the movie or started to express CD48 before the first division. This indicates that these cells had probably already lost their HSC potential at the start of the movie (Figure 5.14A). All the cells of the pedigree express CD48 as indicated by the blue lines. As can be seen in the corresponding Supplementary Movie 5.4, CD48 expression is visible both on the cell surface and within the cytoplasm of the cells, where endocytosed antibody accumulates (Figure 5.14B).

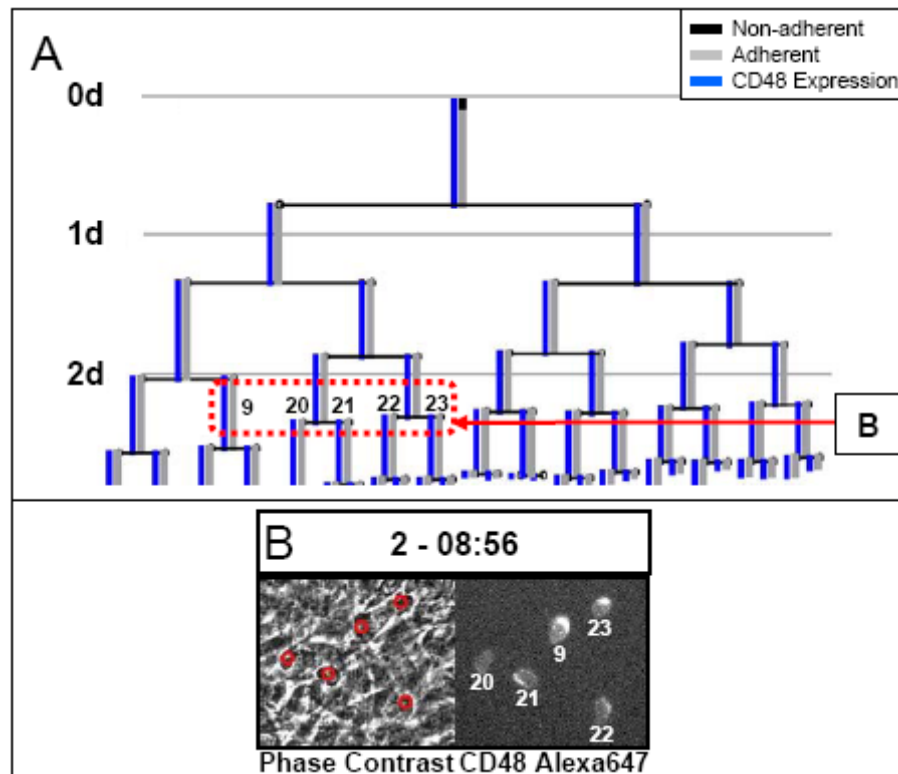


**Figure 5.14: Pedigree of a colony with CD48 expression onset in the mother cell.** The pedigree originates from an MPP and expresses CD48 (blue lines) from the starting cell and in all progeny. Orange arrow indicates cells shown in panel B (A). Frame from corresponding Movie 4 shows cells in phase contrast and fluorescence positive for CD48 expression (B). Scale bars are 10 $\mu$ m. time scale: days – hours:minutes

We also observed pedigrees that did not show CD48 expression in the starting cell, however showed start of CD48 expression in one or more progeny cells (Figure 5.15A and B). This pedigree stays CD48<sup>-</sup> until CD48 is switched on in all 4 cells of generation 3 at the same time (Figure 5.15A and C). At the time point when CD48 is first switched on, the expression of CD48 is very weak (Figure 5.15C and Supplemental Movie 5.5) and increases over time, until 8h 36min later a very strong CD48 signal can be observed (Figure 5.15D). When analyzing CD48 expression we noticed cells with stronger and weaker CD48 expression levels, however we did not quantify this and recognized all of these cells as CD48<sup>+</sup>.

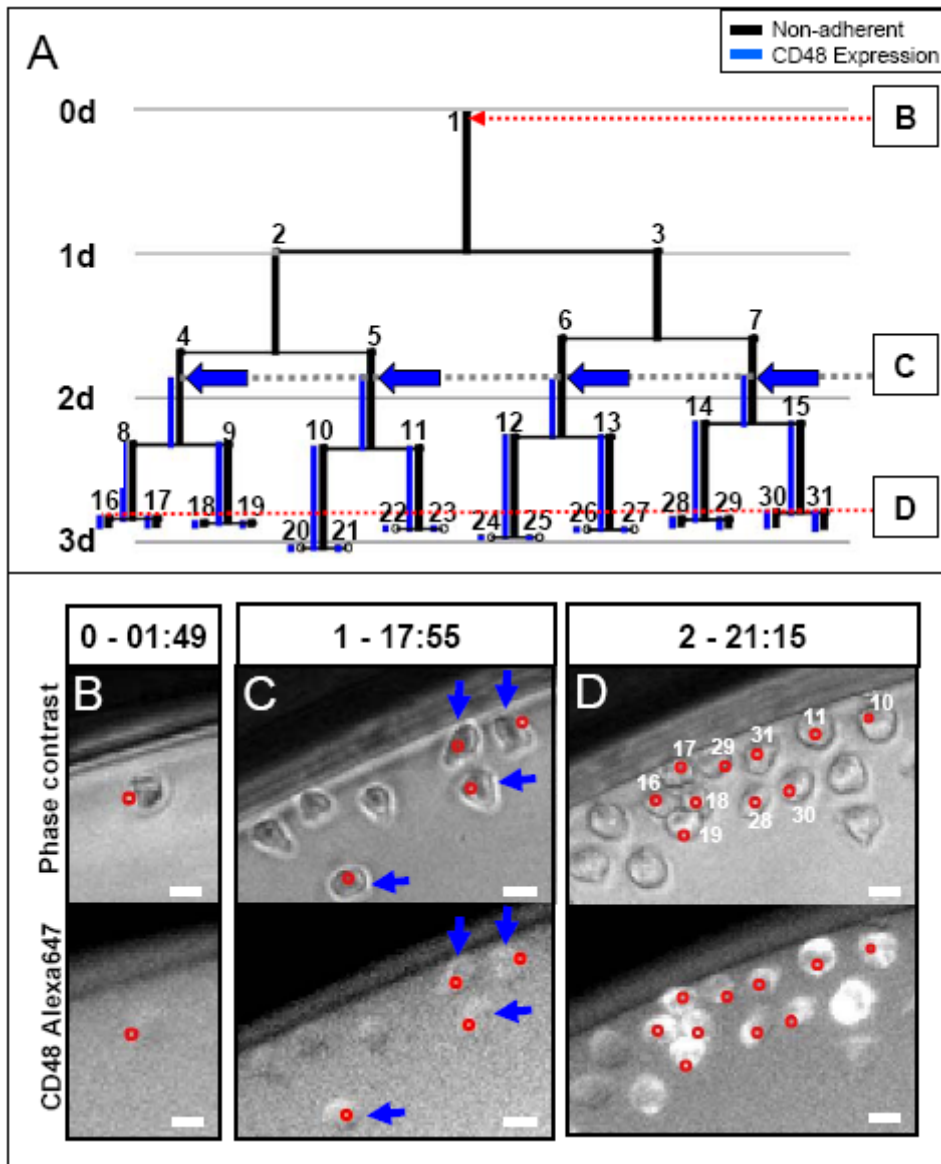


**Figure 5.15: Pedigree of a colony with CD48 expression onset in progeny: Symmetric onset.** Pedigree originates from an HSC and shows onset of CD48 expression in all cells of generation 3 indicated by blue arrows that correspond with frame in panel C (A). Frames corresponding to Movie 5 (B, C, and D). The starting cell is negative for CD48 (B). Weak expression of CD48 in cells marked by blue arrows (C). Stronger expression of CD48 in cells marked by track marks (D). Scale bars are 10 $\mu$ m, time scale: days – hours:minutes

When we quantified pedigrees according to the mentioned categories, we found for HSC cultured on PA6 44.5% ( $\pm 20.3$ ) of trees remaining negative for CD48 for 4 days, whereas only 5.2% ( $\pm 4.7$ ) of trees starting with an MPP remained CD48<sup>-</sup> (Figure 5.16A). Only 2.5% ( $\pm 4.3$ ) of HSC expressed CD48 in the mother cell but 42.2% ( $\pm 13.0$ ) of MPP starting cells turned on CD48 expression. The number of

trees with a later onset of CD48 was the same in HSC and MPP when cultured on PA6 ( $53.0\% \pm 24.6$  and  $52.6\% \pm 8.5$ ). The differences between HSC and MPP regarding the number of negative trees and trees with CD48 mother cell onset were significant ( $p=0.04$  and  $p=0.03$  respectively) meaning that a large number of HSC contain cells with HSC potential that is not lost within the first 4d according to CD48 expression. In contrast, MPP contain a large number of cells that have lost their HSC potential at the start of the movie or shortly thereafter.

We could observe a similar result for cells cultured in stroma free suspension culture containing self renewal cytokines (Figure 5.16B). Under these conditions, again a higher number of trees remained negative when started with a HSC ( $50.0\% \pm 7.1$ ) compared to an MPP ( $2.2\% \pm 3.1$ ,  $p=0.018$ ). As on PA6 stroma, we again found less HSC trees ( $10.0\% \pm 7.1$ ) than MPP trees ( $65.4\% \pm 6.5$ ;  $p=0.007$ ) with mother cell onset in stroma free self renewal conditions. For trees that showed CD48 onset in a progeny, the percentage of HSC ( $40\% \pm 14.1$ ) and MPP ( $32.4\% \pm 3.4$ ) derived pedigrees did not differ ( $p=0.3$ ). In summary, HSC cultured in stroma free self renewal conditions also produced a high percentage of pedigrees that did not express CD48 during a 4d culture period, indicating that these cells still possessed HSC potential. Only very few HSC lost their reconstitution ability within the mother cell as indicated by CD48 expression and less than half of initial HSC lost their potential during the 4d tracking period in one or all of their daughter cells. For MPP, we found almost no cells that remained CD48<sup>-</sup> during 4d of culture but found a high percentage of cells that had differentiated very early on as indicated by CD48 mother cell onset. In addition, a third of initial MPP differentiated and expressed CD48 during the course of the movie.

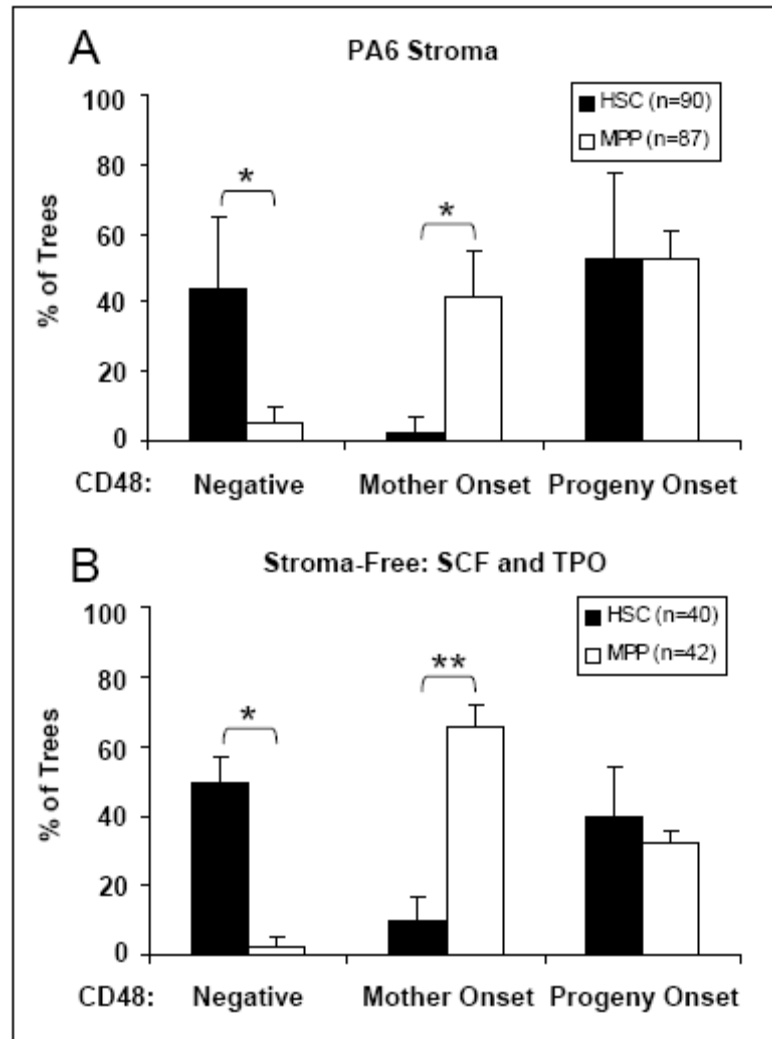


**Figure 5.16: Type of CD48 onset in self renewal conditions.** Percentage of CD48 onset types in trees originating from MPP and HSC cultured on PA6. Data shows the average of 5 independent experiments with 90 HSC and 87 MPP pedigrees analyzed (**A**). Percentage of CD48 onset types in trees originating from MPP and HSC cultured in stroma free culture containing SCF and TPO. Data shows the average of 2 independent experiments with 40 HSC and 42 MPP pedigrees analyzed (**B**). CD48 expression onset was followed for 4 days. Error bars show standard deviation, \* =  $p < 0.05$  \*\* =  $p < 0.01$

When cells were cultured in differentiation promoting cytokines we expected the distribution of trees in the CD48 onset types to closer resemble that of MPP than that of HSC. When we looked at HSC cultured in SCF and IL3, this was partly true, as we found 4.8% ( $\pm 6.7$ ) CD48 negative trees (Figure 5.17A). The number of cells that showed CD48 onset of expression in the mother cell however was lower than in MPP

but higher than in HSC cultured in self renewal conditions ( $19.5\% \pm 0.7$ ). The amount of trees that showed CD48 onset in progeny cells when HSC were cultured in SCF and IL3 was higher than that of both HSC and MPP in self renewal conditions ( $75.7\% (\pm 6.1)$ ). These results confirm that the rapid loss of HSC potential in differentiation promoting conditions is also reflected by an earlier CD48 onset in the cultured cells.

When we examined trees that started with HSC cultured in SCF and IL6, we expected this trend to continue and CD48 onset properties to resemble MPP cultured under self renewal conditions even closer. IL6 is known to promote a complete loss of HSC potential within three days (Ema, Takano et al. 2000). However, our results do not agree with the published data, instead we saw similar behavior of HSC cultured in SCF and IL6 as in self renewal conditions (Figure 5.17B). We detected  $64.0\% (\pm 10.5)$  of trees being negative for CD48,  $2.2\% (\pm 3.1)$  of trees that turned on CD48 in the starting cell and  $33.9\% (\pm 7.5)$  of the examined trees starting to express CD48 in progeny cells. These results indicate that either IL6 in our hands allows maintenance of HSC potential or that IL6 differentiates cells into a lineage that remains CD48<sup>-</sup> or actively suppresses CD48. It is also possible that these conditions promote maintenance of a cell type that has lost self renewal potential but that are still CD48<sup>-</sup> like the MPP1 described in the introduction (Wilson, Laurenti et al. 2008).

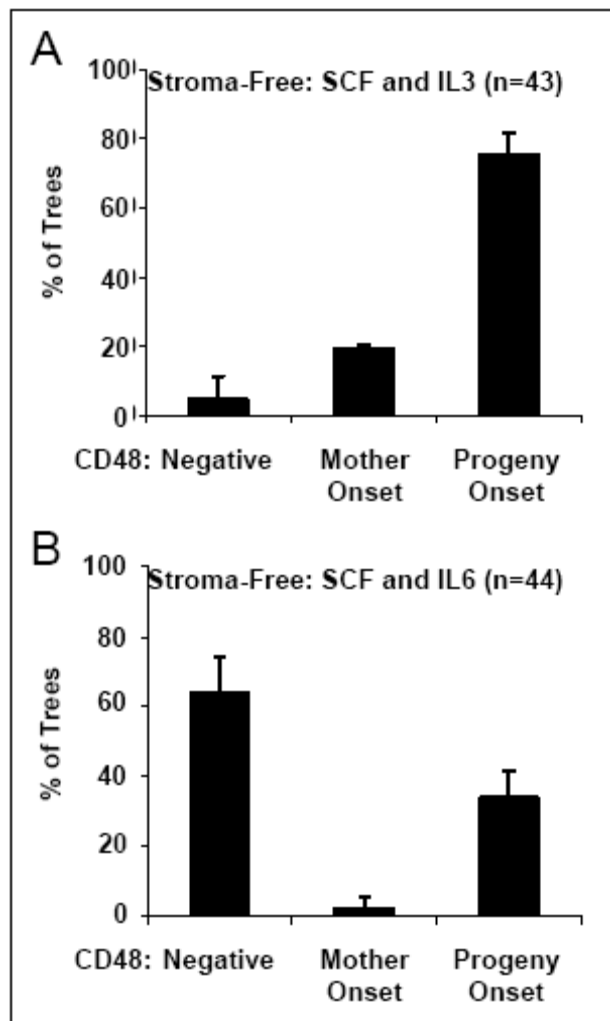


**Figure 5.17: Type of CD48 onset in differentiation conditions.** Percentage of CD48 onset types in trees originating from HSC cultured in stroma free culture containing SCF and IL3. Data shows the average of 2 independent experiments with 43 pedigrees analyzed (**A**). Percentage of CD48 onset types in trees originating from HSC cultured in stroma free culture containing SCF and IL6. Data shows the average of 2 independent experiments with 44 pedigrees analyzed (**B**). CD48 expression onset was followed for 4 days. Error bars show standard deviation.

#### 5.1.4.3. Time of CD48 Expression Onset in HSC and MPP Pedigrees

After determining the types of CD48 onset in pedigrees, we also were interested in when CD48 is first expressed in pedigrees of cells cultured in the different conditions. When HSC were cultured in PA6, we saw 2.8% ( $\pm 4.9$ ) of trees at 12h after movie start to express CD48 (Figure 5.18A). The percentage of trees expressing CD48 did not increase significantly until 60h when 21.3% ( $\pm 4.0$ ) of trees expressed CD48. This increase in CD48 expressing trees leveled off at 72h (39.4%  $\pm 9.2$ ) and did not increase much until 96h (54.9%  $\pm 17.5$ ). MPP in contrast showed an initial 31.1 $\pm$ 19.7% of CD48 expressing trees, recapitulating that already a large proportion of MPP were CD48<sup>+</sup> when isolated. The proportion of CD48<sup>+</sup> MPP trees continued to increase until it reached 94.5% ( $\pm 5.5$ ) at 96h. HSC and MPP were significantly different at all time points except at 12h.

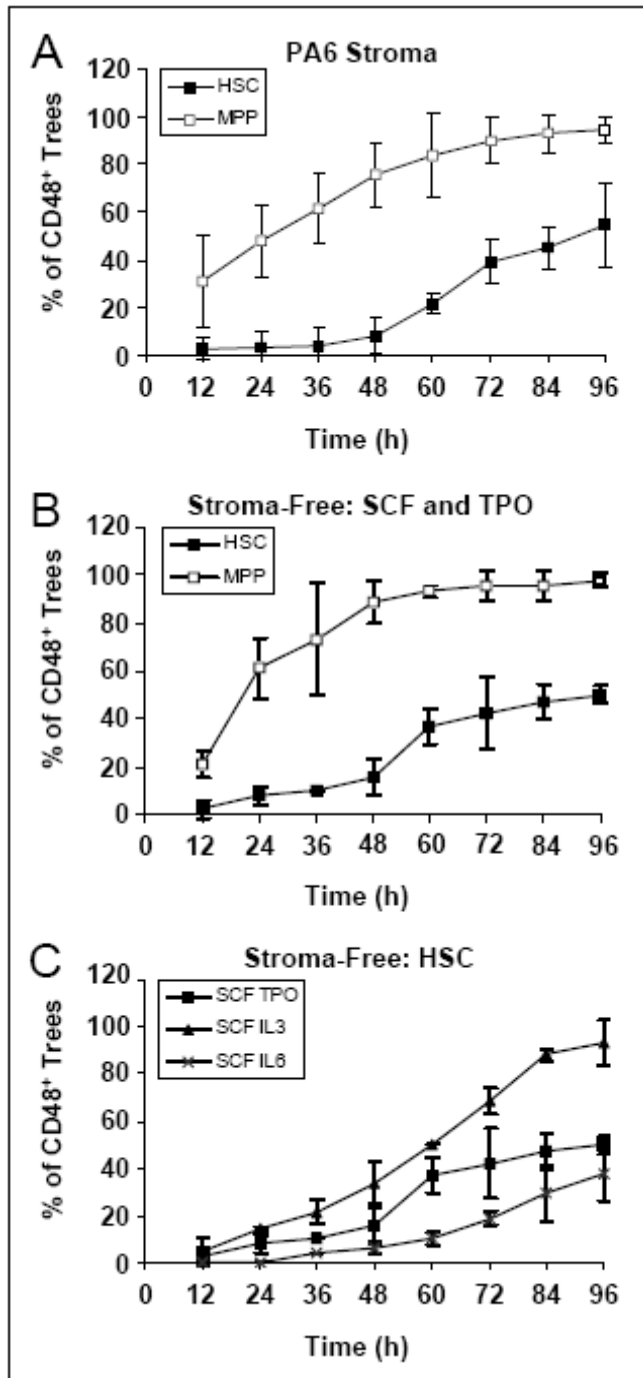


**Figure 5.18: CD48 onset kinetics in pedigrees of cells cultured in self renewal and differentiation conditions.** Percentage of trees containing at least one CD48 expressing cell starting with an MPP or HSC cultured on PA6 (**A**). Percentage of trees containing at least one CD48 expressing cell starting with an MPP or HSC cultured in stroma free culture containing SCF and TPO (**B**). Percentage of trees containing at least one CD48 expressing cell starting with an HSC cultured in stroma free culture (**C**). CD48 expression onset was followed for 4 days. Error bars show standard deviation.

When we examined CD48 onset kinetics in stroma free self renewal conditions, we found a similar trend. In HSC the initial percentage of CD48 was low ( $2.6\% \pm 3.7$ ) at 12h and did not rise significantly until 60h when  $36.8\% (\pm 7.4)$  of trees expressed CD48 (Figure 5.18B). The percentage of CD48<sup>+</sup> trees increased slightly from thereon until at 96h  $50\% (\pm 3.7)$  of the trees were positive for CD48. In MPP, similar to when cultured on PA6, we found  $21.2 (\pm 5.4)$  of CD48<sup>+</sup> trees at 12h. After an initial sharp increase in the number of CD48<sup>+</sup> trees to  $61.1\% (\pm 12.6)$  the

increase in CD48<sup>+</sup> trees leveled off until at 96h when 97.8% ( $\pm 3.1$ ) of trees were positive for CD48. HSC and MPP were significantly different at all time points except at 36h, showing that HSC when cultured in self renewal conditions, remained CD48 negative for a longer time than MPP, which adopted CD48 expression much faster.

We then compared the behavior of HSC cultured in stroma free culture of self renewal and differentiation promoting cytokine conditions. CD48 expressing trees from cells cultured in SCF and IL3 increased with a steep incline linearly to 93.2% ( $\pm 9.6$ ) at 96h, while trees from culture in SCF and IL6 increased also linearly, but less quickly to only 37.5% ( $\pm 11.8$ ) (Figure 5.18C). CD48 onset kinetics between these two cytokine conditions differed significantly at 24h ( $p=0.03$ ), 60h ( $p=0.03$ ), 72h ( $p=0.02$ ), and 96h ( $p=0.04$ ). The CD48 onset kinetics in cells cultured with SCF and TPO overall showed less CD48<sup>+</sup> trees (not significant, 2 tailed t-test) than when cultured in SCF and IL3. SCF and TPO did not induce a significantly higher number of CD48<sup>+</sup> trees than SCF and IL6. The data concerning the CD48 onset kinetics of cells cultured in stroma free culture recapitulates data from the CD48 onset types in Figures 5.16 and 5.17. IL3 clearly promotes differentiation as shown by an increasing number of CD48<sup>+</sup> trees over time, while IL6 allows almost two-thirds of trees to remain CD48 negative after 4d in culture.

#### **5.1.4.4. Asymmetric CD48 Expression Onset Reveals Intrinsic Control of Asymmetric Fates of HSC Daughters**

Having established CD48 detection as a means of detecting loss of HSC potential, we used this marker to identify asymmetric fate decisions of HSC. We were interested in trees that showed an asymmetric onset of CD48 expression in progeny cells. In Figure 5.19A the pedigree corresponding to Supplemental Movie 5.6 is shown, where the daughters of the starting cell display CD48 onset at different time points. While cell 2 starts to express CD48, marked by a blue arrow and shown in B, cell 3 remains negative (Figure 5.19B). The progeny of cell 2 continue to express CD48, but the daughters of cell 3 first do not express CD48, as shown in Figure 5.19C, until shortly before division, cell 6 starts to express CD48 (Figure 5.19D). At the same time cell 7 still remains negative, until just after division, when its daughters start to express CD48.

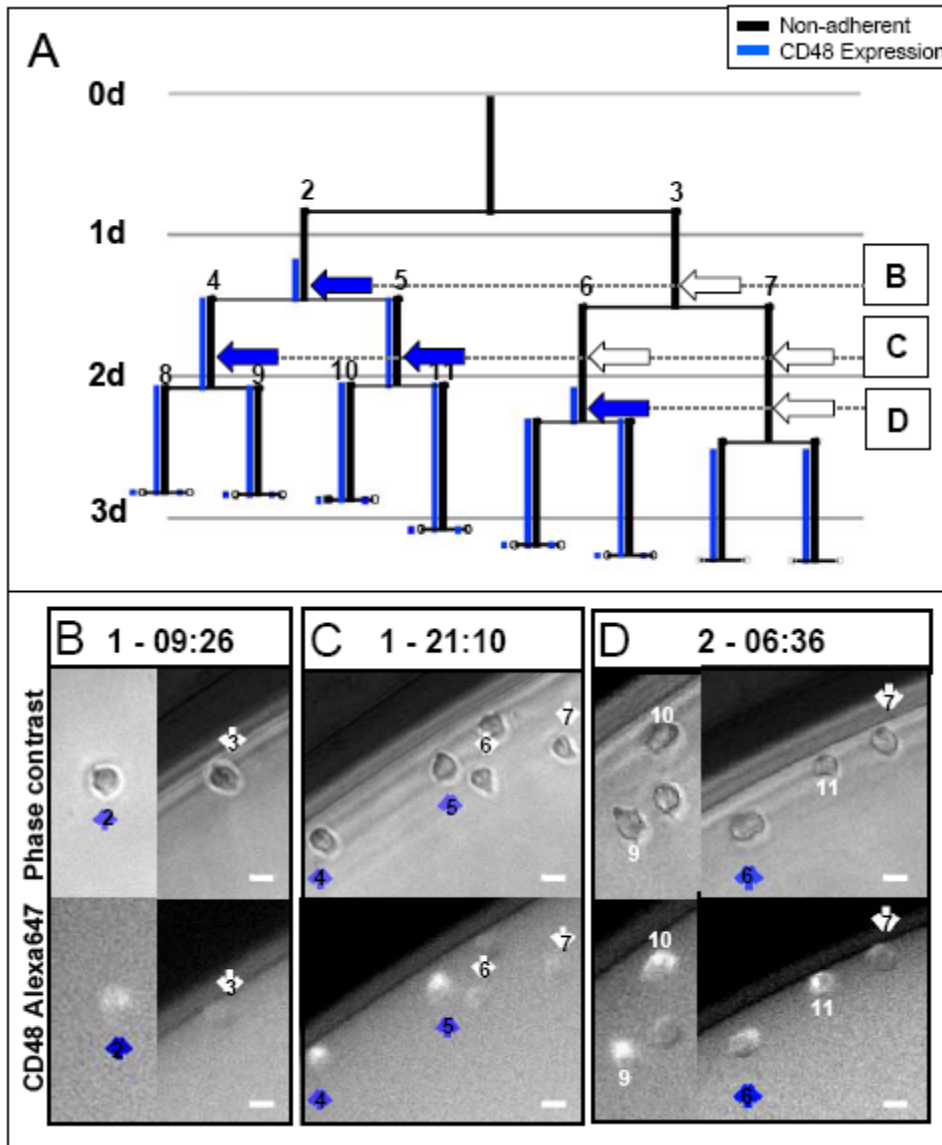


**Figure 5.19: Pedigree of colony with CD48 expression onset in progeny: Asymmetric onset.** Pedigree starting with an HSC shows asymmetric onset (more than 12h) of CD48 expression. Blue arrows indicate CD48 expressing cells in corresponding frames while white arrows indicate CD48 negative cells in corresponding frames (A). Frames corresponding to movie 6 (B, C, and D). Cell 2 indicated by a blue arrow expresses CD48, while cell 3 indicated by a white arrow at the same time does not express CD48 (B). Cells 4 and 5 indicated by blue arrows express CD48, while cells 6 and 7 indicated by white arrows are still negative for CD48 (C). Cell 6 indicated by a blue arrow is now CD48<sup>+</sup> while cell 7 indicated by a white arrow remains CD48<sup>-</sup> (D). Scale bars are 10 $\mu$ m, time scale: days – hours:minutes

Another example of asymmetric onset of CD48 expression is shown in Figure 5.20. The pedigree corresponding to Supplemental Movie 5.7 shows daughters 2 and 3 initially negative for CD48 (Figure 5.20B). Shortly before division, cell 2 starts to express CD48, as shown in Figure 5.20C, and all further progeny of cell 2 also remain

CD48<sup>+</sup>. In contrast, cell 3 remains negative and also its progeny do not upregulate CD48 (Figure 5.20C and Figure 5.20D).

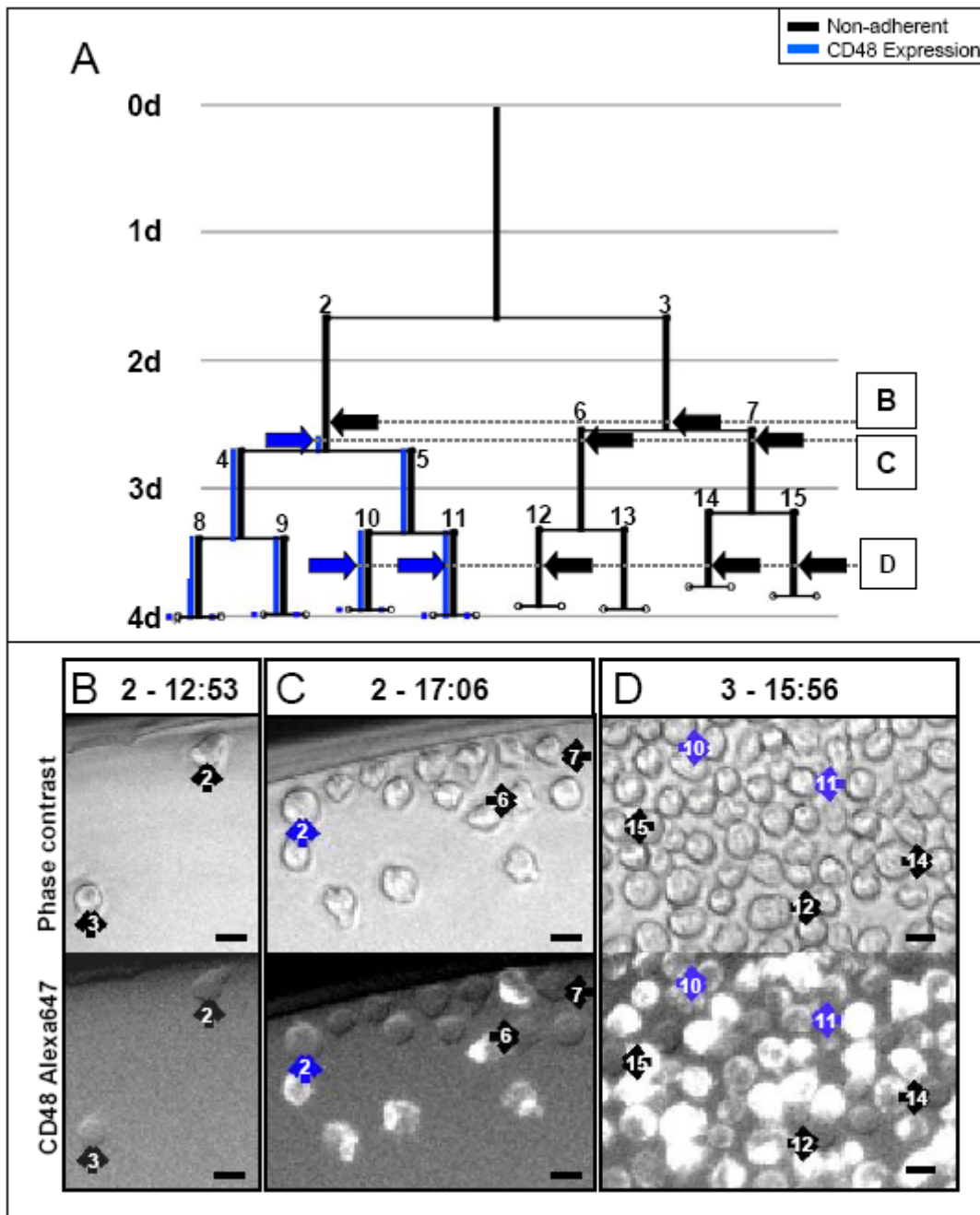


**Figure 5.20: Another example: Pedigree of colony with CD48 expression onset in progeny: Asymmetric onset.** Pedigree starting with an HSC shows asymmetric onset of CD48 expression. Arrows indicate corresponding frames. The left branch of the tree turns on CD48 in cell 2 and remains CD48<sup>+</sup>, while the right branch of the tree remains CD48<sup>-</sup> (A). Frames correspond to Movie 7. Cell 2 and 3 indicated by white arrows are negative for CD48 expression (B). Cell 2 indicated by a blue arrow is CD48<sup>+</sup> while cells 6 and 7 indicated by white arrows remain CD48<sup>-</sup> (C). Progeny of cell 2 express CD48 (blue arrows) while daughters of cell 3 remain CD48<sup>-</sup> (white arrows) (D). Scale bars are 10 $\mu$ m, time scale: days – hours:minutes

To define trees with asymmetric onset of CD48 expression, we chose a minimal time difference of 12 hours. This eliminates differences in onset of CD48 expression of two or three hours which could be attributed to technical detection delays, and is the approximate length of one generation.

Of HSC cultured on PA6 stroma that showed onset of CD48 expression in their progeny, we found 69.5% ( $\pm 13.0$ ) of pedigrees with asymmetric onset (Figure 5.21A). In contrast, only 10.5% ( $\pm 10.6$ ) of MPP progeny were asymmetric in the onset of CD48 expression ( $p=0.03$ ). A similar trend could be observed when cells were cultured in stroma free self renewal culture containing SCF and TPO. Here 53.3 ( $\pm 8.9$ ) of HSC trees showed asymmetric CD48 onset, whereas only 20.8% ( $\pm 5.9$ ) of MPP trees were asymmetric regarding the onset of CD48 expression ( $p=0.1$ , Figure 5.21B). HSC cultured in differentiation conditions also showed similar percentages of asymmetric CD48 onset as when cultured in the presence of self renewal cytokines. When cultured in SCF and IL3 54.6% ( $\pm 11.2$ ) of HSC progeny showed asymmetric onset of CD48 expression, while 50.0% ( $\pm 23.6$ ) of pedigrees with onset of CD48 expression in their progeny were asymmetric when cultured in SCF and IL6 (Figure 5.21B). These results show, that asymmetric onset of CD48 expression is specific to HSC and not MPP and that it is independent of the environment that cells are cultured in. This leads to the conclusion that asymmetric CD48 onset in HSC pedigrees is intrinsically controlled. Therefore, the onset of CD48 expression serves as a live marker of loss of self renewal that helps to identify asymmetric fate decisions in HSC.

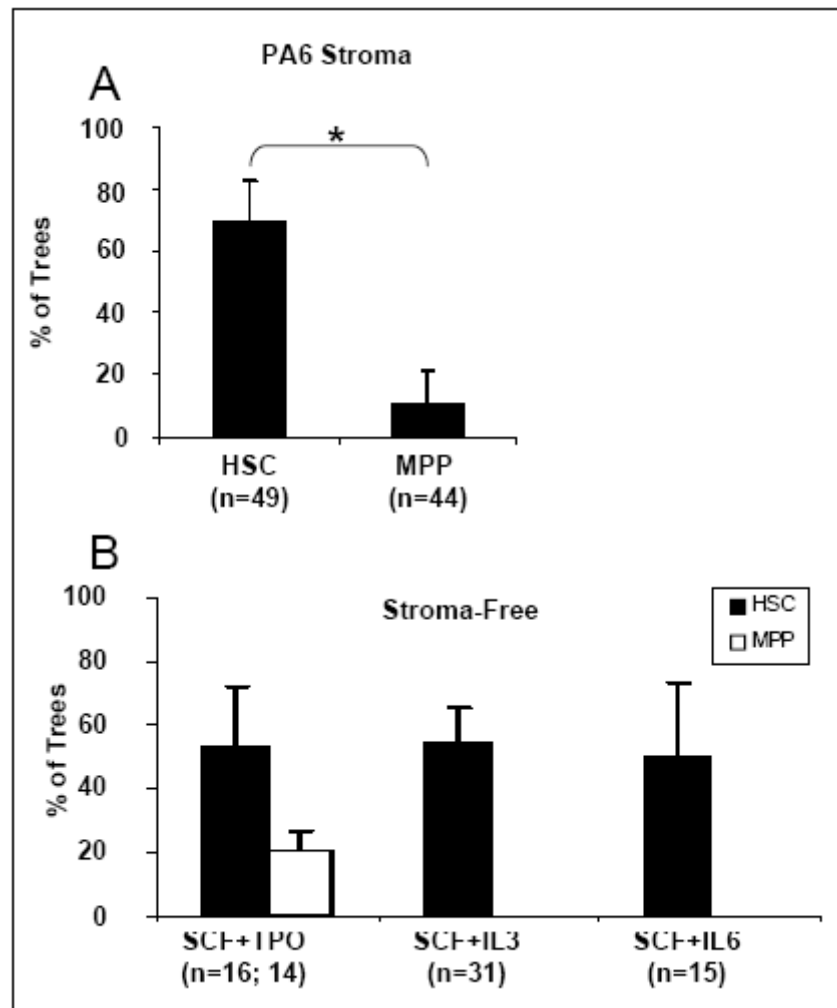


**Figure 5.21: More HSC than MPP produce pedigrees with asymmetric CD48 onset.** Percentage of pedigrees with asymmetric onset of CD48 expression in progeny cells derived from HSC and MPP and cultured on PA6 stroma. Data shows the average of 5 independent experiments with 49 HSC and 44 MPP pedigrees analyzed (A). Percentage of pedigrees with asymmetric onset of CD48 expression in progeny cells derived from cells cultured in stroma free conditions. Data shows the average of 2 independent experiments for each condition. For cells cultured in SCF and TPO, 16 HSC and 14 MPP pedigrees were analyzed. For HSC cultured in SCF and IL3 and SCF and IL6, 31 and 15 pedigrees were analyzed respectively (B). Error bars show standard deviation, \* =  $p < 0.05$

## 5.2. Examining Candidate Protein Segregation as a Potential Mechanism Controlling Asymmetric Fate Decisions of HSC

### 5.2.1. Expression of Candidate Genes in Bone Marrow Populations

To evaluate whether the candidate genes mentioned in the introduction might play a role in ACD, we first set out to examine their presence in mouse HSC, MPP and other major myeloid progenitor population. For this, we isolated these populations by FACS sorting and measured candidate expression at the mRNA level. In detail, KSL cells were subdivided to yield HSC, MPP and MPP4. HSC and MPP were isolated like shown above as CD48<sup>-</sup>CD34<sup>-</sup>Flt3<sup>-</sup>KSL and as CD34<sup>+</sup>Flt3<sup>-</sup>KSL respectively. MPP4 were isolated as CD34<sup>+</sup>Flt3<sup>+</sup>KSL (Figure 5.22A), (Wilson, Laurenti et al. 2008). Myeloid progenitors are lineage marker negative, lack expression of Sca-1 and express high levels of c-kit. This KLS<sup>-</sup> population can be subdivided according to the expression of Fc $\gamma$  receptor (Fc $\gamma$ R) and CD34 (Figure 5.22B). GMP, which can give rise to cells of the monocytic and the granulocytic lineage, express Fc $\gamma$ R as well as CD34. MEP, which can give rise to megakaryocytes and erythrocytes, are negative for both markers. In addition, MEP do also not express CD71, as CD71 expressing cells have already committed to the erythroid lineage. CMP, which can give rise to GMP and MEP do not express Fc $\gamma$ R, but do express CD34.

In order to avoid detection of genomic rather than cDNA with our primers, we chose exon-spanning primers to detect all selected genes (Table1). We could not detect Prominin1 expression in HSC or other immature progenitors (Figure 5.22C), however we found that GMP are the only population tested that expressed Prominin1 mRNA. Since we could detect as low as one copy of Prominin1 in plasmid dilutions (data not shown) we could exclude that the lack of Prominin1 expression in HSC is due to insensitivity of the primers to low copy numbers of the mRNA. These results were confirmed by Affymetrix chip analysis (Dr. M. Rieger). In contrast, Pumilio1 and Pumilio2 were both expressed in HSC as well as MPP and all myeloid progenitors, but not in MPP4 (Figure 5.22C). Quaking1 expression was analyzed using primers recognizing all three splice isoforms. We were able to detect Quaking1 expression in HSC as well as MPP populations and all myeloid progenitors (Figure 5.22C). To assess Staufen1 expression we used primers recognizing both Staufen1 and Staufen<sup>l</sup>.

Like Quaking1, we detected Staufen1 expression within the HSC population and in all other analyzed progenitor populations except for MPP4 (Figure 5.22C).

Gene	Direction	Location	Primer Sequence
Prominin1	Forward	Exon 19	TGGACCCTCCAGCAAACAAG
	Reverse	Exon 22	GGTCCGCAACATAGCCACAC
Pumilio1	Forward	Exon 20	AGCAGAGATCCGAGGCAATG
	Reverse	Exon 21	ATGACAATCTTCCGCTGACC
Pumilio2	Forward	Exon 20	TGAGGTCTGCTGTCAGAATG
	Reverse	Exon 21	CCAAGTGGCCAGTATATGC
QuakingI	Forward	Exon 1	CGGTGGGACCCATTGTTTCAG
	Reverse	Exon 3	TCACTTCTTCAACCGCTCTC
Staufen1	Forward	Exon 9	TGATAGCCCGAGAGTTGTTG
	Reverse	Exon 10	TGTGAGGAGCAGTTGATGAG
$\beta$ -actin	Forward	Exon 4	CCTGACGGCCAGGTCATCACTATTG
	Reverse	Exon 5	GGTGCTAGGAGCCAGAGCAGTAATC

**Table 5.1: RT-PCR primers for candidate genes.** Sequence and binding location of primers to detect candidate RNA expression in hematopoietic progenitors.

In summary, all candidate genes except for Prominin1 were expressed in HSC and in most of the other analyzed progenitor populations. Since Staufen1 and both Pumilio1 and 2 genes are expressed in HSC we decided to continue our studies concerning protein segregation with these candidates. We also were interested in their effect on HSC lineage choice. Prominin1 was not expressed in HSC so we did not pursue this candidate any further. Despite the fact that we found Quaking1 to be expressed in HSC, since so far it has not been directly implicated in protein segregation, we decided to not employ Quaking1 in protein segregation experiments. Rather, Quaking1 seems to be an effector gene, executing decisions of upstream genes that are segregated asymmetrically. Therefore, we decided to evaluate the effect of Quaking1 on fate choices of HSC only.

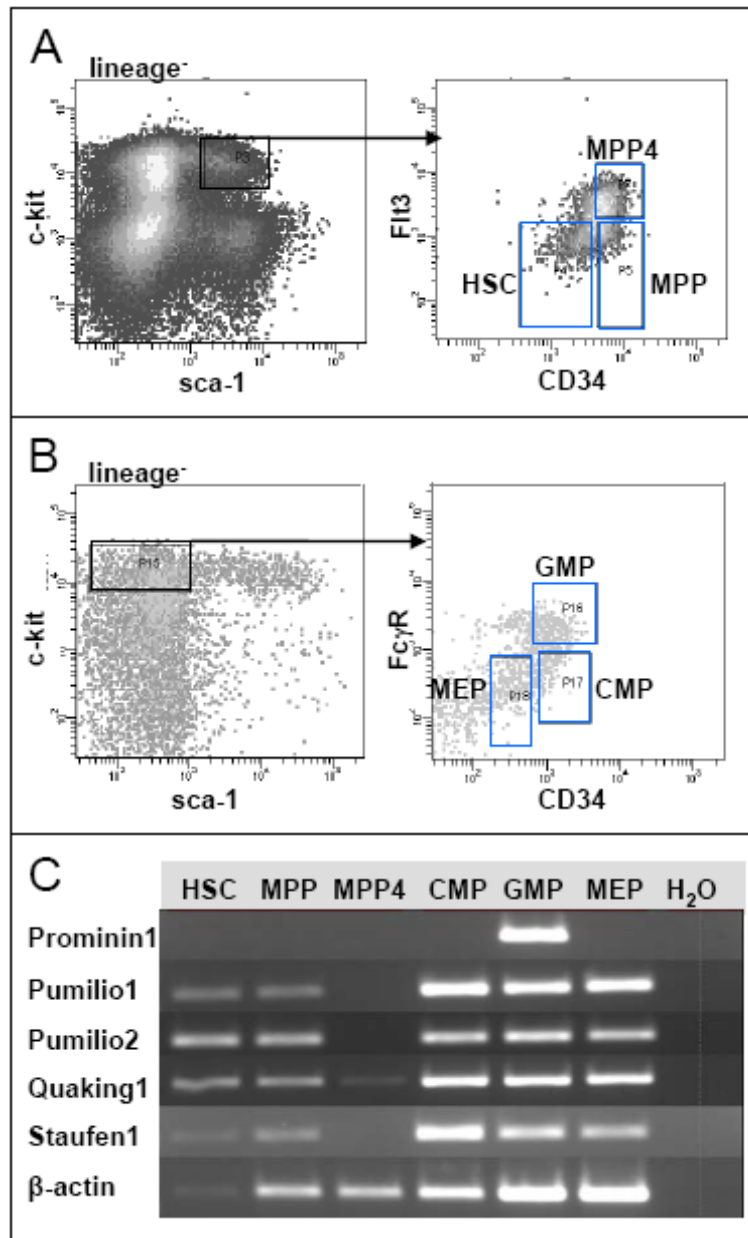


**Figure 5.22: RT-PCR of candidate genes in bone marrow progenitor populations.** Sorting scheme of HSC and myeloid bone marrow progenitors (A). mRNA expression of candidate gene specific sequences (see Table 1) in 50 cell equivalents of bone marrow progenitors (B).

### 5.2.2. Cloning of Candidate Expression Constructs

For each of the candidates, two different lentiviral expression constructs were generated. The first, used to analyze protein segregation of candidate proteins, consists of a direct fusion of the candidate protein to the VENUS fluorescent protein. For analysis of the influence of candidate genes on fate decisions, we had to exclude

that the fusion to a fluorescent protein alters the function of the wild type candidate protein. Therefore, constructs were generated whereby the expression of the candidate gene was separated from VENUS expression by an internal ribosome entry site (IRES). This results in the production of one mRNA containing two separate translation initiation sites for the candidate and VENUS and ensures that every cell expressing the introduced candidate gene also expresses VENUS under the control of the same promoter. In addition, VENUS expression was targeted to the nuclear membrane by the addition of an importin sequence (Imamoto, Shimamoto et al. 1995).

### 5.2.3. Optimization of Lentivirus Infection

Viruses expressing candidates either as fusions to VENUS or as IRES constructs were produced using an optimized protocol from Dr. Christopher Baum's laboratory (Schambach, Galla et al. 2006). We used an ecotropic envelope protein to produce virus that can only infect rodents, but not humans. We tested the virus on HSC isolated from mouse bone marrow using a multiplicity of infection (MOI) of 600. Infection of these cells with vector control virus expressing only VENUS resulted in infection efficiencies of 7% ( $\pm 11.9$ , black bar, Figure 5.23A), while virus containing either Staufen1, Staufeni or Quaking1 resulted in infection efficiencies of 2% ( $\pm 0.7$ ), 2% ( $+1.3$ ) and 1% ( $\pm 2.0$ ) respectively. Infection efficiencies in this range are challenging to work with, as HSC are a rare population (maximum 1000 cells per mouse) and a large number of positive cells are needed to yield significant results. We tried to increase infection efficiency by centrifuging virus, cells and protamine sulfate, which should facilitate virus infection by bringing virus and cells in close contact. However, the percentage of VENUS positive cells did not increase using this spin infection method (white bars, Figure 5.23A). Also, variation of temperature and MOI during spin infection as well as precoating of plates with retronectin did not increase infection efficiency (Figure 5.23A and B and data not shown), as these methods yielded efficiencies of not more than 6%.

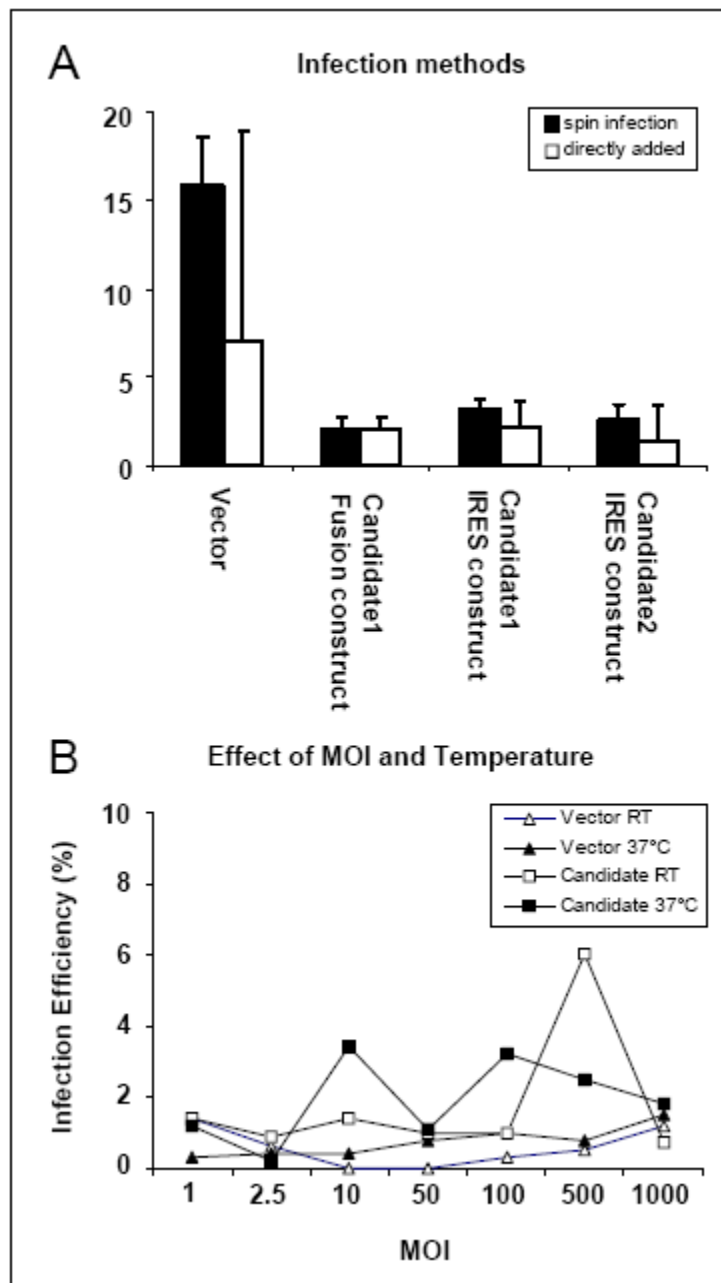


**Figure 5.23: Optimization of lentiviral infection: Infection conditions.** Comparison of infection efficiencies of 4 different lentiviruses with two infection methods. Data shows average of two independent experiments (A). Comparison of lentivirus infection efficiency using various MOIs and spin infection at three different temperatures. Data shows results of one experiment (B). Error bars show standard deviation.

Finally, we decided to test vesicular stomatitis virus G protein (VSVG) pseudotyped lentivirus to infect HSC. VSVG protein can recognize and bind to receptors present on rodent as well as human cells and renders the virus more stable

---

during ultracentrifugation. Using VSVG pseudotyped virus poses a potential risk for the researcher, especially when working with suspected oncogenes, and hence work needs to be performed under strict S2 conditions. Using GFP containing VSVG lentivirus (kindly provided by Dr. Christopher Baum) to infect HSC, resulted in more than 80% of infected cells when directly adding the lentivirus. Using this same condition for infection of HSC with several of our ecotropic lentiviral vectors resulted in infection efficiencies below 10% irrespective of construct or method (Figure 5.24A). Therefore, we decided to produce VSVG pseudotyped lentivirus and compare it to the obtained GFP VSVG virus resulting in similar infection efficiencies at two different MOI (Figure 5.24B). At an MOI of 10 VSVG GFP virus showed 43% and VENUSnucmem virus showed 33% of infected cells. At an MOI of 100 VSVG GFP virus showed 73% and our self produced virus showed 79% of VENUS positive cells. Therefore, we decided to produce all our viruses as VSVG pseudotype and use them at an MOI of 100.

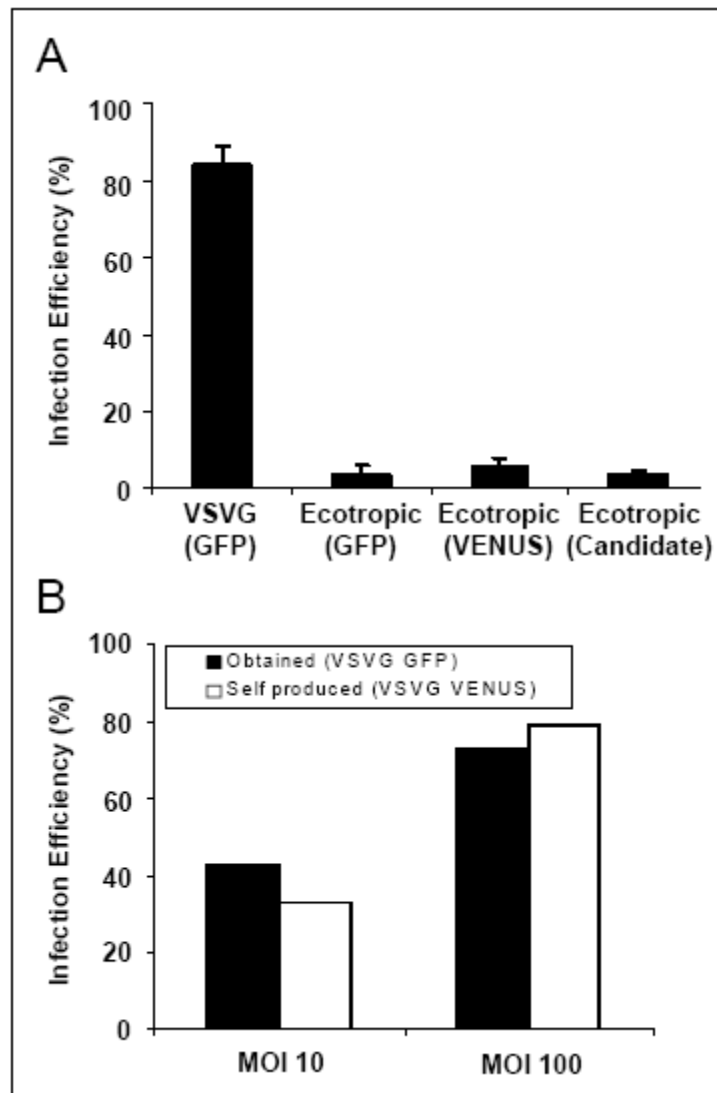


**Figure 5.24: Higher infection efficiency of VSVG compared to ecotropic pseudotyped virus.** Comparison of infection efficiency of VSVG and ecotropic pseudotyped lentivirus using different infection methods. Virus was directly applied to the cell suspension. Data shows results of one experiment with three replicates (A). Comparison of infection efficiency between obtained and self produced VSVG pseudotyped lentivirus (B). Data shows results of one experiment. Error bars show standard deviation.

#### 5.2.4. Segregation of Candidate Proteins during HSC Divisions

##### 5.2.4.1. Experimental Setup for Analysis of Protein Segregation

ACD is assumed to be a mechanism used by HSC to generate asymmetric self renewal fates of daughter cells. Thus, cells that have lost their HSC capacity could be no longer able to segregate fate determining proteins asymmetrically to generate

asymmetric daughter cell fates. To analyze a potential role of ACD in HSC self renewal control, it is crucial to analyze cells that have not lost their HSC potential yet. HSC, when cultured under self renewal maintenance (not expansion) conditions, will divide either symmetrically to give rise to two differentiated cells that have both lost their HSC capacity or they will asymmetrically divide to yield an HSC and a differentiated cell. Therefore, it is important to analyze protein segregation during the first division, since the identity of the cell can only then be assured.

Examining the role of candidate proteins in ACD of HSC, we decided to isolate a cell population that contains the highest possible percentage of cells with reconstitution potential. Using  $CD150^+CD48^-$  within the  $CD34^+KSL$  cell population yields HSC with a purity of over 47% (Kiel, Yilmaz et al. 2005; Wilson, Laurenti et al. 2008) (Figure 5.25A). We isolated this cell population and infected them in stroma free culture in the presence of only SCF for 44h, washed them and initially replated them onto PA6 stroma to analyze protein segregation (Figure 5.25B). However, as we discovered that the PA6 cells were also infected by the virus, thus complicating the analysis of protein segregation in the blood cells, we switched to stroma free culture containing SCF and TPO.

After the infection period, we observed the infected cells and tracked and quantified only presumed first divisions, which we found occurred mostly within the first two days of the time lapse movie (Figure 5.25C). We compared the fluorescence intensity of sister cells normalized to background immediately after division and recorded the difference as a ratio. We assumed ratios above 2 as a potential asymmetric segregation of protein between the two sister cells. In addition, any sister cells producing a ratio higher than 1.5 were again closely examined to determine the reason for the higher ratio. In most cases, a ratio above 1.5 was due to uneven background illumination or imprecise area definition before quantification and after adjustment of area yielded a lower ratio.

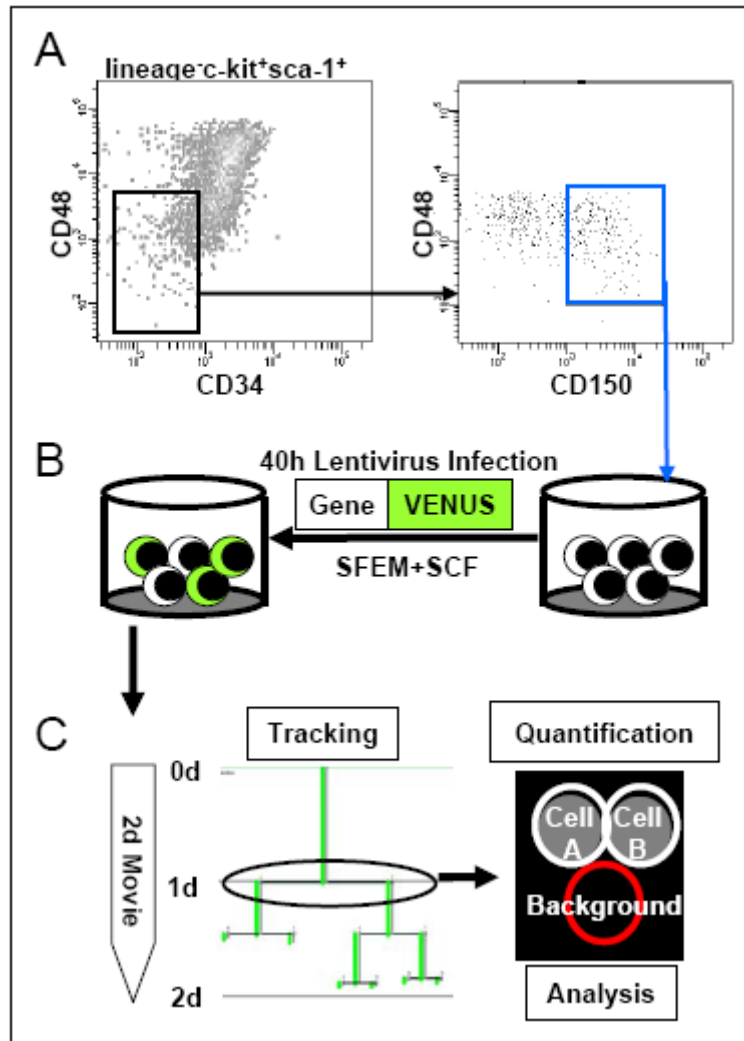


**Figure 5.25: Experimental setup to examine protein segregation in HSC.** HSC sorting scheme, isolation of CD34<sup>-</sup>CD48<sup>-</sup>CD150<sup>+</sup> KSL cells for protein segregation experiments (A). Experimental setup of lentiviral infection (B). Time lapse movie, single cell tracking and quantification of fluorescence in sister cells (C).

#### 5.2.4.2. Staufen1 and Staufeni Are Not Segregated during HSC Divisions

We analyzed a total of 650 divisions of VENUS positive cells for Staufen1 and Staufeni segregation, but we did not find any sister cells that significantly differed in their fluorescent intensity, i.e. a ratio of more than 2 (Figure 5.26A and B). We still took a closer look at the data and noticed background intensity variations across the field of vision in a range from 0 to 14000 fluorescence units (FU) for Staufen1VENUS movies and a range of 500 to 10000 FU for StaufeniVENUS movies (data not shown). Differences in background ranges between Staufen1 and Staufeni movies are due to

differences in histogram adjustment at acquisition and do not have an effect on real signal intensities and cell ratios. We also noticed that the fluorescence intensity over background (FOB) varied widely within a movie (Figure 5.26A and B). This is probably due to different numbers of lentiviral integrations into the genome of the cells, some cells containing multiple and other cells containing single copies of fusion genes. To evaluate the influence of FOB on sister cell ratio we plotted cell ratios against FOB and found that cells with the lowest FOB also had the highest ratios (Figure 5.26A and B). Presumably, the lower the absolute fluorescence intensity of a cell, the higher the error rate coming from imprecise area definition around the cell and limitation in recognizing pixel intensity differences. However, also in cells with a very low FOB, we did not find sister cell ratios above 2, indicating that our measurement tools were actually quite sensitive. We decided to take a closer look at sister cell pairs that displayed cell ratios above an arbitrary line that would exclude cells with very low signals, as we assume a higher error rate in these cells, as well as cells with a high intensity but very low cell ratio, as those cells are unlikely to contain sister pairs that display asymmetric protein segregation. Examples of protein segregation during division of HSC can be observed for *Staufen1* expressing cells (Supplemental Movies 5.8A, 5.8B, 5.8C, and 5.8D) and for *Staufen<sup>1</sup>* expressing cells (Supplemental Movies 5.9A, 5.9B, 5.9C, and 5.9D).

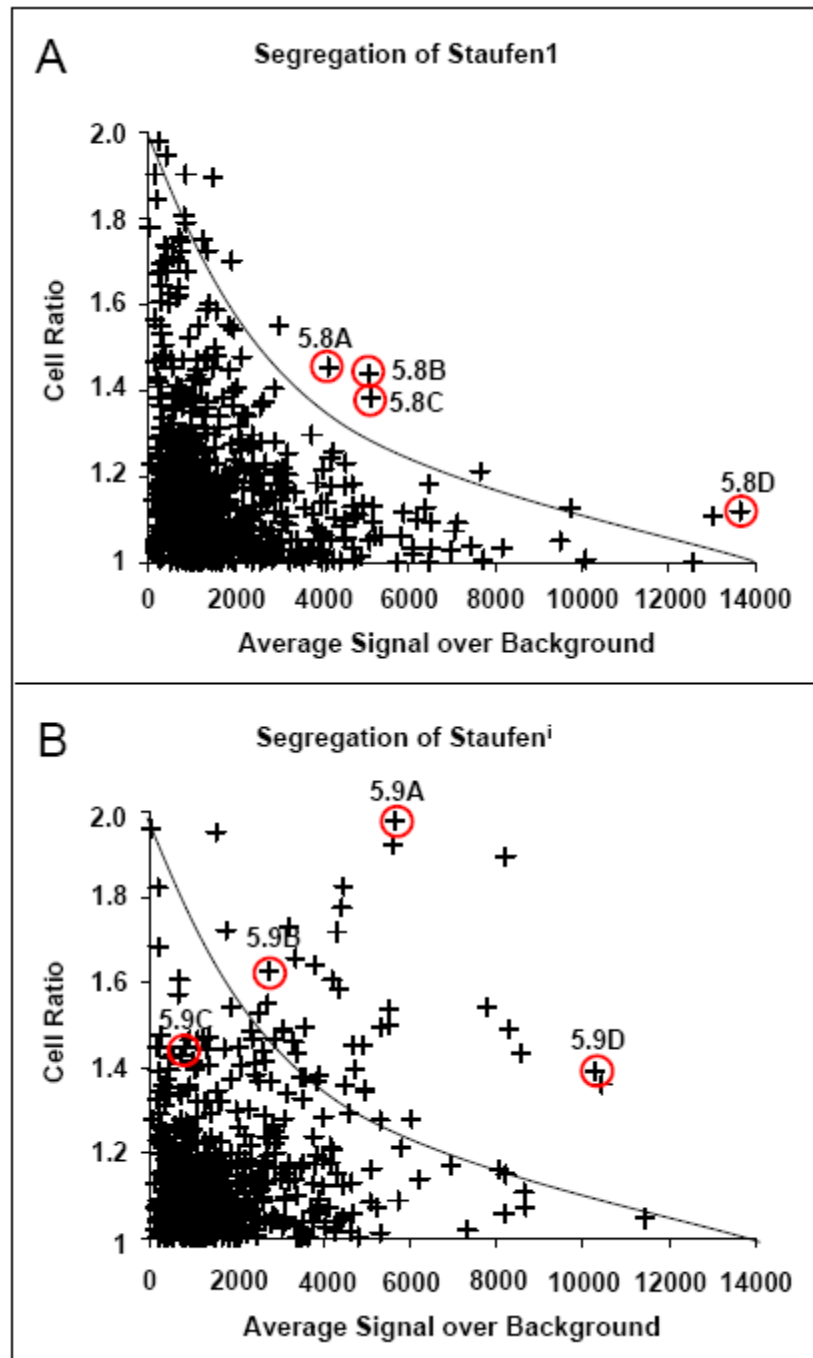


**Figure 5.26: Quantification of Staufen protein segregation.** Circled data points correspond to Movies 5.8A-D and 5.9A-D. Ratio of sister cell fluorescence over average fluorescence signal of sister cells of Staufen1 expressing cells (A). Ratio of sister cell fluorescence over average fluorescence signal of sister cells of Staufen<sup>I</sup> expressing cells (B). Results show data points from 2 independent experiments.

Supplemental Movie 5.8A shows dividing Staufen1 expressing cells that differ in their focal plane shortly after division, which may account for a high cell ratio. In Supplemental Movie 5.8B the dividing cells are located at the edge of the cell culture dish which causes uneven background fluorescence and therefore also a high fluorescence ratio. Supplemental Movie 5.8C shows dividing cells with equally strong signal in both sister cells. No obvious difference can be observed that would account for the high fluorescence ratio. In Supplemental Movie 5.8D sister cells both express equally high levels of VENUS protein which is reflected in the low cell ratio, but high FOB.

Supplemental Movie 5.9A shows a Staufen<sup>i</sup> expressing cell that appears to contain clumps of fluorescent protein. Upon division these clumps are segregated unevenly and it seems that the upper cell receives more protein. This uneven segregation of clumpy protein is reflected by a cell ratio of 1.98. Also in Supplemental Movie 5.9B Staufen<sup>i</sup> overexpression causes the formation of clumps which appear to be segregated unevenly during division resulting in a high cell ratio. In Supplemental Movie 5.9C cells express a low level of Staufen<sup>i</sup> and seem not to differ in their expression strength. In contrast, Supplemental Movie 5.9D shows cells that express a high level of Staufen<sup>i</sup> in clumps that seem to get segregated slightly unevenly during division.

It is evident from the plots denoting Staufen1 and Staufen<sup>i</sup> cell ratios, that in Staufen<sup>i</sup> overexpressing cells, the number of cells with potential asymmetric segregations is higher than in Staufen1 overexpressing cells. When analyzing these events closely, however, we found that Staufen<sup>i</sup> overexpressing cells often contain clumps that make correct quantification difficult. According to published data (Duchaine, Wang et al. 2000), these clumps are an overexpression artifact and are not an indicator of asymmetric protein segregation. In concordance with the literature we could only see these clumps in cells with high Staufen<sup>i</sup> signal.

In summary, we did not find asymmetrically segregated Staufen1 or Staufen<sup>i</sup> fusion proteins in HSC. Sister cell fluorescence intensity ratios stayed below the cutoff of 2 and cells that displayed ratios between 1.5 and 2 were due to uneven background or in the case of Staufen<sup>i</sup> due to overexpression artifacts and do not reflect asymmetrically segregated protein.

#### 5.2.4.3. Evaluating the Number of Analyzed Divisions

We have monitored 650 divisions for each of the Staufen1 isoforms. This seems like a large number of divisions; however a number of factors have to be taken into consideration. First, it is important to know if the monitored divisions were really first *in vitro* HSC divisions. Second, not all cells in the isolated starting population possess HSC capacity. And third, not every HSC may undergo asymmetric division.

To address the first point it is necessary to elucidate the number of cells that had divided before the start of the movie monitoring protein segregations. As mentioned above, our movies were started only after a non visualized 44h infection period. This time frame for infection was chosen, since by this time the infection of HSC was completed and a fluorescent signal could be detected by microscopy (data not shown). We did not know however if during this infection period the plated cells had divided already. Therefore, we decided to elucidate the divisional behavior of cells during the infection period. To this end we visualized cell behavior of freshly isolated HSC cultured under the same conditions as the cells during infection. When we analyzed the behavior of cells cultured under infection conditions during the first 70h, we found that 46% of cells divided at least once, 48% of cells died and only 6% of cells survived without division until the end of the movie (Figure 5.27A).

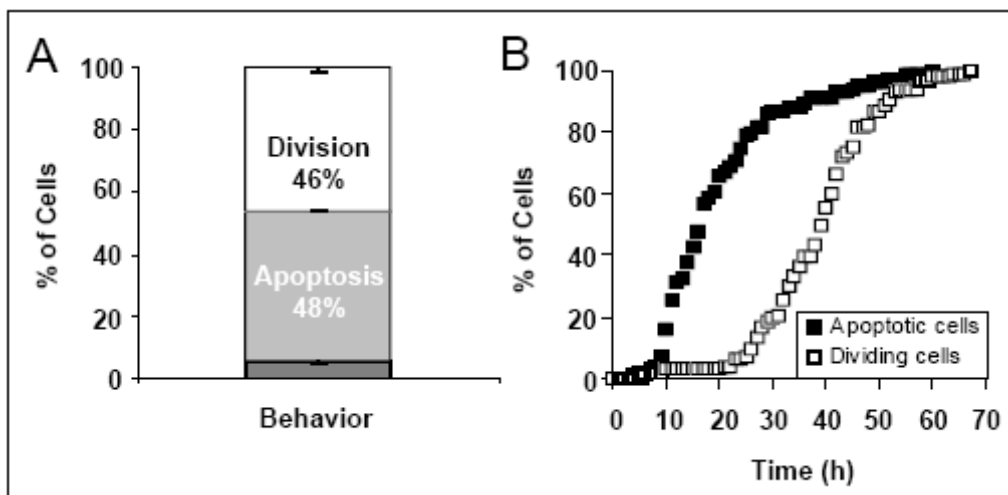


**Figure 5.27: Evaluation of cell behavior during non video monitored infection period.** Cell fates of HSC after 70h in SCF. Fate of starting cell is shown: Division, Apoptosis and Nothing (does not divide or apoptose). Data shows average of two independent experiments with 207 colonies analyzed (A). Kinetics of first division and apoptosis over time during first 70h. Data

The high percentage of divisions and apoptoses was a surprise, as we had assumed SCF without the addition of any proliferative signal to be neutral, providing survival and quiescence signals to the cells. We wanted to know if within the dividing cells the first division already took place during the 44h infection period or if they divided at a later time during which we had already started our movie and could then visualize and quantify divisions.

We found that after 44h 73% of surviving cells had undergone their first division (Figure 5.27B). Therefore, we could deduct from this that only 27% of the divisions monitored in our segregation movies were really first divisions. Having quantified 650 divisions each for *Staufen1* and *Staufen1*<sup>i</sup>, we can conclude from the divisional behavior in SCF within the first 44h, that only 27%, that is 175 divisions, were really first divisions. Combining HSC isolation protocols (Osawa, Hanada et al. 1996; Kiel, Yilmaz et al. 2005; Wilson, Laurenti et al. 2008) we know that within the monitored cells more than 47% are true HSC. That leaves us with at least 82 first HSC divisions out of the initial 650. And if we assume that asymmetric cell division only occurs in e.g. a third of total divisions (a much lower probability of ACD would render this process not important for cell specification) we have 27 divisions in which we would expect to see asymmetrically segregated protein. From this we can conclude that it should be sufficient to monitor 650 divisions in this matter, and that

neither Staufen1 nor Staufen<sup>i</sup> segregate asymmetrically in HSC when overexpressed as fusion genes as we would have recorded these asymmetric segregations within the number of divisions quantified.

As we recorded apoptosis in 48% of cells during the first 70h when cultured under infection conditions, we were curious to know if these cells that died during this time, did so after or before the end of the 44h culture period. When we looked at the kinetics of apoptosis of these cells, we found that more than 90% of apoptotic cells had died before the cells were switched to SCF and TPO at 44h (Figure 5.27C). Therefore, those cells would be dead already at the start of the movie examining segregations. The early time of apoptosis of such a high number of cells can be caused by negative influence of the sorting process on the cells, but when culturing cells in SCF and TPO, apoptosis of starting cells was not higher than 25% (Figure 5.7B), indicating that the high number of apoptoses cannot be due to damage from the sorting process alone. It is possible that a subtype of cells with HSC surface phenotype is not responsive to SCF and therefore, does not receive survival signals. HSC are sorted for cells that express high levels of c-kit, the receptor of SCF. Therefore, a lack of SCF responsiveness cannot be due to a complete lack of c-kit, but to either rapid downregulation of c-kit or blocked signaling pathways downstream of c-kit (Wandzioch, Edling et al. 2004) inducing apoptosis in a subset of cells. However, our results for division and survival of SCF cultured cells are similar to data from Selta et al., who found a slightly higher division rate (55% compared to our 46%) but a lower apoptosis rate (30% compared to our 48%) when culturing HSC in SCF for 72h (Seita, Ema et al. 2007).

#### **5.2.4.4. Pumilio1 Is Not Segregated during HSC Divisions**

When planning segregation movies for Pumilio1, we decided that we would be able to observe a higher percentage of first divisions when our infection period would be shorter than the 44h. In addition, infection of HSC with Pumilio1VENUS fusion virus showed in initial experiments, that VENUS signal could be detected as soon as 30h after start of infection (data not shown). Therefore, we decided to reduce the infection period for Pumilio1 to 30h during which time less than 20% of HSC had

divided in infection condition time lapse movie, another 51% of cells had divided between 30h and 44h (Figure 5.27B).

For Pumilio1 we initially monitored 266 divisions in a two day time-lapse movie. Of these 266 divisions, 212 divisions were first divisions and out of these, 99 divisions were generated from cells with true HSC potential. If a third of these cells divide asymmetrically and use the segregation of Pumilio1 as a means to accomplish an asymmetric fate choice, we would expect to observe 33 divisions with a fluorescence sister cell ratio above 2. However, we did not find sister cell pairs that differed in their fluorescent intensity as much (Figure 5.28).

Like in time-lapse movies monitoring Staufen1 and Staufen<sup>i</sup> protein segregations, we found variations in background intensity ranging from 463 to 7589 fluorescence units (FU) when examining Pumilio1 segregation (data not shown). FOB also varied widely in Pumilio1 expressing cells from only 78 to 5350 (Figure 5.28A), which is probably due to cells containing different copy numbers of the fusion gene.

Even though there were no sister cell pairs with a ratio of fluorescence of above 2, we still took a closer look at divisions that had a FOB of above 3000 or a fluorescence ratio above 1.4. Supplemental Movie 5.10A shows a Pumilio1 expressing cell that is dividing. No obvious difference in intensity of fluorescence can be observed between the two sister cells. The cell pair depicted in Supplemental Movie 5.10B also displays cell ratio and FOB slightly above the arbitrary threshold. Observing the corresponding Supplemental Movie 5.10B the two sister cells seem to have different sizes in addition to laying on top of fluorescent debris. This may account for the high cell ratio, however as we did not find any cell pairs with similar size difference it might be an overexpression artifact. In Supplemental Movie 5.10C the two Pumilio1 expressing sister cells seem to be slightly out of focus at the time of division. Shortly thereafter though, they express relatively high amounts of Pumilio1 in their cytoplasm. In Supplemental Movie 5.10D the sister cells expressing Pumilio1 both have low levels of fluorescence (average FOB 1189) as can be also seen in Figure 5.28. A bit of fluorescent debris is present underneath the cells and in addition with higher measuring error in low expressing cells can account for the cell ratio of 1.42.

Overall these results indicate that Pumilio1 when overexpressed in HSC as a fusion protein does not segregate asymmetrically in daughter cells. Fluorescence

ratios of sister cell pairs shortly after division only rise above an arbitrary threshold when fluorescent debris is present, the background fluorescence is uneven, or the area definition for the fluorescence measurement was imprecise.

When we analyzed Pumilio2 segregation during HSC divisions, we found that the fluorescence signal from the fusion gene was barely detectable over the background. We found maximum signal strength of 11.5% of background fluorescence in Pumilio2 expressing cells (data not shown), whereas we had found maximum signal strength of 267.7% of background fluorescence in Pumilio1 expressing divisions. In addition, we found only very few sister cell pairs positive for Pumilio2 signal. This was probably due to the low titer of the virus which we used to infect HSC. Virus titer for Pumilio2 fusion gene was never higher than  $2 \times 10^6$  per ml, whereas titers of other fusion genes ranged from  $1 \times 10^7$  to  $1 \times 10^8$  per ml. We think that the long ORF of Pumilio2 (3.2kb) or structural problems influence proper VENUS signal and that thereby titers and infection efficiency stay low because single integrations might give a too low signal and cannot be detected. In any case, we decided that our fusion gene overexpression approach cannot be used for the Pumilio2VENUS fusion and therefore did not monitor any further divisions of Pumilio2 expressing HSC. We cannot conclude if Pumilio2 is segregated during HSC divisions as not enough divisions of Pumilio2 expressing cells could be monitored due to inefficiency of Pumilio2 lentivirus.

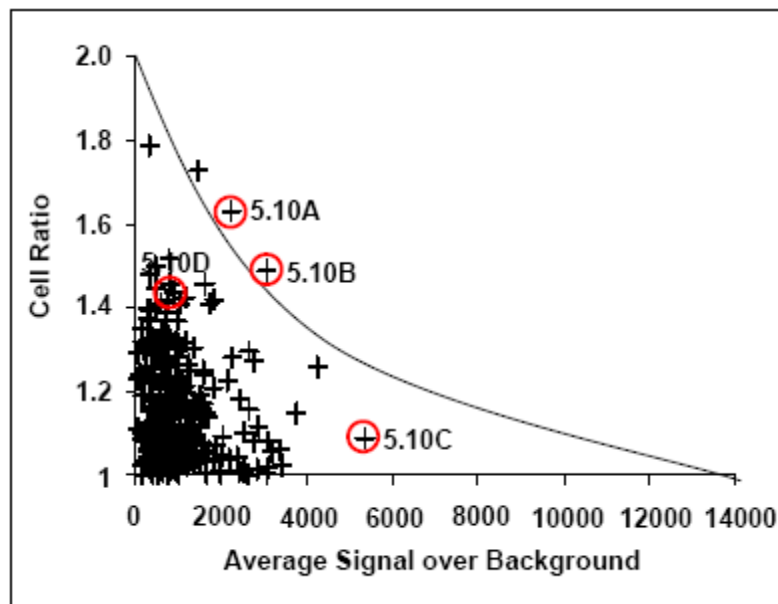


**Figure 5.28: Quantification of Pumilio1 protein segregation.** Circled data points correspond to Movies 5.10A-D. Ratio of sister cell fluorescence over average fluorescence signal of sister cells of Pumilio1 expressing cells. Results show data points from 2 independent experiments.

### 5.2.5. Influence of Candidate Genes on Fate Decisions

In addition to the role of our candidate genes in protein segregation during HSC division, we wanted to know if these genes play a role in fate decisions of HSC. Therefore, we overexpressed candidate genes in HSC by using a lentiviral vector and observed the influence of candidate genes on colony potential, lineage choice and proliferation ability. For this purpose we used our viral vectors containing IRES expression cassettes to allow for wildtype overexpression of candidates in HSC.

As for experiments examining protein segregation, we again sorted CD150<sup>+</sup>CD48<sup>-</sup>CD34<sup>+</sup>KSL as HSC population (Figure 5.29A). HSC were infected with lentivirus during a 72h infection period in stroma free culture containing SCF and TPO (Figure 5.29B). During this time frame virus was allowed to integrate into the genome and cells to proliferate. The longer infection period also allowed time for accumulation of VENUS protein in these cells to yield a stronger fluorescence signal. We know that after 3d of culture in SCF and TPO only 61-72% of initial HSC potential is left (Ema, Takano et al. 2000). However, a colony formation assay does not read out HSC potential but rather multipotency of cells and therefore, these infection

conditions are good enough for this *in vitro* analysis of fate potential. After the infection period, cells positive for VENUS expression, reflecting successful infection and overexpression of candidate genes, were resorted, counted and plated into methylcellulose containing cytokines allowing formation of all myeloid lineages (M3434) (Figure 5.29C). We had found it to be very difficult and time consuming to judge if a colony is positive for VENUS expression in dense colonies in methylcellulose. Therefore, by plating only VENUS positive colonies, we ensured that all colonies within the dish were positive and did not have to be analyzed for VENUS expression when determining colony type at the end of the experiment.

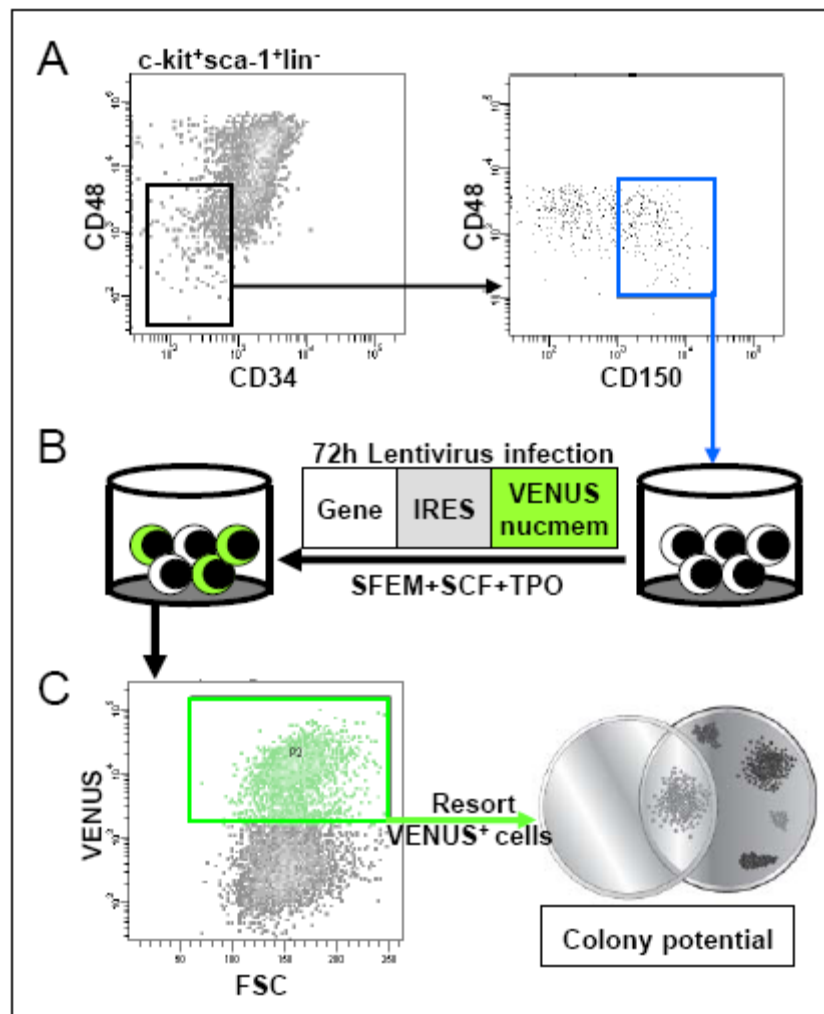


**Figure 5.29: Experimental setup examining the *in vitro* effects of candidate genes on progenitors.** Sorting scheme, isolation of CD34<sup>+</sup>CD48<sup>+</sup>CD150<sup>+</sup> KSL cells for experiments examining *in vitro* effects (A). Experimental setup of lentiviral infection (B). Resort of VENUS<sup>+</sup> cells and plating into colony assay (C).

As infection efficiency as well as signal strength varied widely between fusion gene lentiviral vectors, we decided to first analyze these two parameters using the IRES construct lentiviral vectors before examining the effect of candidate genes on HSC lineage potential *in vitro*. As described above, for the vector control virus we saw an infection efficiency of 92.8% ( $\pm 5.0$ ) (Figure 5.30A), whereas lentiviral infection with viruses containing various candidate genes resulted in lower efficiencies. *Staufen1* expression resulted in 18.5% ( $\pm 10.7$ ) of positive cells, while infection with *Staufen<sup>i</sup>* containing virus yielded 42.6% ( $\pm 20.5$ ) of cells positive for VENUS expression. Infection efficiencies for the two *Quaking1* isoforms were similar: overexpression of *Quaking1-6B* and *5A* resulted in 35.5% ( $\pm 9.6$ ) and 36.1% ( $\pm 11.1$ ) of cells respectively being positive for VENUS expression. When we examined lentiviral vectors containing *Pumilio1* and *Pumilio2* we found only 3.9% and 4.6% of cells respectively to express VENUS.

The mean fluorescence of VENUS<sup>+</sup> cells denotes the signal strength and gives information as of how well positive and negative populations can be separated by FACS. When cells were infected with control virus we detected a mean fluorescence of 27852.2 FU ( $\pm 11090.6$ ) in VENUS<sup>+</sup> cells (Figure 5.30B). Mean fluorescence of cells infected with candidate gene vectors was much lower. *Staufen1* and *Staufen<sup>i</sup>* overexpression led to similar values of mean fluorescence of positive cells (5726.2 FU  $\pm$  3027.1 and 7044.6 FU  $\pm$  4040.4 respectively). *Quaking1 6B* and *5A* showed a mean fluorescence of 15054.7 FU ( $\pm 999.0$ ) and 14452.7 FU ( $\pm 446.4$ ) respectively. Overexpression of *Pumilio1* and *Pumilio2* however resulted in only 1619 FU and 2768 FU respectively of mean fluorescence in VENUS<sup>+</sup> cells.

In summary, infection efficiencies for IRES containing lentiviral vectors co expressing either *Staufen1*, *Staufen<sup>i</sup>*, *Quaking1-5A* and *6B* were not as good as for vector control virus, but still high enough to answer questions regarding fate decisions in HSC progeny. Similarly, mean fluorescence levels of VENUS positive cells in candidate infected cells were lower than in vector control infected cells, but still high enough such that the VENUS<sup>+</sup> population could be easily separated in FACS from the VENUS<sup>-</sup> population. In contrast, infection efficiencies for *Pumilio1* and *2* were extremely low and also mean fluorescence levels of those few positive cells did not allow clean separation of VENUS<sup>+</sup> from VENUS<sup>-</sup> cells. We therefore decided to use *Pumilio1* fusion virus instead of the IRES virus to examine the effect of *Pumilio1*

on lineage decision, even if the fusion protein could have altered function compared to the wild type. Pumilio1 fusion virus showed high infection efficiencies of 31.5% ( $\pm 2.4$ ) and high mean fluorescence of positive cells of 13740.5 FU ( $\pm 598.8$ ). Unfortunately, for Pumilio2 we could not use the fusion virus since this also resulted in a low number of infected cells with barely detectable mean fluorescence, as shown above.

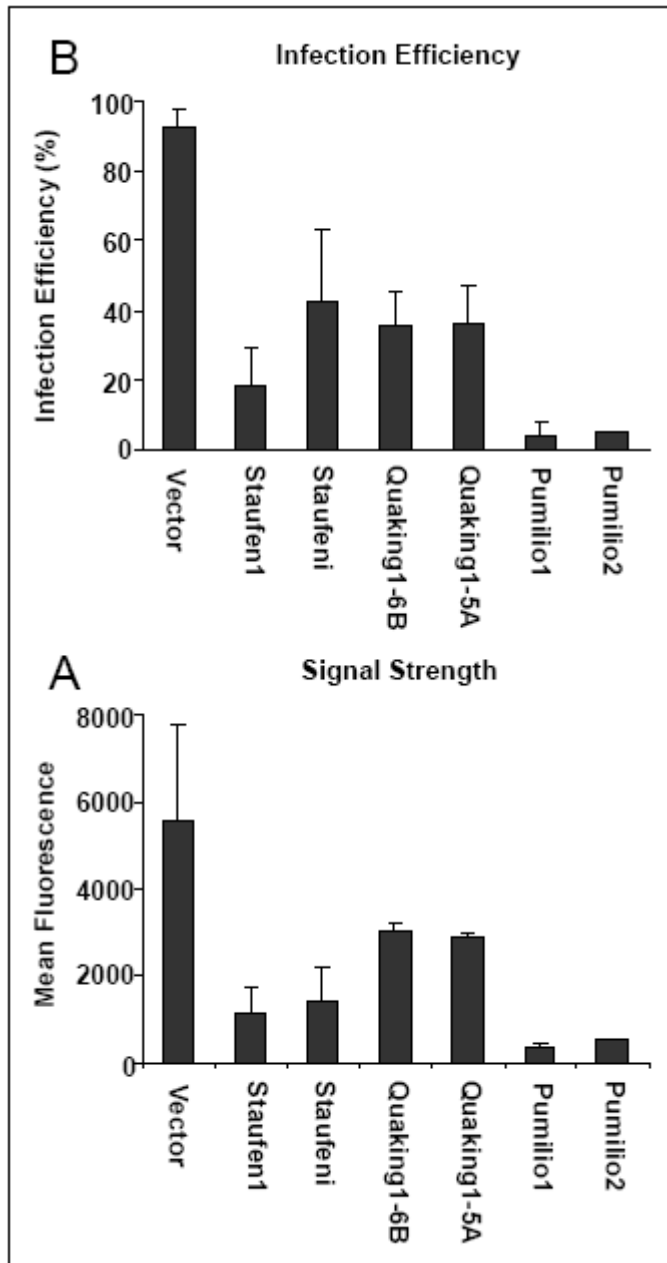


**Figure 5.30: Properties of IRES construct lentivirus vectors.** Efficiency of lentiviral vector infection from different candidate genes as measured by FACS, all are IRES constructs (A). Mean fluorescence of VENUS positive cells of candidate lentivirus infected cells as measured by FACS (B). Results show average of three independent experiments. Error bars show standard deviation.

#### **5.2.5.1. No Influence of Staufen1 and Staufen<sup>i</sup> on Proliferation and Lineage Choice of Progenitor Cells *In Vitro***

We analyzed the influence of Staufen1 and its splice isoform Staufen<sup>i</sup> on HSC lineage decision. We found that both isoforms allowed formation of all mature myeloid lineages. Colony formation potential and proliferation was also not affected by either Staufen1 or Staufen<sup>i</sup> overexpression. In addition, we found that the proportions of different colony types were similar to those produced by vector control overexpressing HSC (Figure 5.31A). However, since a role for Staufen in leukemia was suggested previously (Faubert, Lessard et al. 2004), we decided to look at colony potential during serial replatings. Leukemic cells should be able to be replated indefinitely, retaining a constant colony potential efficiency. When we replated colonies for five times we saw varying percentages of colony potential, however overall colony potential decreased in vector control as well as Staufen1 and Staufen<sup>i</sup> infected cells, until almost no more cells grew in culture after the fifth replating (Figure 5.31B and 5.32A). In addition to similar colony potential, the absolute number of colonies was also similar in Staufen1, Staufen<sup>i</sup> and vector control infected cells (Figure 5.32B). Therefore, Staufen1 and Staufen<sup>i</sup> are unlikely to cause aberrant cell proliferation seen in leukemia.

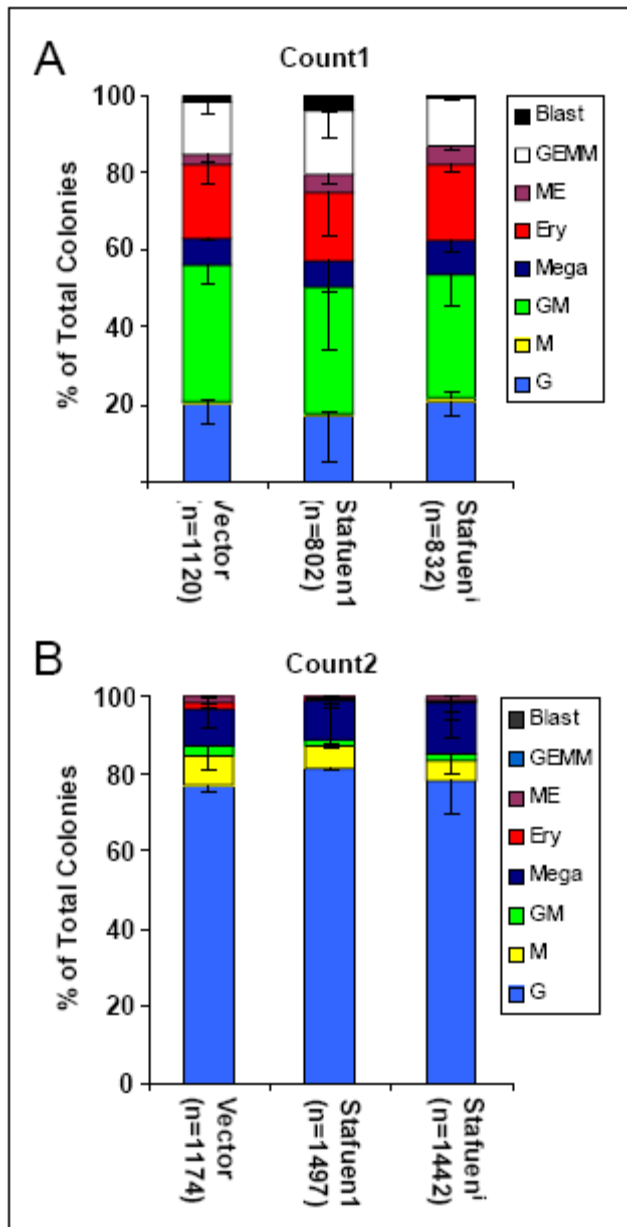


**Figure 5.31: No influence of Staufen1 on *in vitro* fate decisions.**

Influence of Staufen1 isoforms on lineage choice and colony formation of HSC, count1 (**A**). Colony formation and lineage choice of Staufen1 and Staufen<sup>i</sup> expressing cells after first replating, count2 (**B**). Data shows the average of three independent experiments with three replicates each. Error bars show standard deviation

When we analyzed the multipotency of colonies we found that it decreased already after the first replating. In the first count we could observe 20% ( $\pm 5.2$ ) of G colonies and 13.4% ( $\pm 3.1$ ) of multipotent GEMM colonies in vector controls (Figure 5.31A). In the second count after the first replating however, we counted 77.3% ( $\pm 1.9$ ) G colonies, but no multipotent GEMM colonies (Figure 5.31B). In the third count we could observe almost 100% G colonies with only very few Megakaryocytes present (data not shown). Similar results were obtained for cells overexpressing Staufen1 or Staufen<sup>i</sup> (Figure 5.31A and B).

In summary we found that although at least one of the Staufen1 splice isoforms is expressed at the mRNA level in HSC and bone marrow progenitor

populations, overexpression of neither form influences lineage decisions and proliferation ability of progenitor cells *in vitro*.

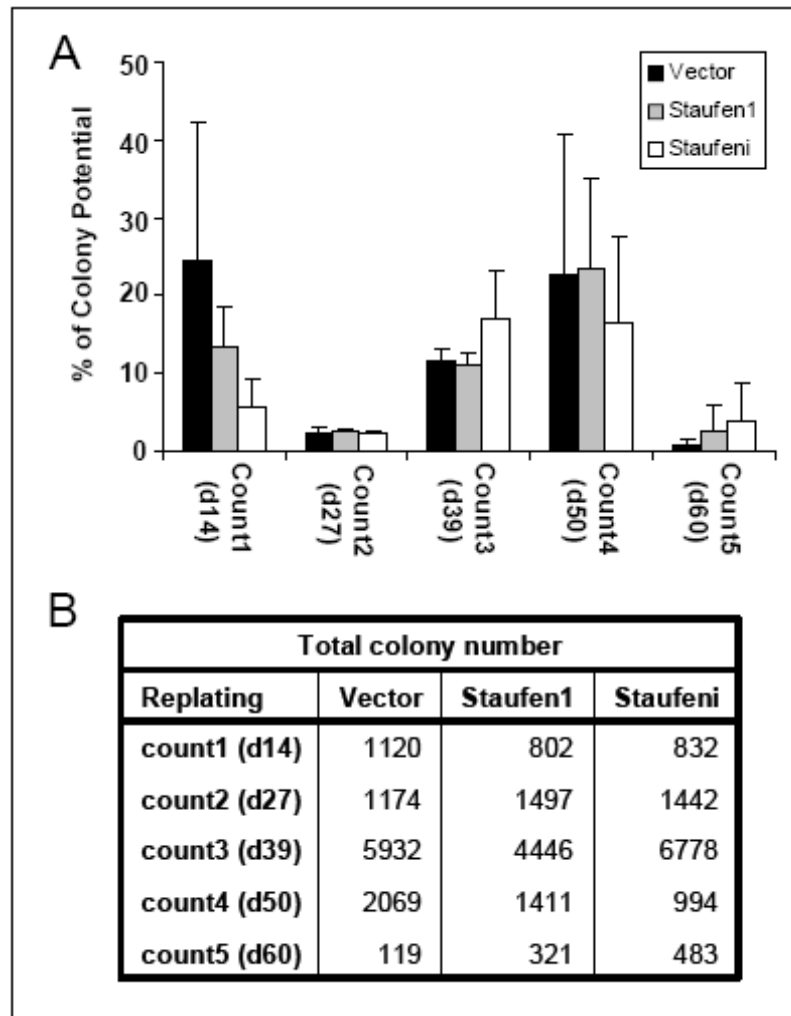


**Figure 5.32: Staufeni does not cause aberrant proliferation *in vitro*.** After analysis of colonies in methylcellulose, colonies were dissociated and resulting cells replated in fresh methylcellulose. Colony potential is the number of seeded cells divided by the number of resulting colonies. Colony potential of infected cells over five replatings (**A**). Total colony number in each replating (**B**). Data shows the average of two independent experiments with three replicates each. Error bars show standard deviation

#### 5.2.5.2. Negative Influence of Pumilio1 on *In Vitro* Progenitor Potential

As shown above, when trying to overexpress Pumilio1 using an IRES construct, we found that virus titers and efficiencies of expression in HSC were very

low ( $6 \times 10^5$  and 4% respectively). As discussed earlier we therefore decided to use the Pumilio1VENUS fusion constructs instead, which we had successfully used in segregation studies, to analyze Pumilio1 function on HSC fate decisions. When we infected HSC with Pumilio1 VENUS containing lentiviral vector we found 31.5% ( $\pm 2.4$ ) of cells to be infected with the virus. A colony assay of VENUS<sup>+</sup> replated cells resulted in normal proliferation and the formation of colonies of all myeloid lineages. We saw however decreased colony formation potential from 25.1% in vector control expressing cells to 10.3% in Pumilio1 expressing cells. Moreover, we saw an increase in the percentage of GM colonies from 31.9% ( $\pm 6.0$ ) to 66.3% ( $\pm 6.4$ ,  $p=0.007$ ) and a decrease of G colonies from 38.6% ( $\pm 1.9$ ) to 9.6% ( $\pm 1.1$ ,  $p=0.03$ ) when cells expressed Pumilio1 compared to vector control. Therefore, Pumilio1 seems to have an influence on GM fate decisions. In addition, when we reanalyzed VENUS expression by FACS after counting of colonies, we found only 3% ( $\pm 0.3$ ) VENUS<sup>+</sup> cells, while 64.2% ( $\pm 11.6$ ) of vector infected cells were still VENUS<sup>+</sup>. We do not know if only individual cells of Pumilio1 expressing colonies were negative or if whole colonies did not express Pumilio1. This indicates that cells Pumilio1 expression was detrimental to either cell survival or proliferation leaving only cells without exogenous Pumilio1 expression. As control infected cells also displayed a reduced percentage of VENUS<sup>+</sup> cells, it is likely that some cells silenced both VENUS and candidate gene expression (Figure 5.33).

For Pumilio2 we encountered the same problem as for Pumilio1. Although viral titers for Pumilio2 IRES viral vectors reached  $1 \times 10^7$ , infection efficiencies of HSC did not exceed 5%. Unlike Pumilio1, where we could increase infection efficiency using virus expressing a fusion gene, using Pumilio2VENUS fusion constructs did not increase the efficiency of viral infection. Therefore, we decided not to analyze the effect of Pumilio2 on fate decisions in HSC by this method. In summary we think that Pumilio1 and 2 could have a toxic effect on HSC or their progeny resulting in a low number of Pumilio2 overexpressing cells and loss of Pumilio1 positive cells after differentiation.

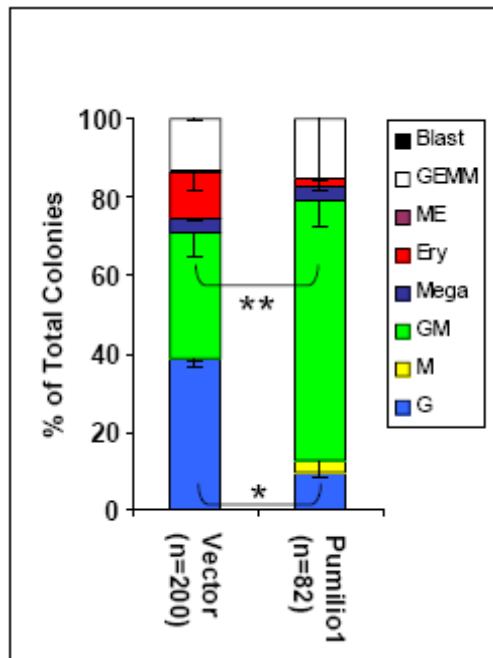


**Figure 5.33: Pumilio1 alters lineage choice *in vitro*.** Influence of Pumilio1 on lineage choice and colony formation of HSC. GM colonies are increased ( $p=**$ ) and G colonies reduced ( $p=*$ ) in Pumilio1 expressing colonies. Data shows the average of two independent experiments with three replicates each. Error bars show standard deviation, \* =  $p<0.05$  \*\* =  $p<0.01$

### 5.2.5.3. Quaking1 Influences GM Lineage Decisions

We chose to evaluate the influence of Quaking1 on fate decisions of HSC because of indications that it could be a downstream target of Pumilio. In *C.elegans* the Quaking1 homolog Gld1 is regulated by Fbf, a Pumilio homolog, and acts as Pumilio's effector to carry out fate decisions (Crittenden, Bernstein et al. 2002; Suh, Jedamzik et al. 2006). In addition, Quaking also plays a role in germ cell fate decisions and regulates targets at the RNA level (Francis, Maine et al. 1995; Ebersole, Chen et al. 1996).

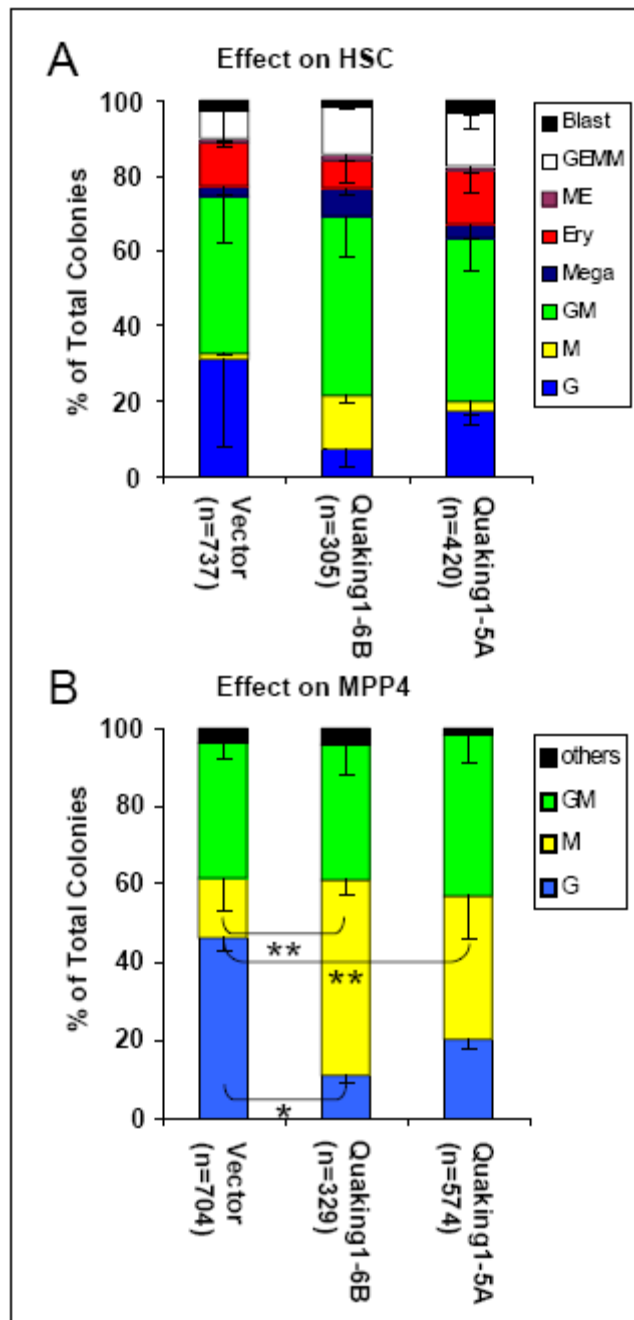
Quaking1 gene produces three different known isoforms that provided us with natural mutants and would make any observed effects caused by one isoform but not the others more significant. Quaking1-7B ORF is identical to Quaking1-6B ORF. These two splice isoforms only differ within their 3'UTR but not within their ORF. The third Quaking1 isoform, Quaking1-5A differs within the 3' portion of its ORF from the other two isoforms. Therefore, we generated two constructs containing the two different ORF which we will subsequently refer to as Quaking1-5A and Quaking1-6B. Introducing these two splice variants into HSC by lentiviral overexpression allowed formation of all myeloid lineages, including megakaryocytes, erythrocytes, granulocytes and macrophages. The colony formation and proliferation capacity of HSC was also not affected by overexpression of either transgene as can be seen in

Figure 5.34A. Moreover, all types of colonies including multipotent GEMM colonies could be produced by Quaking1 overexpression. However, we saw an increase of macrophage (M) colonies in Quaking1-6B expressing colonies ( $14.0\% \pm 1.8$ ,  $p=0.07$ ) compared to empty vector control ( $1.5\% \pm 0$ ). Therefore, we decided to focus on the role of Quaking1 in GM progenitors.

To analyze Quaking1 effects in GM progenitors, it was important to choose the right starting population that would after a 72h proliferation period still contain bipotent cells that can produce GM colonies as well as unipotent cells with either G or M potential. Using CMP as a starting population, we found that after 72h in SCF and TPO, these cells could give rise to only very small and few unipotent colonies (data not shown). Therefore, we decided to use cells that had lost their self renewal capacity, but that were still multipotent. We chose MPP4 (Wilson, Laurenti et al. 2008) and isolated them as  $CD34^+Flt3^+CD48^+KSL$  cells. When we infected these cells and cultured them for three days in SCF and TPO, we found that mainly colonies of the GM, G and M type were produced, but very few colonies with ME type (Figure 5.34B). Therefore, this population was useful to examine the effect of Quaking1 isoforms on GM lineage decisions.

Introducing Quaking1-6B and -5A into these MPP4, we found a higher number of M colonies ( $50\% \pm 4.5$ ,  $p=0.04$ , and  $36\% \pm 10.8$ ,  $p=0.09$ , respectively) compared to control ( $15.8\% \pm 9.0$ ). The number of G colonies was reduced in Quaking1-6B and 5A ( $11.2\% \pm 2.3$ ,  $p=0.006$  and  $20.4\% \pm 2.7$ ,  $p=0.008$ , respectively) compared to empty vector control infected MPP4 ( $46.8\% \pm 3.5$ , Figure 5.34B). We then checked absolute colony numbers produced by Quaking1-5A and -6B infected MPP4 and normalized them to absolute colony numbers of vector control infected cells. We found that in Quaking1-6B expressing cells the number of M colonies was higher at the expense of G colonies and constant GM colonies compared to vector controls, indicating that Quaking1-6B influenced lineage choice between G and M in bipotent progenitors. In Quaking1-5A expressing cells the number of GM colonies was higher at the expense of G colonies compared to vector controls. This indicates that bipotent GM progenitors preferentially produced GM colonies than G colonies. In summary, Quaking1 isoforms when overexpressed in HSC and progenitor cells allow differentiation and maturation into all myeloid lineages. However, Quaking1 isoforms

seem to influence lineage decisions within the GM lineage and slightly interfere with formation of G colonies.



**Figure 5.34: Influence of Quaking1 on in vitro fate decisions.** In HSC, Quaking1-6B affects G versus M lineage decisions (A). In MPP4, both Quaking1 isoforms affect G versus M lineage decisions. Quaking1-6B and -5A increase G ( $p=**$ ), Quaking1-6 decreases M ( $p=**$ ) (B). Data shows the average of two independent experiments with three replicates each. Error bars show standard deviation, \* =  $p < 0.05$  \*\* =  $p < 0.01$

## **5.2.6. Influence of Candidate Genes on *In Vivo* HSC Potential**

### **5.2.6.1. Reconstitution Potential of Candidate Transduced HSC Reveals Influence of Candidates during Expansion Conditions**

#### **5.2.6.1.1. Contribution to Peripheral Blood of Recipient Mice**

Except for Pumilio1, our other candidate genes had little or no effects on lineage decisions of hematopoietic progenitors and none of the candidates seemed to be segregated during HSC division. However, as *in vitro* assays can not adequately assess HSC function, we decided to analyze effects of candidate genes on HSC themselves *in vivo*. To this end we transduced HSC with virus containing overexpression constructs of Staufen1, Staufen<sup>l</sup>, Pumilio1, Quaking1-5A and Quaking1-6B for two days in medium containing SCF only. Following assessment of the infection efficiencies by counting positive and negative cells in a snapshot image, all the cells (both transduced and non-transduced) were transplanted into recipient mice (Figure 5.35A, transplants performed by Angelika Roth). For recipient mice we again chose the W<sup>41</sup>/W<sup>41</sup> Gpi1a Ly5.1 strain that does not require irradiation before receiving a bone marrow transplant. We examined the peripheral blood (PB) of these mice at 4, 8, 12 and 16 weeks after transplant for the presence of VENUS positive cells and CD45.2 donor type cells within the CD45<sup>+</sup> white blood cells (Figure 5.35B).

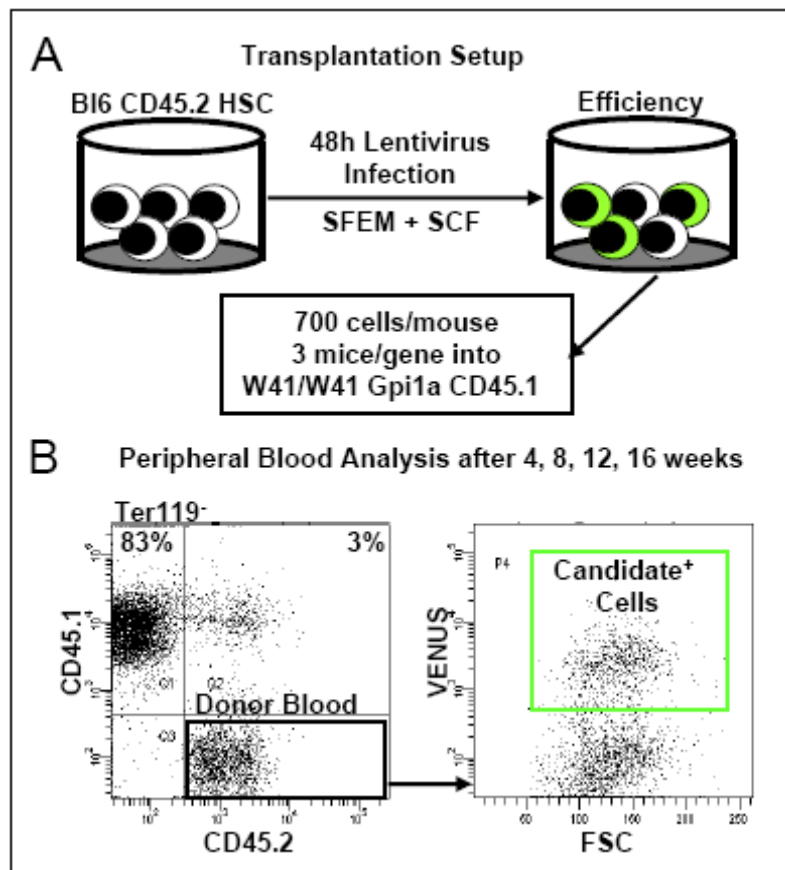


**Figure 5.35: Transplantation of candidate gene expressing HSC into  $W^{41}/W^{41}$  Gpi1a Ly5.1 mice.** Experimental setup of HSC infection and transplantation (A). Analysis of peripheral blood for percentage of donor contribution (CD45.2) and VENUS<sup>+</sup> cells (B).

All mice that had been transplanted showed donor type blood cells in their PB. The percentage of CD45.2 expressing blood cells increased from 0.5% to 1.5% at 4 weeks to 12.7% to 18% at 16 weeks in all mice irrespective of transgene expression (Figure 5.36A).

The transplanted cells had initially been transfected by viral vectors containing candidate genes separated by IRES from VENUS or in the case of Pumilio1 by vectors containing the VENUS fusion gene. Therefore, the percentage of VENUS expressing cells first reflects infection efficiency after the two day infection period and later, when isolating cells from the mouse, indicates survival of cells with overexpressed candidate genes. After the infection period, control cells showed an infection efficiency of 94%, whereas cells transduced with the various candidate genes showed infection efficiencies ranging from 13% to 45%. To account for the different

initial percentages of VENUS positive cells we normalized percentages of VENUS expressing cells isolated from the PB of the transplanted mice to the initial efficiencies (Figure 5.36B). However, we still observed a high difference in the percentage of VENUS<sup>+</sup> cells which we derived from mice transplanted with vector control infected cells compared to mice transplanted with candidate infected cells (Figure 5.36B).

The presence of donor type blood cells in the PB of the recipients 16 weeks after transplant is a good indicator for the presence of true HSC in the initial donor population as only HSC are able to continuously produce mature cells over the course of 16 weeks. If after 16 weeks the percentage of VENUS<sup>+</sup> cells within the donor type blood remains the same as in the starting population, this would indicate that infected cells and non infected cells possess the same amount of HSC potential and that there is no negative effect of overexpression on HSC behavior as read out by contribution to PB.

For control cells we found 72.9% ( $\pm 13.8$ ) VENUS<sup>+</sup> cells within the donor type population of the PB after 16 weeks (Figure 5.36B) compared to an initial 94% of VENUS<sup>+</sup> cells after infection. This could indicate that the virus per se has a slightly negative effect on HSC survival or behavior. In mice transplanted with Pumilio1 transduced cells we could barely detect any VENUS positive cells (highest: 2.7%  $\pm$  2.0 at 12 weeks), compared to 25% of initially infected cells, indicating a negative effect of Pumilio1 on HSC function. In mice transplanted with Staufen1 infected cells the percentage of VENUS<sup>+</sup> cells increased up to 14.6% ( $\pm 15.4$ ) at 8 weeks after which the percentages of VENUS<sup>+</sup> cells dropped to 8.7% ( $\pm 10.2$ ) at 16 weeks. In mice transplanted with Staufen<sup>i</sup> transduced cells the percentage of VENUS<sup>+</sup> cells rose continuously until 7.6% ( $\pm 0.4$ ) of cells were positive at 16 weeks. This indicates that Staufen1 and Staufen<sup>i</sup> overexpression in HSC allowed some HSC potential to be maintained as read out by the percentage of VENUS<sup>+</sup> cells in PB after 16 weeks however, it is likely that HSC function is influenced somehow. When analyzing PB of mice transplanted with isoforms of Quaking1 a decrease over time in PB contribution of VENUS positive cells was observed for both Quaking1-6B (from 9.7%  $\pm$  3.1 to 0.6%  $\pm$  0) and for Quaking1-5A (from 14.5%  $\pm$  0.7 to 2.3%  $\pm$  2.0).

In summary, the overexpression of Pumilio1, both Staufen1 isoforms as well as both Quaking1 isoforms in HSC proved to be detrimental to normal HSC function

as read out by contribution to PB. This result however does not explain how HSC function is affected by transgene overexpression. Therefore, we decided to analyze the bone marrow of the transplanted mice and examine the percentages of VENUS<sup>+</sup> cells in progenitor and HSC populations directly.

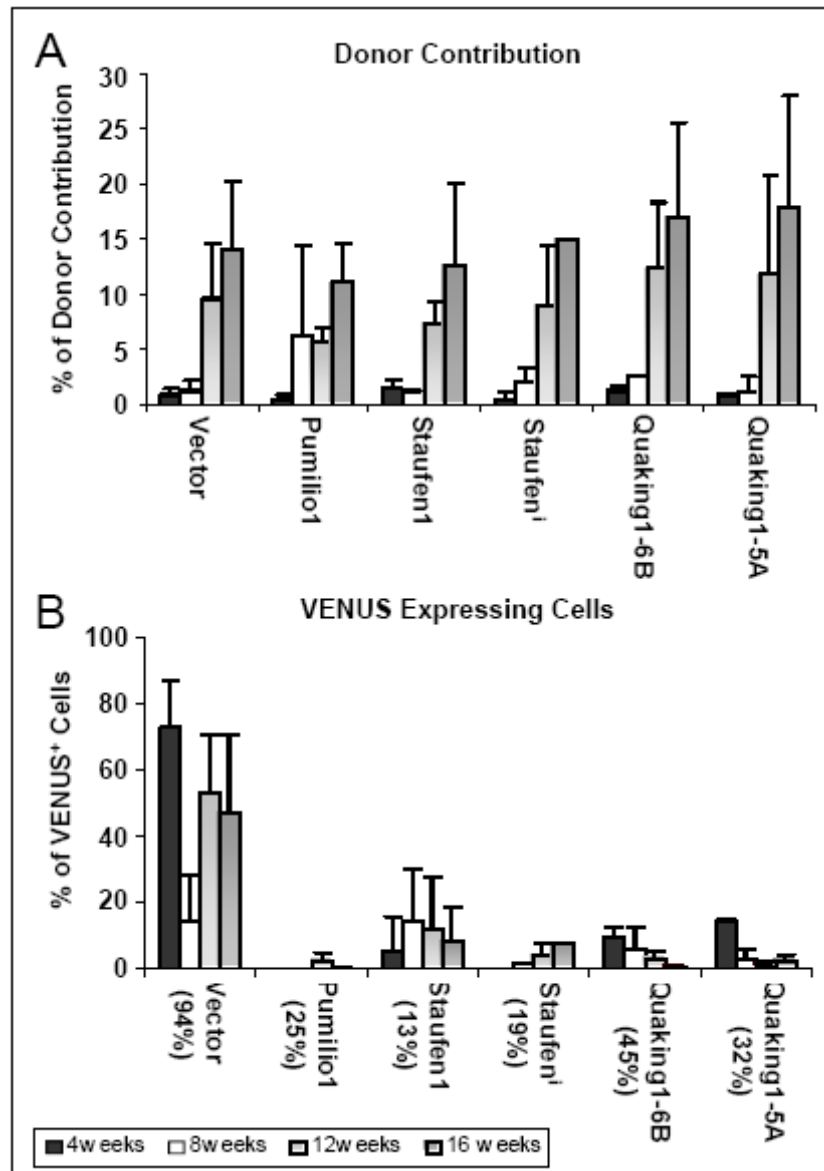


**Figure 5.36: Result of peripheral blood analysis of candidate transplanted mice.** Donor contribution in PB over 16 weeks (A). Percentage of VENUS<sup>+</sup> cells of PB donor type cells over 16 weeks. Percentages in parenthesis show initial infection efficiency before transplantation (B). Data shows the

### 5.2.6.1.2. Contribution to Bone Marrow Populations of Recipient Mice

Bone marrow populations of transplanted mice were analyzed at 18 weeks after transplant to elucidate the type of effect of candidate gene overexpression on HSC. We decided to first analyze one mouse each from the mice transplanted with cells transduced with the different viral constructs to be able to decide if and how secondary transplants should be performed with the bone marrow from the remaining mice. We assessed the percentage of CD45.2 cells within the CD45 expressing bone marrow cells. As was seen in the peripheral blood, donor type blood cells were equally contributing to the total bone marrow in all analyzed mice irrespective of transgene expression (a range of 32 - 48% of CD45.2 cells within total CD45 expressing cells). When we analyzed VENUS expression in the bone marrow, we assessed the percentage of VENUS<sup>+</sup> cells within each population. For example, 30.4% of all KSL cells in control mice are positive for VENUS expression (Figure 5.37A and B). We further found 85.1% of donor type cells positive for VENUS expression (Figure 5.37B). This percentage is very close to the initial infection efficiency of 94%. When examining HSC populations in the bone marrow of transplanted mice, we found however a lower percentage of cells to be VENUS positive. Only 39.4% of CD150<sup>+</sup>CD48<sup>-</sup>CD34<sup>-</sup>KSL cells expressed VENUS. This indicates that the viral vector alone has a slightly negative effect on stem cell maintenance; however, it allows normal production of progenitors and mature blood cells as we found the expected number of VENUS expressing donor blood cells.

Examining the bone marrow of mice transplanted with cells transduced with the various candidate genes, the results are quite different. Overexpression of Pumilio1 in transplanted HSC allowed only 1.2% of total donor type blood cells to survive in the bone marrow until 18 weeks and to still express VENUS (Figure 5.37C). No HSC maintenance was allowed by Pumilio1 overexpression as read out by the percentage of VENUS<sup>+</sup> cells within the CD150<sup>+</sup>CD48<sup>-</sup>CD34<sup>-</sup>KSL population. Staufen1 as well as Staufen<sup>i</sup> allowed only 3.1% and 1.6% respectively of total donor type blood cells to survive as measured by the percentage of VENUS positive cells. Neither isoform allowed the maintenance of HSC, however, in Staufen<sup>i</sup> transplanted mice we found 1.1% of VENUS<sup>+</sup> cells within the KSL population, a population which encompasses true HSC but has otherwise lost self-renewal capacity.

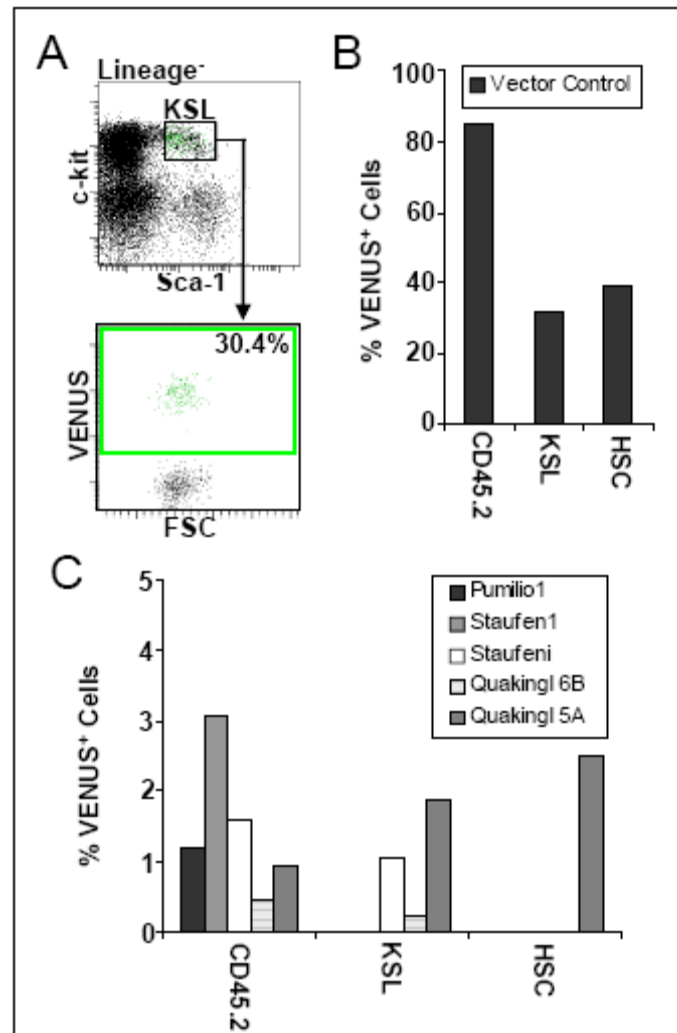


**Figure 5.37: Bone marrow population analysis of transplanted mice: HSC.** Example of FACS analysis: Percentage of VENUS<sup>+</sup> cells within the KSL population are analyzed (A) Percentage of VENUS<sup>+</sup> cells within CD45.2, KSL and HSC of vector control transplanted mice (B). Percentage of VENUS<sup>+</sup> cells within CD45.2, KSL and HSC of candidate gene transplanted mice (C). Results show data of one mouse.

For Quaking1-5A and Quaking1-6B we found only 0.4 % and 0.9% respectively of donor type blood cells to be positive for VENUS. Within the KSL population, only 0.2% of cells expressed Quaking1-6B, whereas 1.9% expressed Quaking1-5A. Concordantly, for Quaking1-6B no positive cells were found in the HSC compartment, whereas 2.5% of the cells within the HSC compartment expressed Quaking1-5A (Figure 5.37C). This indicates that Quaking1-5A overexpression allows at least a small number of cells with an HSC surface marker phenotype to survive for

18 weeks in the bone marrow of recipient mice, whereas overexpression of all the other candidate genes cause such severe defects in HSC when overexpressed that no HSC expressing these candidates could be detected after this time.

Examining progenitor populations in the mouse transplanted with vector control transduced cells we again determined the percentage of VENUS expressing cells within the various progenitor populations (Figure 5.38A). We found VENUS expression in 92.5% of CMP and 90.4% of GMP (Figure 5.38B). However, when examining lymphoid cells and common lymphoid progenitors (CLP), we found 66.0% and 39.9% of VENUS<sup>+</sup> cells respectively. This indicates that vector control transduction per se does not negatively affect generation and maintenance of myeloid progenitors. However, it may have an inhibiting effect on the lymphoid progenitors.

In mice transplanted with Pumilio1 infected cells, we did not find any VENUS<sup>+</sup> cells within CMP or GMP (Figure 5.38C). However, we found 3.6% of early lymphoid cells but not CLP to express VENUS. In Staufen1 transplanted mice we saw VENUS expression in 2.3% of MEP but no VENUS positive cells in CMP and GMP. Staufen1 expression as detected by VENUS signal could be found to a high extent in CLP and other early lymphoid cells where we found 26.9% and 28.5% of cells respectively expressing VENUS. Mice transplanted with Staufen<sup>l</sup> transduced cells showed VENUS<sup>+</sup> cells in 2.1% of the CMP, 1.1% of the GMP and 2.6% of the MEP and 10.5% of the early lymphoid cells, but no VENUS<sup>+</sup> cells in CLP (Figure 5.38C). This indicates that overexpression of the two Staufen1 isoforms has differential effects on myeloid and lymphoid cell populations. When we analyzed mice transplanted with cells transduced with Quaking1-6B, we found no VENUS<sup>+</sup> cells within CMP, GMP, MEP and CLP and only 3.1% VENUS expressing cells in early lymphoid cells. For mice transplanted with Quaking1-5A transduced cells, we found 0.3% CMP, 0% GMP, 0.3% MEP, no CLP and 0.9% of lymphoid cells (Figure 5.38C).

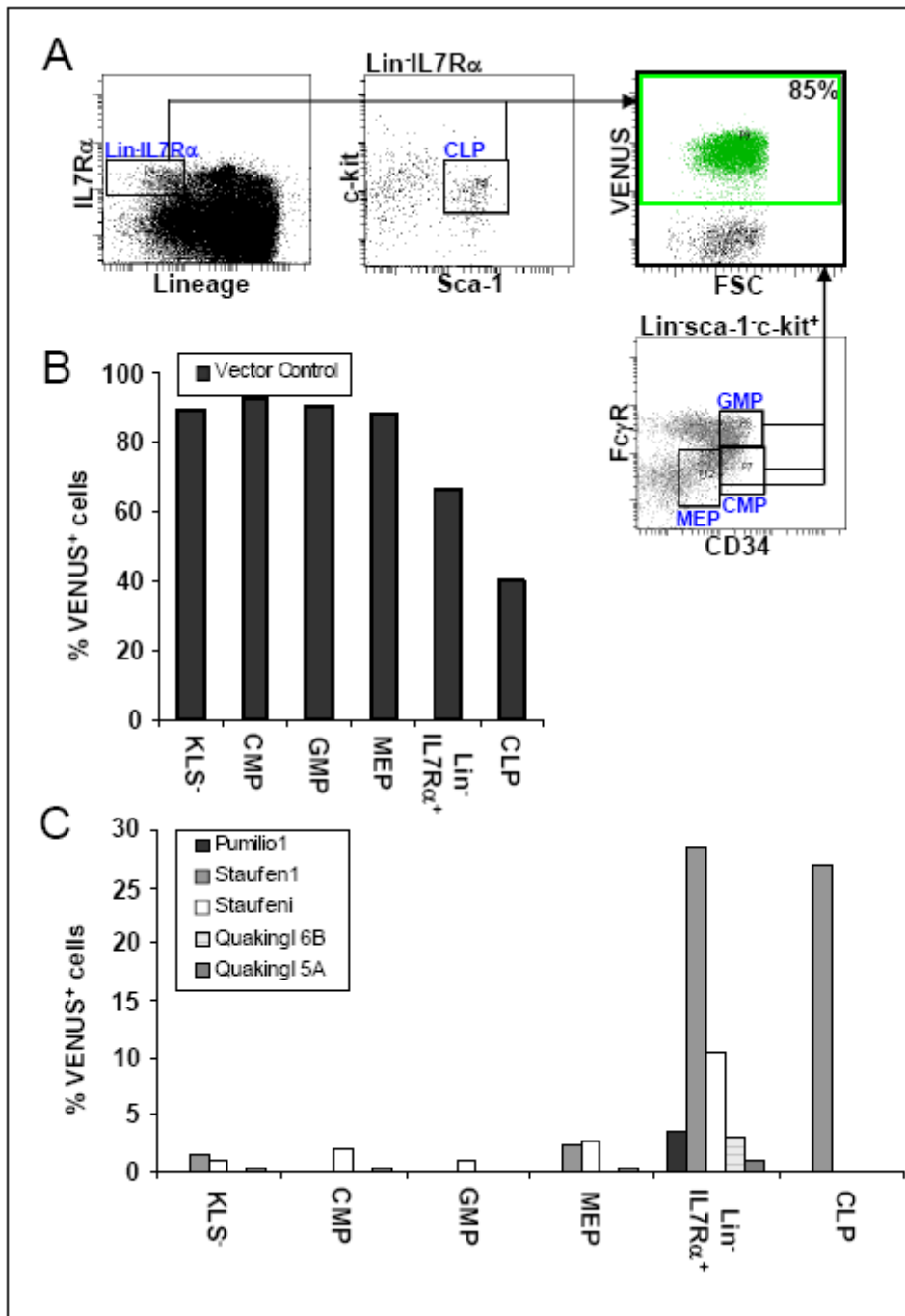


**Figure 5.38: Bone marrow population analysis of transplanted mice: Progenitors.** Example of FACS analysis: Percentage of VENUS<sup>+</sup> cells within progenitor populations are analyzed (A). Percentage of VENUS<sup>+</sup> cells of vector control transplanted mice in myeloid and lymphoid progenitors (B). Percentage of VENUS<sup>+</sup> cells of candidate gene transplanted mice in myeloid and lymphoid progenitors (C). Results show data of one mouse.

We wanted to take a closer look at more mature cells residing within the bone marrow. We analyzed the GM lineage which is negative for Ter119 expression. We distinguished cells of the granulocytic and monocytic lineage by their expression of granulocyte specific Ly6G, a subtype of Gr-1, and Mac-1, a marker that can be found on both granulocytes and monocytes. Therefore, granulocytes were identified by being Ly6G<sup>+</sup>Mac-1<sup>+</sup> (M2) and distinguished from monocytes that are Ly6G<sup>-</sup>Mac-1<sup>+</sup> (M1, Figure 5.39A). When we analyzed cells from control transplanted mice we found 72.3% and 86.2% of VENUS<sup>+</sup> cells in monocytic and granulocytic cells respectively (Figure 5.39B). For mice transplanted with Pumilio1 overexpressing cells we found 0.4% VENUS<sup>+</sup> cells in immature cells that were not committed to either myeloid lineage, but no VENUS<sup>+</sup> cells in mature monocytic or granulocytic cells (Figure 5.39C). Staufen1 allowed the formation of few (0.8%) granulocytic cells but no monocytic cells, whereas Staufeni allowed the generation of both monocytes and granulocytes at low percentages (0.5% and 1.6%, respectively). In Quaking1-6BA transplanted mice we did not see any VENUS<sup>+</sup> cells in either myeloid lineage, but we found a low number (0.6%) of VENUS<sup>+</sup> cells in both myeloid lineages in Quaking1-5A transplanted mice. These data indicate that candidate gene overexpression in HSC allowed for little or no mature myeloid VENUS<sup>+</sup> cell formation 18 weeks after transplants.

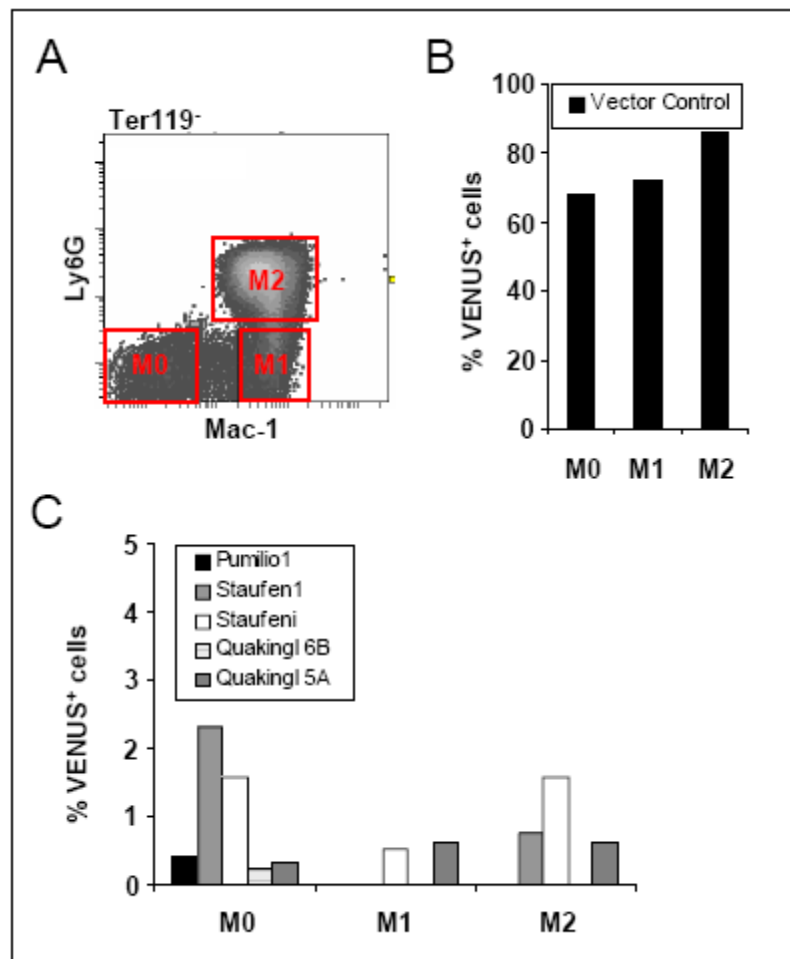


**Figure 5.39: Bone marrow population analysis of transplanted mice: Myeloid lineage.** Expression of Ly6G and Mac-1 in Ter119<sup>-</sup> bone marrow cells (A). Percentage of VENUS<sup>+</sup> cells of vector control transplanted mice within myeloid lineage cells (B). Percentage of VENUS<sup>+</sup> cells of candidate gene transplanted mice within myeloid lineage cells (C). Results show data of one mouse.

We also looked in detail at cells of the erythroid lineage, which were negative for myeloid markers Gr-1 and Mac-1 and lymphoid markers CD19 and B220. We distinguished three maturation stages within the erythroid lineage and analyzed only stages that still express CD45 since this marker is used to determine donor or recipient blood type (Figure 5.40A). More mature stages that lack CD45 expression were not analyzed. The Ter119 and CD71 double negative population encompasses all immature cells and no cells that are committed to the erythroid lineage (S0). Stage1 characterized by CD71<sup>+</sup>Ter119<sup>-</sup> expression identifies cells committed to the erythroid lineage (S1). Stage2 encompasses CD71<sup>+</sup>Ter119<sup>mid</sup> cells that are defined as proerythroblasts (S2) and stage3 contain double positive cells that are basophilic

erythroid cells (S3). All subsequent stages of erythroid maturation contain only very low numbers of CD45 expressing cells and were therefore not analyzed for VENUS expression.

Analyzing cells from vector control transplanted mice we found 94.7% VENUS<sup>+</sup> cells in S1 and 88.6% in S3 cells, but only 54.8% in the S2 population (Figure 5.40B). Since we are excluding CD45<sup>-</sup> cells from our analysis, this lower percentage might not indicate a negative effect of viral vector expression on this compartment. However, also in mice transplanted with cells overexpressing the various candidate genes, we always found the lowest percentage of VENUS<sup>+</sup> cells in S2 cells, indicating that this population might be less represented in virus transduced cells (Figure 5.40C). We found that *Staufen1* as well as *Staufen1*<sup>i</sup> expression allowed generation of 2.3%, 0.8% and 5.4% of VENUS<sup>+</sup> cells in stages 1 through 3 of the erythroid lineage, whereas *Pumilio1* positive cells could only generate 0.8% of VENUS<sup>+</sup> cells up to S1. Percentages below 1% of *Quaking1-6B* and *-5A* expressing cells could be found in all erythroid stages. In summary it seems that *Staufen1* as well as *Quaking1* allow the generation of few erythroid cells, whereas *Pumilio1* seems to block at least part of this lineage.

From all these analyses of bone marrow populations of transplanted mice we can conclude that HSC that were initially transduced with vector control virus and transplanted into recipients can be maintained for at least 18 weeks *in vivo* as identified by surface marker expression. Overexpression of our candidate genes in HSC did not allow HSC maintenance over this time period *in vivo*. Only *Quaking1-6B* overexpression allowed survival of a few cells with HSC phenotype.

As for the other bone marrow populations, we found that *Staufen1* as well as its splice isoform *Staufen1*<sup>i</sup> allowed the survival of a few mature myeloid and erythroid cells as well as MEP. Only *Staufen1*<sup>i</sup> allowed the survival of a few myeloid progenitors (CMP and GMP) and maintenance of some early lymphoid cells that were more mature than CLP. It is interesting to note, that overexpression of *Staufen1* led to the survival of quite large numbers of CLP, but no *Staufen1*<sup>+</sup> cells could be found in the KSL compartment.

Confirming our *in vitro* assays, *Pumilio1* does not allow survival of cells over longer periods of time. We could only find very few *Pumilio1*<sup>+</sup> cells in lymphoid and

early erythroid cells, but since the number of observed VENUS<sup>+</sup> events was so low, this could have also been an artifact.

In mice transplanted with Quaking1 expressing cells, we found that neither isoform allowed the survival of any myeloid or lymphoid progenitors, apart from very few early lymphoid cells. Both isoforms seem to allow survival of a few myeloid and erythroid committed cells though. Quaking1-6B was the only candidate that allowed survival of cells within the KSL compartment and specifically of HSC. We were not able to confirm that these cells truly had self renewal capacity by transplanting them into secondary recipients because the other Quaking1-6B transplanted mouse died of unknown reason before we could conduct the experiment.

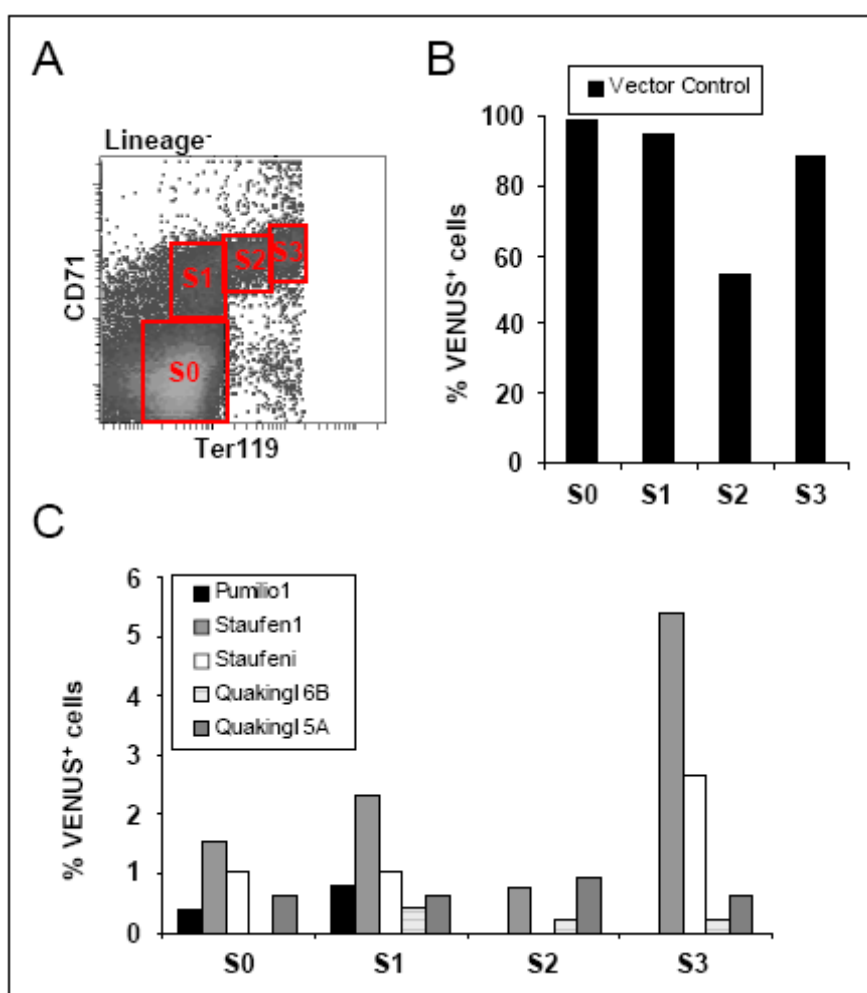


**Figure 5.40: Bone marrow population analysis of transplanted mice: Erythroid lineage.** Expression of CD71 and Ter119 in lineage<sup>-</sup> bone marrow cells (A). Percentage of VENUS<sup>+</sup> cells of vector control transplanted mice within the erythroid lineage (B). Percentage of VENUS<sup>+</sup> cells of candidate gene transplanted mice within the erythroid lineage (C). Results show data of one mouse.

## **5.2.6.2. Candidate Transgenic Mice Allow Analysis of Candidate Influence on Hematopoiesis during Homeostasis Conditions**

### **5.2.6.2.1. Testing Functionality of Transgenes: Expression in the Skin**

Transplanting HSC into compromised mice results in HSC expansion and differentiation, that does not occur in normal homeostasis conditions. In order to analyze effects of candidate genes on hematopoiesis under homeostasis conditions transgenic mice carrying inducible expression constructs of candidate genes were generated by Dr. Timm Schroeder in Japan. Expression of a candidate gene either as a fusion gene or from an IRES construct was driven by a chicken beta actin promoter (pCAG). Insertion of a loxP site flanked STOP cassette in front of the promoter rendered the expression cassette inactive. CRE expression in these cells results in recombination of the two loxP sites thereby excising the STOP cassette and initializing gene expression by the pCAG promoter. By crossing transgenic mice containing this expression cassette to mouse lines expressing CRE under cell and stage specific promoters the effects of transgene expression can be analyzed in a cell type and developmental stage specific manner during homeostasis.

The F1 offspring of the initial six transgenic founders were transferred to the Helmholtz center mouse facility. Mice were genotyped for VENUS presence in the genomic DNA and positive mice backcrossed to the C57/Bl6 background (Table 3). Genotype positive mice were further tested for functional VENUS expression upon CRE recombination. We decided to first use fibroblasts grown out of tail clips from transgenic mice to analyze for VENUS functionality. To this end, fibroblasts were isolated from the tails of transgenic mice and infected with a lentivirus expressing CRE and TOMATO fluorescent protein localized to the mitochondria. Using fibroblasts from our inducible mouse lines, successfully infected cells express TOMATO as well as CRE which then recombines the two loxP sites and excises the STOP cassette in front of the transgene, thus inducing expression of both the candidate gene and VENUS. Seven days after infection of the fibroblasts with the CRE virus cells were analyzed by FACS analysis to check for TOMATO and VENUS expression.

Analysis of infected and CRE recombined fibroblasts showed a large proportion of negative cells, that show high auto fluorescence in both TOMATO and VENUS channels (Figure 5.41A). Cells above the negative cells indicate TOMATO positive

infected cells, whereas cells below the negative cells indicate VENUS positive cells. We did not see any VENUS positive cells in non-infected fibroblasts, therefore, we were sure that the latter cells were in fact double positive for TOMATO and VENUS, but appeared to be singly VENUS positive due to compensation artifacts.

In mice containing a *Staufen1*VENUS expression cassette we found mice from all three founders to be functional for VENUS expression in the skin (Table 2). Not all the mice of each line were found to be positive. This is probably due to the fact that from some mice only very few fibroblasts grew out of tail clips and therefore, we could have missed the low number of double positive cells. In mice containing the *Staufen1* IRES VENUSnucmem expression cassette we did not find fibroblasts from any mouse with functional VENUS expression. This means that *Staufen1* overexpression does not work in skin fibroblasts in these mice. In *Pumilio2* IRES VENUSnucmem containing mice we found all four mice tested (1 Founder) to be positive for VENUS expression indicating functional *Pumilio2* overexpression in these cells.

<b>Staufen1VENUS</b>		
<b>Founder</b>	<b>mice tested</b>	<b>mice positive</b>
20	4	3
24	8	2
26	10	4
<b>Staufeni IRES VENUSnucmem</b>		
<b>Founder</b>	<b>mice tested</b>	<b>mice positive</b>
17	7	0
21	0	0
<b>Pumilio2 IRES VENUSnucmem</b>		
<b>Founder</b>	<b>mice tested</b>	<b>mice positive</b>
18	4	4

**Table 5.2: Functionality of expression cassette in the skin of inducible transgenic mice.** Functionality of expression cassette was analyzed by FACS coexpression of VENUS and TOMATO in tailclip derived fibroblasts infected with CRE-IRES-mitoTOMATO.

Staufen1 VENUS						
Founder	Parameter	F1	F2	F3	F4	F5
20	Genotype positive (%)	64	59	25	67	
	Breeding partner	b16	b16	b16		
	Functionally tested mice				4	
	Double positive mice				0	
24	Genotype positive (%)	20	25	43	47	91
	Breeding partner	b16	b16	F3	F4	
	Functionally tested mice				3	2
	Double positive mice				0	0
26	Genotype positive (%)	44	55	73	64	
	Breeding partner	b16	b16	b16		
	Functionally tested mice				4	
	Double positive mice				0	
Staufen1 IRES VENUSnucmem						
Founder	Parameter	F1	F2	F3	F4	F5
17	Genotype positive (%)	57	35	43	67	44
	Breeding partner	b16	b16	F3	b16	
	Functionally tested mice				1	5
	Double positive mice				0	0
21	Genotype positive (%)	27	20	80	57	40
	Functionally tested mice	b16	b16	b16	b16	
	mice functionally tested					2
	Double positive mice					0
Pumilio2 IRES VENUSnucmem						
Founder	Parameter	F1	F2	F3	F4	F5
18	Genotype positive (%)	70	46	45	67	T2C
	Breeding partner	b16	b16	b16	b16	
	Functionally tested mice			3	2	
	Double positive mice			3	2	

**Table 5.3: Inducible candidate gene expressing mice: breeding scheme and functionality of expression cassettes in bone marrow.** Transgenic mice were bred to C57/Bl6 mice for several generations as indicated. Functionality of expression cassette in transgenic mice was determined by coexpression of VENUS and TOMATO in CRE-IRES-mitoTOMATO lentivirus infected c-kit<sup>+</sup>lin<sup>-</sup> derived cells.

#### 5.2.6.2.2. Testing Functionality of Transgenes: Expression in Bone Marrow Cells

As we were interested in the overexpression of candidate genes in the bone marrow, the presence of VENUS expression in skin fibroblasts is a good indicator for functionality in other tissues, but cannot substitute for a functional characterization of bone marrow cells themselves. We decided to analyze the bone marrow of all previously tested mice, including the ones that did not show expression in the skin. Therefore, we sorted c-kit<sup>+</sup> lin<sup>-</sup> bone marrow cells from the transgenic mice and infected them with the same CRE expressing lentivirus we had used for the fibroblasts (Figure 5.41B). A functional inducible N-CadherinVENUS mouse and a C57/Bl6 mouse were used as positive and negative controls, respectively.

Re-analysis of cells was done after 6 days, when enough time had passed for infection, CRE expression and recombination and subsequent VENUS expression to have been completed. As shown in Figure 5.42C, cells were analyzed for TOMATO and VENUS expression. Gates were set using uninfected C57/Bl6 cells. Negative as well as positive control cells infected with mock control (IRES-mitoTOMATO) showed 22% TOMATO positive cells but no VENUS positive or double positive cells. This result shows that the infection *per se* worked and that the inducible system is not active without CRE recombination. C57/Bl6 cells infected with the CRE lentivirus showed again 22% of TOMATO positive cells but 0% of VENUS or double positive cells as these mice do not contain VENUS coding sequences in their genome. However, CRE lentivirus infection of cells from N-Cadherin VENUS mice resulted in 22% TOMATO positive cells as well as 3% VENUS and TOMATO double positive cells. With this system we could now test functionality of the transgenic mice in bone marrow cells.

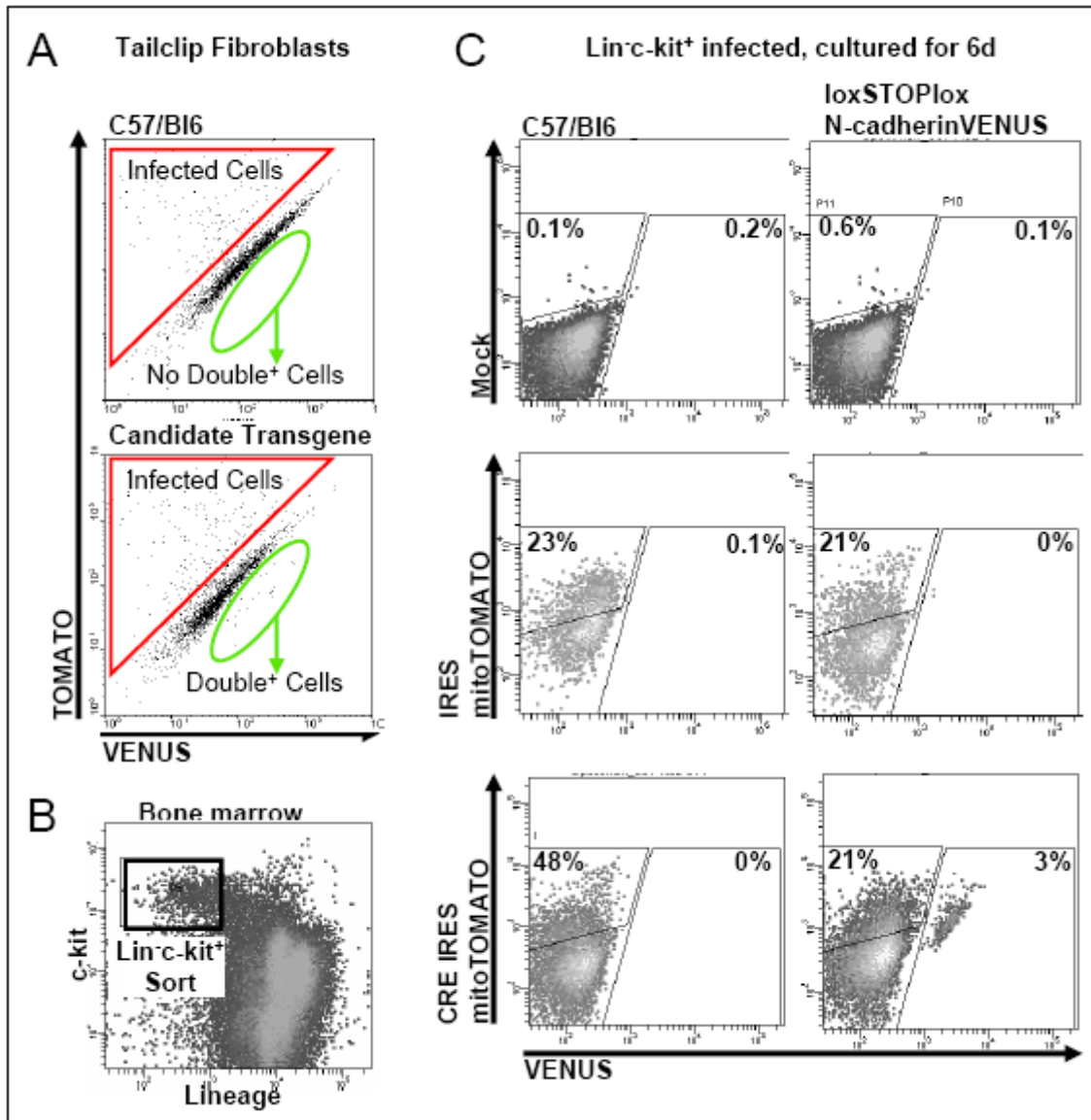


**Figure 5.41: Experimental setup testing VENUS functionality of transgenic mice.** FACS analysis of infected tailclip derived fibroblasts of C57/Bl6 and candidate inducible transgenic mouse. Red triangle: infected cells. Green ellipse: VENUS and TOMATO double positive cells (A). Sorting scheme of c-kit<sup>+</sup>lin<sup>-</sup> bone marrow cells (B). FACS analysis of infected c-kit<sup>+</sup>lin<sup>-</sup> from negative and positive control mice (C).

Two to six mice from each of the six different founders were tested in the described manner from the following mouse lines: Staufen1VENUS, Staufen<sup>i</sup>-IRES-VENUSnucmem, and Pumilio2-IRES-VENUSnucmem. Unfortunately we found that no progeny from the founders of either Staufen1VENUS or Staufen<sup>i</sup>-IRES-VENUSnucmem mouse lines expressed VENUS after CRE-mediated recombination in bone marrow cells (Figure 5.42 and Table 3). However, bone marrow cells from Pumilio2-IRES-VENUSnucmem mice showed 0.2-1.1% VENUS positive cells upon CRE

recombination (Figure 5.42), and it was therefore possible that these mice contained functional expression cassettes in bone marrow cells.

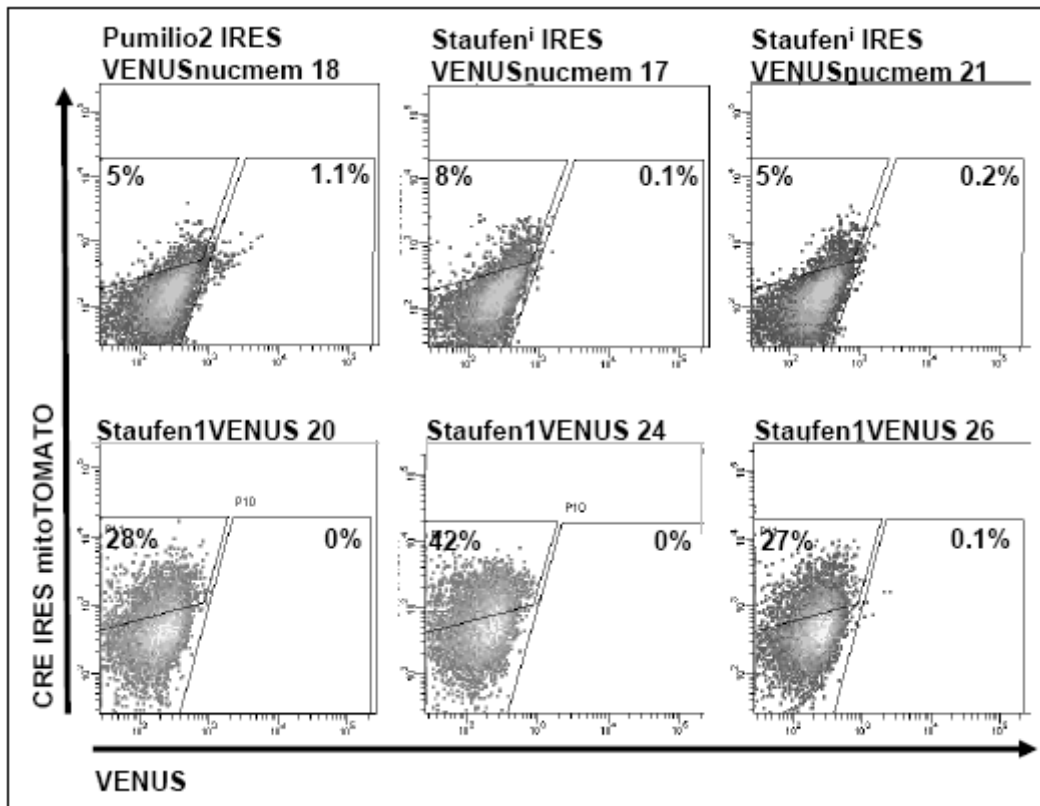


**Figure 5.42: Functionality of expression cassette in the bone marrow of inducible transgenic mice.** Functionality of expression cassette was confirmed by coexpression of VENUS and TOMATO in  $c\text{-kit}^+\text{lin}^-$  derived cells infected with a lentivirus containing CRE-IRES-mitoTOMATO. FACS analysis of VENUS and TOMATO expression in  $c\text{-kit}^+\text{lin}^-$  derived cells. The shown graphs are

### 5.2.6.3. Tie2 Controlled Homeostatic Pumilio2 Overexpression Allows Maintenance of Cells with HSC Phenotype

To prove functionality of Pumilio2-IRES-VENUSnucmem mice, we crossed them to Tie2-CRE mice to induce candidate gene overexpression in blood and endothelial cells directly in the mouse (Table 3). Crossing of heterozygous Pumilio2-IRES-VENUSnucmem with heterozygous Tie2-CRE mice resulted only in one genotype double positive mouse. At 12 weeks of age, this mouse was analyzed for VENUS expression in the peripheral blood and bone marrow progenitor populations. In addition, bone marrow cells from this mouse were compared to wild type C57/Bl6

cells to check for effects of *Pumilio2* overexpression on lineage decision and distribution of cells within the progenitor populations.

Within the lineage negative population of the *Pumilio2*<sup>+/-</sup>*CRE*<sup>+/-</sup> mouse, we found 0.75% ( $\pm 1.06$ ) of cells were VENUS positive (Figure 5.43B) and also the myeloid progenitors did not show a higher percentage of VENUS<sup>+</sup> cells (0.2%  $\pm 0$  for KLS<sup>-</sup> cells, Figure 5.43B). However, analysis of populations enriched for stem cells revealed that VENUS<sup>+</sup> cells were present in the KSL population (1.85%  $\pm 0.49$ ), and were further enriched in the HSC population defined by CD150<sup>+</sup>CD48<sup>-</sup>CD34<sup>-</sup>KSL markers (5.75%  $\pm 4.03$ , Figure 5.43A). Analysis of cells with lymphoid potential showed 14.65% ( $\pm 10.67$ ) cells positive for VENUS expression within the common lymphoid progenitor populations (CLP, Figure 5.43A).

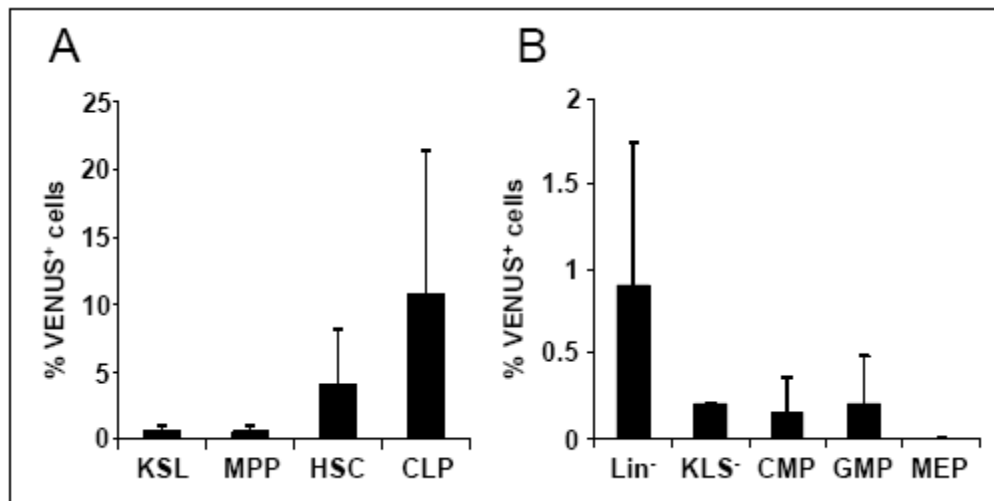


**Figure 5.43: Bone marrow analysis of *Pumilio2*-IRES-VENUSnucmem x *Tie2*-CRE transgenic mouse.** Percentage of VENUS<sup>+</sup> cells within myeloid progenitor populations (A). Percentage of VENUS<sup>+</sup> cells within HSC populations and CLP (B). Data shows average of two transgenic mice analyzed. Error bars show standard deviation.

When we compared percentages of cells within bone marrow populations of this transgenic mouse to C57/Bl6 we did not find a significant difference in any population. However, since percentages of VENUS<sup>+</sup> cells are rather low we did not expect them to have a marked influence on total bone marrow cells.

The low percentage of VENUS<sup>+</sup> cells in the bone marrow, reflecting the efficiency of CRE recombination in this mouse can be explained by the known low efficiency of *Tie2*-CRE on a C57/Bl6 background (personal communication with Dr.

Lothar Henninghausen). However, the Pumilio2-IRES-VENUSnucmem mouse line is nevertheless useful and will now be crossed to an Mx1-CRE expressing mouse line where high recombination efficiency in C57/Bl6 has been shown (personal communication with Dr. Lothar Henninghausen).

In summary we found that indeed the Pumilio2-IRES-VENUSnucmem transgenic mouse line was functional, expressing VENUS (and presumably Pumilio2) upon recombination in the bone marrow. This was especially advantageous since Pumilio2 proved to be a gene difficult to work with when overexpressing it in lentiviral constructs. Overexpression of Pumilio2 in transgenic mice allowed survival of HSC, CLP and early myeloid lineages. The lack of surviving GMP could reflect the recombination efficiency of Tie2 CRE in Bl6, but could also point towards a detrimental effect of Pumilio2 on this cell type.

### 5.3. Conclusion

In conclusion we identified and quantified asymmetric fates of individual HSC daughter cells but we could not elucidate the molecular mechanism that influences these fate decisions. We found that HSC compared to MPP show an intrinsically controlled delay in cell cycle entry time. A specific difference in sister generation times of HSC daughters can be attributed only to the influence of a certain environment but is not intrinsically controlled. In contrast, the asymmetric onset of the loss of stemness marker CD48 specifically in HSC daughters reflects an intrinsic control of self renewal versus differentiation divisions in HSC.

We could not verify the hypothesis that asymmetric protein segregation during HSC division generates asymmetric daughter cell fates, since none of our candidates could be observed to segregate asymmetrically during division with the methods tested. We found however, that all tested candidates have a detrimental effect on HSC maintenance as tested by reconstitution experiments with candidate overexpressing cells. In addition, some of the candidates also displayed *in vitro* effects on progenitor lineage potential. Pumilio1 inhibited long term survival and colony formation of progenitors and the effector protein Quaking1 influenced myeloid lineage decisions when overexpressed.



## 6. Discussion

It is currently not known how HSC maintain constant numbers throughout the life of an organism and at the same time manage to produce millions of blood cells every day. It is assumed but has not been proven yet that the mechanism of asymmetric cell division enables HSC to achieve this goal by dividing into another HSC and a differentiated daughter cell. This Thesis tries to elucidate the mechanism of asymmetric cell division of mouse HSC by assessing their potential to produce asymmetric fates in vitro in both stroma and stroma free culture and by examining possible mechanisms involved in controlling the generation of asymmetric fates. We found that HSC intrinsically control asymmetric fate decisions of self renewal and differentiation of daughter cells. Further exploration of the mechanism controlling the generation of asymmetric daughter cell fates revealed that selected candidate genes, *Staufen1*, *Staufen1*<sup>i</sup> and *Pumilio1*, are not segregated during HSC division and are unlikely to contribute to the generation of asymmetric fated HSC daughter cells.

### 6.1. Asymmetric Fate Potential of HSC

Previous studies have attempted to elucidate if ACD is a mechanism employed by HSC. As far back as 1983 have researcher quantified asymmetric fates of hematopoietic progenitor cells (Suda, Suda et al. 1983; Ogawa, Suda et al. 1984; Suda, Suda et al. 1984). By separation of cells shortly after their division and by analysing the fate potential of their daughters by colony formation assays, it could be shown that these cells were able to produce asymmetrically fated daughter cells. These studies however were flawed, as they used highly heterogeneous starting cell populations with an unknown percentage of cells with specific reconstitution potential. Later studies used human blood progenitor populations containing extremely low percentages of HSC from various tissues to conduct similar experiments with separation of daughters by micromanipulation (Leary, Strauss et al. 1985; Mayani, Dragowska et al. 1993). As a readout in these studies again colony formation in methylcellulose as well as prolonged colony formation on stroma was

used to assess immaturity and lineage potential (Punzel, Liu et al. 2003; Giebel, Zhang et al. 2006). In addition, label retaining experiments in single cell cultures revealed asymmetric proliferation potential of daughter cells (Huang, Law et al. 1999; Punzel, Zhang et al. 2002). The low percentage of true HSC, that are able to reconstitute the bone marrow of a recipient in vivo for life, within the populations used in these studies, prevent any conclusions as to HSC specific properties.

In contrast, a more recent study examined asymmetric fates using clearly defined bone marrow populations from mouse containing high (41%) numbers of cells with reconstitution potential (Ema, Takano et al. 2000). Daughter and granddaughter cell fates of HSC were analyzed by colony formation and lineage potential as well as reconstitution potential. It was found that HSC produce varying percentages of daughter pairs with asymmetric fates regarding maintenance of HSC potential and multipotency depending on the culture conditions (Ema, Takano et al. 2000; Takano, Ema et al. 2004). However, this study, like previous studies mentioned above, used micromanipulation to transfer daughter cells after their division. It is not clear how this change in microenvironment that is created by the blood cells themselves as well as the mechanical manipulation affects HSC in their lineage choice. In addition, cells were cultured in well defined stroma free media that allows deduction of the influence of single factors on the cells, but does not assess behaviour of HSC in an environment that contains cellular components and resembles closer the niche present in the in vivo situation.

Both problems were attempted to be overcome by Wu et al. (Wu, Kwon et al. 2007), who used time lapse microscopy and highly purified HSC cultured on stromal cells to answer questions regarding ACD. Using a notch activity reporter mouse as readout for immaturity of HSC daughters, they observe asymmetric fates of dividing HSC on 7F2 and OP9 stroma. In our hands however, when we analyzed GFP expression in bone marrow population of this GFP Notch activity reporter mouse line, we found no enrichment of GFP expressing cells in highly HSC enriched populations (personal communication Dr. Masaki Shigeta). Also, the time intervals that Wu et al. used for their time lapse movies are rather long (every 15 min) and we know from our own experiments that identities of cells can easily be mixed when observed in low temporal resolution. For these reasons, no conclusion can be drawn from their results regarding asymmetric fate potential of HSC.

To overcome all the mentioned flaws of previous studies, the present study used CD34<sup>+</sup>KSL mouse bone marrow cells, which contain a high percentage of cells with reconstitution potential. We further observed cells continuously with a high temporal (every 2 min) and spatial resolution using time lapse microscopy and recorded their divisional kinetics as well as fate potential by single cell tracking for at least 4 days. We cultured cells on stroma as well as in stroma free suspension culture and used self renewal as well as differentiation promoting culture conditions to be able to compare the effects of different environments on HSC behaviour and to distinguish extrinsically from intrinsically controlled HSC behaviour. In order to assess asymmetric fate potential of individual HSC we used two different readouts, generation time of daughter cells as well as loss of reconstitution potential as assessed by a live marker. And we compared the asymmetric fate potential of HSC as well as their divisional kinetics to MPP, which are closely related cells that have lost reconstitution potential. This enabled us to distinguish characteristics that are unique to true HSC from behaviour common to all immature hematopoietic progenitor cells. Therefore, the identification of HSC specific properties, especially regarding their divisional behaviour and fate choice, is a first step required to be able to expand HSC for the use in clinical transplantations.

## **6.2. Choice of Culture Conditions**

In order to study asymmetric fate decisions of HSC it is important to choose culture conditions that promote HSC homeostasis where asymmetric divisions of HSC yielding a self renewed and a differentiated daughter could take place. That means that HSC potential has to be maintained for several days by the environment, but without expanding HSC which can only be achieved by symmetric self renewal divisions. Our chosen stromal environment, PA6, has been proven to support HSC maintenance and does not expand HSC. Another stromal cell line, OP9, is widely used to support hematopoiesis, however it was not sufficiently studied if and how much HSC potential they maintain (Ueno, Sakita-Ishikawa et al. 2003). Sys-1 Stromal cell line in conjunction with LIF slightly expands HSC and therefore is not useful either to study asymmetric divisions.

Stroma free conditions that claim to expand stem cell numbers have been published as well. Cultures containing IL-11 in addition to SCF can expand HSC numbers slightly (Miller and Eaves 1997; Audet, Miller et al. 2002) and expansion of HSC can be also observed in the presence of SCF, thrombopoietin (TPO), insulin-like growth factor 2 (IGF-2) and fibroblast growth factor 1 (FGF-1) (Zhang and Lodish 2005; Noda, Horiguchi et al. 2008). These culture conditions are not appropriate to study ACD as they likely promote symmetric self renewal divisions. However, it might be interesting to compare expansion with maintenance cultures to elucidate cellular pathways that differ in the response to either signal.

Ema et al. have described two stroma free suspension conditions that allow maintenance of various percentages of initial HSC potential as well as one cytokine combination that leads to rapid differentiation (Ema, Takano et al. 2000). Using the maintenance conditions allowed us the analysis of asymmetric fates as well as to study the mechanism behind asymmetric fate choices.

### **6.3. Divisional Kinetics of HSC and MPP**

The use of generation time length of HSC daughters as readout for asymmetric fates was prompted by previous studies showing that cultured HSC compared to MPP showed longer generation time in the first and also in subsequent divisions as measured by label retaining experiments (Nygren, Bryder et al. 2006). This proliferation difference between HSC and MPP that can be observed in vitro is also true for freshly isolated cells. The percentage of cells in G<sub>0</sub> was highest in freshly isolated HSC, indicating a long generation time, and decreased upon differentiation of these cells into MPP and further differentiated populations (Passegue, Wagers et al. 2005; Wilson, Laurenti et al. 2008).

When we compared divisional kinetics of HSC and MPP on stroma containing as well as stroma free environments, we found in our experiments, like expected from previous studies, that HSC enter the cell cycle later than MPP and that HSC also within the first three divisions show a longer GT than MPP. Similar proliferative behaviour in all culture conditions tested indicates intrinsic control of divisional kinetics of HSC and MPP.

Not only seems there to be a difference in divisional kinetics of HSC and MPP but also does generation time length seem to serve as an indicator to distinguish true HSC from other cells in populations that are highly enriched for HSC potential. Dykstra et al., who like the present study used video monitoring of cells, showed that HSC potential was preferentially found in clones of cultured HSC that displayed longer cell cycle times than clones derived from cells with HSC surface phenotype that failed to reconstitute mice (Dykstra, Ramunas et al. 2006). Again the in vitro behaviour reflects in vivo properties of HSC. Label retaining in vivo experiments showed that phenotypic HSC that are slowly dividing within the organism have a clear advantage in competitive repopulation experiments compared to faster dividing cells with the same phenotype (Nygren, Bryder et al. 2006; Wilson, Laurenti et al. 2008). Therefore, a change in proliferate capacity was assumed to precede a change in surface phenotype that marks the loss of reconstitution potential.

#### **6.4. Asymmetries in Generation Time Length of Daughter Cells**

As generation time length clearly distinguishes HSC from MPP but also seems to identify reconstitution potential in phenotypically identical cells, we concluded that daughter cells of single HSC that showed longer generation time would be more immature than daughters with short generation time. Therefore, HSC daughters that are asymmetric in their generation time length could indicate an asymmetric fate decision in the mother cell. In accordance with this Dykstra et al. saw a greater difference in generation time length of daughter cells in clones containing HSC potential than in clones without reconstitution potential when cultured in stroma free conditions. Our results showed in support of this theory more trees with asymmetric generation time of HSC daughters than of MPP daughters when cells were cultured on PA6 stroma.

However, culture of HSC and MPP in stroma free environment showed no difference in the number of cells with asymmetric generation time of daughter cells and thus revealed environmental rather than intrinsic control of asymmetric generation time of daughter cells. It is widely assumed that asymmetric cell division, yielding a self renewed and a differentiated daughter would be an intrinsic property

of HSC. As we showed that asymmetric generation time is not intrinsically controlled, it could, rather than indicating asymmetric fate decisions, indicate the effect of non uniform stromal cells on identical HSC daughter cells to yield different cell fates that are accompanied by asymmetric generation time. In absence of these signals from stromal cells different fates of initially equal daughter cells could not be produced.

### **6.5. Intrinsic Control of Asymmetric Fate Decisions**

The recent establishment of the SLAM code enables isolation of highly purified bone marrow populations containing a high percentage of HSC (Kiel, Yilmaz et al. 2005). Freshly isolated HSC are negative for the expression of CD48 and also recently it was shown that cultured HSC remain negative for CD48 expression (Noda, Horiguchi et al. 2008). Therefore, we have used live CD48 staining in time lapse movies to assess loss of HSC potential of daughter cells. By comparing the time of onset of CD48 expression in sister cells we were able to quantify asymmetric and symmetric fate decisions in HSC progeny. This revealed that more HSC compared to MPP have progeny with asymmetric CD48 onset and this could be observed on stroma as well as in stroma free environments and is therefore an intrinsic property of HSC.

Asymmetric fates of human hematopoietic progenitors (HPC), which are ill defined and contain only low percentages of true HSC, have been previously described. Giebel et al (Giebel, Zhang et al. 2006) found that a high percentage of the most immature cells produced daughter cells of which only one daughter received the immature fate of the mother cell. Also Punzel et al. (Punzel, Liu et al. 2003) found a constant percentage of progenitors with asymmetric daughter cell fates within dividing cells when cells were cultured on AFT024 stroma and in stroma free culture containing different cytokine combinations (Punzel, Zhang et al. 2002; Punzel, Liu et al. 2003). As these studies did not utilize purified HSC as described in this thesis, no conclusion about asymmetric fates of HSC daughters can be made from their data.

In the present study we used unmanipulated, highly purified HSC and found similar percentages of asymmetric fates, read out by asymmetric CD48 onset in HSC

progeny cells, when HSC were cultured in stroma free self renewal and differentiation conditions. In contrast, Takano et al. when using micromanipulated HSC, found varying percentages of asymmetric fates of HSC daughters depending on the culture conditions (Takano, Ema et al. 2004). In addition, this study used colony potential to distinguish differently fated daughter cells. Only in a separate study, when culturing HSC in self renewal conditions, was the HSC potential of HSC daughters tested by long term in vivo bone marrow reconstitution (Ema, Takano et al. 2000). Culture condition dependent percentages of HSC with asymmetric daughters described by Takano et al. (Takano, Ema et al. 2004) do not contradict our data, as we assessed the amount of HSC with asymmetrically fated daughters as a percentage of all trees that switched on CD48 in their progeny. Thus, trees which were committed to differentiation in the mother cell or did not differentiate at all were not included in this analysis. As the percentage of trees with progeny CD48 onset differed between environments, also the absolute percentage of HSC with asymmetrically fated daughters differed between culture conditions.

As CD48 not only enables us to read out asymmetric fate choices but also to assess indirectly the reconstitution potential of cultured cells, we compared our data to data obtained by Ema, who compared the reconstitution potential of HSC cultured under self renewal and differentiation conditions (Ema, Takano et al. 2000). Ema showed that HSC cultured in serum free medium containing SCF and TPO retain a large proportion of reconstitution potential for at least 6 days (66.7% of initial potential after 3d, and 26.5% after 6d). Our data from HSC cultured in SCF and TPO confirms this high reconstitution potential. The percentage of CD48 expressing trees remained low and almost half of the trees did not express CD48 in any of their progeny for the course of 4 days. Similar trends could be observed for culture of HSC on PA6, which are able to maintain HSC potential for at least 2 weeks. Our data of HSC cultured in SCF and IL3 still fits data concerning reconstitution potential of cultured HSC from Ema who found 27.5% of initial HSC potential retained in HSC cultured in SCF and IL3. When analyzing CD48 expression in pedigrees at 3 days after start of movie we found that about 30% of trees had not switched on CD48. After 4d however, only a small percentage of trees (5%) remained CD48 negative and thus had not lost HSC potential. Also the overall percentage of CD48<sup>+</sup> trees increased rapidly over time resulting in many trees with progeny onset of CD48.

From previous data of HSC cultured in IL6 it was expected that trees from HSC cultured in IL6 would switch on CD48 even earlier than when cultured in IL3, because HSC cultured in SCF and IL6 for 3 days had lost all their reconstitution potential (Ema, Takano et al. 2000). However in our experiments, more trees remained CD48 negative throughout 4 days of culture when cultured in SCF and IL6 compared to SCF and TPO and also less cells showed early commitment to differentiation of the mother cell.

The explanation for the discrepancy in results can only be explained by the differential readout of HSC potential in the two studies. Ema et al. used reconstitution of single cells after culture in different environments however, we utilized a molecular marker to avoid manipulation of cultured cells (Ema, Takano et al. 2000). It is known that CD48 does not start to be expressed immediately after the loss of reconstitution potential, but rather slightly later. This was shown in Wilson et al and also in this Thesis by analysing the expression of CD48 on freshly isolated CD34<sup>+</sup>KSL cells (Wilson, Laurenti et al. 2008). It is known that murine bone marrow cells that express CD34 have lost their reconstitution potential (Yang, Bryder et al. 2005). However, not all of these cells do express CD48. We also do not know what effect various cytokines have on the expression of CD48. It is possible that IL6 either actively suppresses expression of CD48 in cells that have already lost HSC potential or that IL6 leads to a loss of HSC potential but keeps cells in a pre CD48 expressing state. To clarify these questions it will be necessary to repeat reconstitution experiments of cells cultured in SCF and IL6 in addition to monitoring their CD48 expression status.

### **6.6. Exploring the Mechanism Controlling Asymmetric Fate Choice**

As we show here that individual mouse HSC generate asymmetric fates that are probably intrinsically controlled, the mechanism controlling these asymmetric fate decisions was addressed as well. From invertebrates it is known that asymmetric cell fates are often controlled by the asymmetric segregation of determinants during division (Knoblich, Jan et al. 1995; Broadus, Fuerstenberg et al. 1998). It is widely assumed that protein segregation during division is conserved also in fate decisions

of mammalian stem cells of adult tissues. Evidence for this has been brought forward: For example in the developing mouse cortex the mouse homolog of drosophila Numb, an inhibitor of Notch signalling, was found to segregate asymmetrically during division and is crucial for the formation of two differently fated daughter cells (Zhong, Jiang et al. 2000; Shen, Zhong et al. 2002).

In addition to segregating molecular determinants, it has been postulated that stem cells would also retain one set of chromosomes in the self renewed HSC daughter after division to avoid accumulation of mutations in the stem cell compartment. This "immortal strand hypothesis" could be validated in satellite muscle cells (Shinin, Gayraud-Morel et al. 2006), Nestin<sup>+</sup> neural stem cells (Karpowicz, Morshead et al. 2005) and mammary epithelial label retaining cells (Smith 2005) but was not found true for mouse HSC (Kiel, He et al. 2007).

Furthermore in human HPC, it was shown that several endosomal determinants are segregated during division, however, no conclusion concerning their role in fate specification could be drawn from this data since protein distribution was analyzed in fixed cells (Fargeas, Fonseca et al. 2006; Beckmann, Scheitza et al. 2007). No proof for protein segregation as a measure to specify asymmetric fates in HSC daughters has been brought forward. The only evidence that hematopoietic cells specify fates by segregating determinants asymmetrically during division was found in T-lymphocytes (Chang, Palanivel et al. 2007). T-cells when they recognize an antigen presented by a dendritic cells form an immunological synapse which leads to asymmetric distribution of proteins in the T-cell and subsequent asymmetric segregation of proteins into daughter cells during mitosis. The protein segregation causes asymmetric cell specification into an effector and a memory T-cell.

### **6.7. Candidate Segregation in HSC Divisions**

Observing protein segregation in HSC divisions and following fate decisions of HSC daughters can only be accomplished by using time lapse microscopy and single cell tracking, which allow assessment evaluation if a segregated protein is the cause of the specification of a certain cell lineage. We first quantified fluorescence intensity during divisions of HSC that overexpressed fusions of candidate proteins with

fluorescent reporters. We chose candidates whose asymmetric segregation in invertebrate developing cells is crucial to cell specification and embryonic patterning (Li, Yang et al. 1997; Lin and Spradling 1997). In addition, we found them to be expressed in mouse HSC. We found however, that none of our candidates, *Staufen1*, its splice isoform *Staufen<sup>i</sup>*, and *Pumilio1* segregated asymmetrically during division of HSC. It is possible that these factors fulfil to date unknown functions in HSC and other blood cell lineages. They might not control asymmetric fate decisions or these fate decisions might not be controlled intrinsically despite our data supporting this notion.

Other reasons why we did not see any asymmetrically segregated candidates might lie in the method that was applied. It is possible, that the fusion to a fluorescent protein changes the function of the candidate so that asymmetric segregation is not possible anymore. For *Staufen1* and its splice isoform previous publications showed normal function of similar fusion genes (Wickham, Duchaine et al. 1999; Duchaine, Wang et al. 2000). In agreement with this we also did not see differences in the effect of lineage potential between fusion genes and *Staufen1* IRES constructs (data not shown), indicating that the fusion did not alter *Staufen1* and *Staufen<sup>i</sup>* function. In contrast, *Pumilio1* has not been expressed as a fusion previously. In this Thesis we could not compare effects of fusion and IRES construct, as the latter when overexpressed by lentivirus did not yield a significant number of infected cells. Although this might suggest that *Pumilio1* in its wildtype form is toxic to cells and therefore, the *Pumilio1* fusion could alter the protein as we saw colony formation of *Pumilio1* fusion infected cells.

Another reason for the lack of observed asymmetric protein segregation could be that the overexpressed protein is present in much higher levels than endogenous protein and therefore overloads the segregation machinery. It is possible that not all protein is segregated, but is masked by non segregated protein. This was shown in the *Drosophila* egg, where an increase of *Staufen* protein did not lead to more localized *Staufen* in the presence of constant levels of target mRNA (Ferrandon, Elphick et al. 1994).

Our camera and fluorescence quantification tools are sensitive enough to detect 2 fold differences in protein concentration between the two sister cells. It can not be excluded that even lower differences between sister cells could lead to

asymmetric cell fates. However, this is unlikely since asymmetric segregated proteins observed in fixed cells showed often that differences in protein concentrations are easily detectable by eye from still images (Beckmann, Scheitza et al. 2007).

We observed in cells that overexpressed high amounts of Staufen<sup>i</sup> fusion as measured by VENUS expression the formation of fluorescent clumps. These clumps were described previously by Duchaine et al. as overexpression artefacts arise only from overexpression of Staufen<sup>i</sup> alone but are not apparent in Staufen<sup>i</sup> and Staufen1 coexpressing cells (Duchaine, Wang et al. 2000). We did not observe any toxic effects of these clumps but did see slight differences in sister cell fluorescent intensities of Staufen<sup>i</sup> expressing cells of some monitored divisions, however, we do not think this reflects a biological function of the endogenous protein, but rather is an overexpression artefact.

We did not examine the segregation of a fourth candidate, Prominin1, because unlike the other candidate genes we did not find Prominin1 to be expressed in mouse HSC, but only in GMP. The expression of Prominin1 has been widely studied in human, where it is referred to as CD133 and has been implicated as a stem cell marker in various tissues. CD133 is used for example in the blood (Giesert, Almeida-Porada et al. 2001), the neuronal system (Uchida, Buck et al. 2000), and the intestine (Zhu, Gibson et al. 2009) to identify stem and progenitor cells and is also a marker of cancer stem cells (Vercauteren and Sutherland 2001). The expression of mouse Prominin1 however, has not been studied in the blood and HSC and therefore, our finding that Prominin1 is expressed not in HSC but only in myeloid progenitors is rather interesting.

## **6.8. Candidate Influence on Fate Decisions**

### **6.8.1. Effect of Staufen1 on Fate Decisions**

Although we did not detect asymmetric segregation of our candidate genes, indicating no role in asymmetric fate decisions of HSC, it is still interesting if they influence fate choices of HSC and progenitors in another manner. We found no effect of either Staufen1 or Staufen<sup>i</sup> on in vitro colony potential and lineage choice, however, HSC maintenance was inhibited in HSC overexpressing either Staufen

isoform as measured by reconstitution of bone marrow. This suggests an HSC specific role for Staufen1. It has recently been described that Staufen1 when overexpressed inhibits the formation of oxidative stress induced granules that promote silencing of translation (Thomas, Tosar et al. 2009). As it is especially important for HSC to be protected from oxidative stress, inhibition of stress granule formation by Staufen1 could lead to the observed loss of HSC maintenance. However, further studies are necessary to elucidate the role of stress granules in HSC.

There is no information about Staufen function in blood cells, but Staufen2 was found to be expressed in various leukemias (Faubert, Lessard et al. 2004). We had chosen Staufen1 and not Staufen2 as a candidate gene, because in contrast to Staufen2, Staufen1 ORF was readily available and also expressed in HSC. We also tested in colony replating experiments of Staufen1 expressing progenitors show any leukemic behaviour, but they behaved like the vector control infected cells.

### **6.8.2. Effect of Pumilio on Fate Decisions**

When we overexpressed Pumilio1 in HSC we found that HSC could not be maintained as measured by bone marrow reconstitution. Also *in vitro*, in a colony assay we found reduced colony formation potential but Pumilio1 overexpression in progenitors allowed formation of all myeloid lineages. However, we saw an increase in GM colonies at the expense of G colonies, indicating that Pumilio1 influences bipotent GM progenitors. This result might be not relevant, because upon reanalysis of mature cells by FACS at the end of the colony assay, we found that only 3% of cells still expressed Pumilio1 in contrast to 64% of cells still expressing the vector control. We had seeded only VENUS<sup>+</sup> cells into the colony formation assay and therefore, it is unlikely that so many colonies were produced by uninfected cells. It is also unlikely that Pumilio1 when expressed as VENUS fusion is completely toxic to bone marrow cells as we could detect up to 35% of Pumilio1 positive cells 3 days after virus infection by FACS analysis. It is possible however, that Pumilio1 expression is silenced in many cells as cells expressing Pumilio1 could have a disadvantage compared to cells without it. In time lapse movies of vector and candidate gene

infected cells we sometimes saw sister cells, that first displayed equal intensity of fluorescence immediately after division. Subsequently however, we saw loss or decrease of VENUS signal in only one daughter cell while the other daughter retained its fluorescence signal with the same intensity (data not shown), indicating probably the formation of two different fated cells by extrinsic signals. As VENUS mean fluorescence intensity was much higher in vector control infected cells compared to cells infected with any of the candidates, a decrease in VENUS signal in a candidate infected cell would result more readily in a loss of detectable signal than in vector control infected cells. Therefore, one would expect less VENUS expressing cells in mature cells from candidate infected cells than from vector control infected cells. However, when we measured the percentage of VENUS<sup>+</sup> cells in Staufen1 and Staufen<sup>1</sup> infected cells at the end of the colony assay, we found still up to 40% of VENUS expressing cells (data not shown). As the mean fluorescence of Staufen1 IRES expressing cells is lower than mean fluorescence of Pumilio1 fusion positive cells, we would expect even more VENUS<sup>+</sup> cells in Pumilio1 fusion infected cells. Therefore, it is likely that Pumilio1, when expressed as a fusion, affected on the one hand colony formation by various means: Pumilio1 expression could lead to cell death of progenitors at a certain differentiation stage, it could interfere with proliferation of progenitors so that they could not produce visible colonies, or it could cause fast differentiation of progenitors into mature cells that do not have colony potential. On the other hand since we detected only few VENUS positive cells at the end of this assay, it is for sure that a large number of cells must have silenced Pumilio1 expression to levels that are not detectable by FACS anymore. Gerber et al., looking for mRNA targets of Pumilio in adult *Drosophila* ovary, found Pumilio mRNA as a target of Pumilio protein, although they did not find a consensus binding motif in the Pumilio RNA sequence (Gerber, Luschnig et al. 2006). Also in *C.elegans* it was found that two Pumilio homologues autoregulate each other by translational repression of the mRNAs (Lamont, Crittenden et al. 2004). A Pumilio homolog in *C.elegans* is also inhibited by Notch signalling (Lamont, Crittenden et al. 2004) a target of GLD-3, a subunit of an atypical Poly-A polymerase and the STAR protein GLD-1, which both are themselves also targets of Pumilio (Eckmann, Kraemer et al. 2002; Kimble and Crittenden 2007). Therefore, it is conceivable that also mouse Pumilio controls its own translation either by direct interaction with its mRNA or via a

feedback loop that involves other regulators and thus could explain the observed silencing.

We did not see any or very few VENUS<sup>+</sup> cells in Pumilio1 IRES as well as in Pumilio2 fusion and Pumilio2 IRES infected HSC. There are several explanations for this result. As viral titers were low, either because the constructs were too large or wildtype Pumilio1 and or 2 were interfering with virus production and assembly, this could explain low infection efficiency of HSC. However, we used the same MOIs as for other viral vectors. In addition, infection of PA6 stromal cells, that can be infected easily also with low-titer viruses, yielded barely any infected cells with only weak fluorescence signal. Therefore, the IRES behind the fairly long Pumilio reading frames resulted in insufficient translation of VENUS and therefore too low fluorescence signals. For these proteins it might be of advantage to use 2A sequences instead of IRES to separate the candidate gene from the fluorescent reporter (de Felipe, Martin et al. 1999). Cloning a 2A sequence between the candidate and the reporter leads to translation of one long polypeptide that is subsequently cleaved by cellular proteinases resulting in equal amounts of candidate and reporter.

The other explanation for the low infection efficiencies of these viruses could be that these proteins when overexpressed in wildtype form are toxic to cells and therefore, cells could die even before a VENUS signal becomes apparent. Against a toxicity of Pumilio2 speaks that we saw VENUS positive cells within the HSC compartment as well as other progenitor compartments when Pumilio2 was specifically expressed in the bone marrow by crossing inducible Pumilio2 transgenic mice with Tie2CRE mice. From this result we conclude that at least some cells with HSC phenotype are produced and maintained when Pumilio2 is expressed. This result also speaks against low VENUS signals as a reason for low infection efficiencies since transgenic mice were produced from a Pumilio2 IRES construct and we did not have difficulty detecting VENUS signal in these mice. Further experiments will have to examine Pumilio2 expressing HSC and progenitors from these mice for their reconstitution and fate decision properties.

### 6.8.3. Effect of Quaking1 on Fate Decisions

The overexpression of Quaking1 in HSC and progenitors allowed colony formation and generation of all myeloid lineages in vitro. In vivo reconstitution experiments however showed that Quaking1-6B expression did not allow HSC maintenance as measured by bone marrow reconstitution. Quaking1-5A expression allowed maintenance of very few phenotypical HSC that we found in the bone marrow of reconstituted mice, however, the low number of events positive for VENUS expression within the HSC population leaves doubts as to the relevance of those few percent. The loss of HSC potential in Quaking1 overexpressing cells is not astonishing, when comparing Quaking1 to its *C.elegans* homolog Gld1. Gld1 in the *C.elegans* germline promotes oocyte differentiation from germline stem cells. In null mutants of Gld1, germcell tumors are formed and oocyte differentiation is inhibited (Francis, Barton et al. 1995). If this is transferred to HSC, abolishment of Quaking1 would result in leukemic HSC expansion but gain of Quaking1 in increased differentiation. Indeed only very few progenitor cells as well as more mature cells of the GM and erythroid lineage could be detected in the bone marrow of mice transplanted with Quaking1 expressing HSC. Also PB levels in transplanted mice showed a rapid decrease in Quaking1 expressing cells. Therefore, it is likely that Quaking1 expression led to a fast differentiation in vivo. The in vitro data of Quaking1 expressing cells indicates however, that differentiation could not have progressed too far down the hierarchy of blood development, as these cells could still form normal colonies of all lineages. The reduced G colonies in both Quaking1-5A and -6B as well as more GM and more M colonies in Quaking1-5A and -6B respectively, indicates that G colony formation was somehow inhibited in Quaking1 expressing progenitors. The role of Quaking1 in GM lineage decisions is interesting and should be further explored in time lapse movies. We selected Quaking1 as a candidate partly because its homolog Gld1 is regulated by *C. elegans* Pumilio (reviewed in Kimble and Crittenden 2007). The fact that both Pumilio1 as well as the Quaking1 isoforms seem to have an effect on GM lineage decisions in vitro could hint towards a connection of Pumilio and Quaking1 in mammals, although studies as to their interaction have to be undertaken to confirm this notion.

In summary, *Staufen1*, *Staufen1<sup>i</sup>*, *Pumilio1*, *Quaking1-5A* and *-6B* interfere with HSC maintenance in expansion condition of reconstituted mice. The *Pumilio2* effect on HSC maintenance was not examined under these same conditions, but resulted in at least some HSC maintenance in homeostasis conditions in a transgenic mouse model. It would be interesting to see if *Staufen1* as well as *Quaking1* isoforms and *Pumilio1* would allow HSC maintenance under homeostasis conditions as well. Unfortunately no functional transgenic mice were available expressing these candidates. It will be also interesting to transplant HSC expressing *Pumilio2* from transgenic *Pumilio2* mice into recipients and evaluate the effect of *Pumilio2* on HSC behaviour in expansion situation.

In addition, if the loss of HSC potential caused by candidate overexpression results in rapid loss of HSC potential before the first division of HSC, it is possible that protein segregation of candidates cannot take place anymore if this is an HSC specific mechanism that is not active in non-HSC anymore.

## **6.9. Conclusion**

We could show at the single cell level and with a high temporal resolution that HSC differ in their division kinetics as well as in their fate decision properties from MPP. We show that HSC produce asymmetric fated daughter cells independently of their environment and intrinsically control the decision between self renewal and differentiation as measured by a live marker. The mechanism how this is achieved remains unknown, but we show here a method how a large number of candidate genes can be screened fast and efficiently for their potential role in protein segregation and fate decisions. Although they were not segregated in HSC divisions, the here examined candidate genes, *Staufen1*, *Staufen1<sup>i</sup>*, *Pumilio1*, and *Quaking1-5A* and *-6B*, do influence HSC maintenance and fate decisions and therefore must play a critical role in HSC function.

## 7. Experimental Procedure

### 7.1. Isolation of Stem and Progenitor Populations

For isolation of HSC, MPP populations and CLP, femurs, tibias and hipbones were removed from 12 week old male C57Bl/6J mice, cleaned of muscle tissue and crushed with a mortar and pestle. The obtained cell suspension was passed through a cell strainer (cat no 8240816, BD Biosciences). Cells were resuspended in FACS buffer containing 2% FCS (cat no P30-3302, PAN Biotech GmbH, Aidenbach, Germany), 1mM EDTA (cat no 8043.2, Roth, Karlsruhe, Germany), 0.1% Sodium-Azide (cat no S2002-25G, Sigma, Taufkirchen, Germany) and PBS. PBS was prepared from 8 g NaCl (cat no S/3160/65, Fisher Scientific, Schwerte, Germany), 0.2 g KCl (cat no 4936.1000, Merck, Darmstadt, Germany), 0.2 g KH<sub>2</sub>PO<sub>4</sub> (cat no 1.04873.1000, Merck, Darmstadt, Germany) and 1.18 g Na<sub>2</sub>HPO<sub>4</sub> (cat no T876.2, Roth, Karlsruhe, Germany) dissolved in 1l bidistilled water and sterilized. For isolation of myeloid progenitors, as well as for analysis of bone marrow progenitors of transplanted mice, bone marrow was flushed from tibias and femurs and mononucleated cells were isolated using a Histopaque 1083 gradient (Sigma Aldrich). Cells were then resuspended in FACS buffer for staining.

Cells from bone marrow - PA6 cocultures were dissociated using Hank's enzyme free dissociation buffer (cat no 13150-016, Gibco/Invitrogen, Karlsruhe, Germany) for 40 min at 37°C, resuspended in FACS buffer containing propidium iodide (PI, P4170, Sigma, Taufkirchen, Germany) and filtered through a cell strainer (cat no 352235, BD Falcon, Franklin Lakes, USA) before analysis.

Colonies in semisolid medium were resuspended after counting in 10ml PBS per 35mm cell culture dish, pelleted and resuspended in FACS buffer containing PI.

### 7.2. Antibody Staining

All stainings were performed in 50µl volume of FACS buffer.

For isolation and analysis of HSC, MPP and CLP, cells were stained with 50ng each per  $10^6$  cells of the following biotinylated lineage antibodies: Ter-119 (Ter119, cat no 13-5921), CD11b (M1/70, cat no 13-0112), Gr-1 (RB6-8C5, cat no 13-5931), CD41 (MWRReg30, cat no 130411), CD3 $\epsilon$  (145-2C11, cat no 13-0033), B220 (CD45R, RA3-6B2, cat no 13-0452), and CD19 (1D3, cat no 130193, all eBioscience, San Diego, USA). Cells were lineage depleted according to manufacturer's instruction using 20% of reagents from Easy Sep Biotin Selection kit (cat no 18556, Stem Cells Technology, Vancouver, Canada). Lineage depleted cells were stained with the following antibodies for HSC and MPP stains per  $10^6$  cells each: 40ng Streptavidin Alexa750 (cat no 47-4317, eBioscience), 60ng c-kit PECy7 (2B8, cat no 25-1171, eBioscience), 40ng sca-1 Pacific Blue (D7, cat no 108120, Biolegend, San Diego, USA), 100ng CD34 Alexa647 (RAM34, cat no 51-0341, eBioscience), and 40ng CD48 PECy5 (HM48-1, cat no 103420, Biolegend). For experiments analyzing asymmetric fates,  $10^6$  cells were additionally stained with 60ng Flt3 PE (A2F10, cat no 12-1351, eBioscience). For protein segregation experiments and viral infections,  $10^6$  cells were stained instead with 40ng CD150 PE (TC15-12F12.2, cat no 115904, Biolegend) in addition to HSC antibodies. For isolation of CLP, lineage depleted cells were stained with 40ng Streptavidin Alexa750, 60ng c-kit PECy7, 40ng sca-1 Pacific Blue, and 40ng IL7R $\alpha$ -PE (A7R34, cat no 12-1271, eBioscience).

For isolation of myeloid progenitor populations  $10^6$  isolated mononucleated bone marrow cells were stained with 50ng each of the following biotinylated antibodies: Ter-119, Gr-1, CD41, CD3 $\epsilon$ , B220, CD19, IL7R $\alpha$  (A7R34, cat no 13-1271, eBioscience), with the addition of 50ng biotinylated Flt3 (A2F10, cat no 13-1351, eBioscience) for CMP isolation and 50ng biotinylated CD71 (R17217, cat no 13-0711, eBioscience) for MEP isolation. For the isolation or analysis of CMP, GMP and MEP, cells were additionally stained with 60ng c-kit PECy7, 40ng sca-1 Pacific Blue, 100ng CD34 Alexa647, 40ng Fc $\gamma$ R FITC (2.4G2, cat no 553144, Pharmingen/BD Biosciences, Heidelberg, Germany) and 40ng Streptavidin APC-Cy7.

For analysis of bone marrow progenitors of transplanted mice,  $10^6$  mononucleated cells were stained with 40ng CD45.2 PECy5.5 (104, cat no 35-0454, eBioscience). For analysis of myeloid lineage cells,  $10^6$  isolated cells were stained with 40ng Ter119 APC Alexa780, 50ng biotinylated Mac-1, and 40ng Ly6G PE (1A8, 551461, Pharmingen/BD Biosciences). For analysis of erythroid lineage cells,  $10^6$  cells

were stained with 40ng the following lineage antibodies, all in APC: Mac-1 (M1/70, cat no 170112, eBioscience), Gr-1 (RB68C5, ) cat no 17-5931, eBioscience), B220 (RA3-6B2, cat no ,17-0452, eBioscience), as well as 50ng biotinylated CD71 (R17-217, cat no 130711, eBioscience), 50ng Ter119 PE (Ter119, cat no 556673, Pharmingen/BD Bioscience) and 40ng Streptavidin Pacific Blue.

### 7.2.1. Labelling of CD48 Antibody

CD48 (HM48-1, cat no 103408, Biolegend) was labelled with Alexa647 (cat no A20186, Bioprobes/Invitrogen, Karlsruhe, Germany) according to the manufacturer's instructions.

### 7.2.2. Titration of CD48 Antibody

The CD48 antibody was titrated using 0.2, 0.5, 1, and 2  $\mu\text{g}$  labelled antibody per  $10^6$  lineage<sup>+</sup> bone marrow cells, which were a by-product of the lineage depletion. Lineage<sup>+</sup> cells were suspended in 50 $\mu\text{l}$  of FACS buffer, stained with antibody for 30 minutes at 4°C, and analyzed with the FACS Aria.

For in culture titration, KSL cells were cultured in SFEM (SFEM, no 09650, Stem Cell Technologies) containing 100 ng/ml SCF (cat no 250-03, PeproTech, Hamburg, Germany), 10ng/ml IL3 (cat no 213-13, PeproTech), and 10ng/ml IL6 (cat no 216-16, PeproTech) for 4 d in the presence of CD48 Alexa647 at the following final concentrations: 0, 2, 1, 0.2, and 0.1 $\mu\text{g}/\text{ml}$ . After 4 d of culture, cells were pelleted, washed, resuspended in FACS buffer and stained with CD48 FITC (cat no 11-0481, eBioscience) for 30 minutes on ice before FACS analysis.

## 7.3. Flow Cytometry

Cells were analyzed by flow cytometry using a FACS Calibur System (Becton Dickinson, San Jose, USA) equipped with 488 nm and 635 nm lasers. FITC and

VENUS signals were detected using the filter 530/30, PE and tdTOMATO signals were analyzed with the 585/42 filter, PI was detected with the filter 630 LP and APC and Alexa647 signals were detected with the filter 661/16.

A FACSAria cell sorter (Becton Dickinson, San Jose, USA) was employed to isolate individual populations by cell sorting. VENUS and FITC signals were analyzed using the 488 nm laser and 530/30 emission filter. PE and tdTOMATO were excited with the 488 nm laser and detected using the emission filter 575/26. PE-Cy7 signals were recorded using the 488 nm laser and the 780/60 emission filter. APC and Alexa647 were illuminated with the 633 nm laser and detected in the 660/20 emission filter. PI was excited using the 407 nm laser and detected using the 610/20 emission filter. Sorting was performed with a maximal flow rate of 3 using high precision mode (0/32/0). Sorting purity was ensured either by reanalysis of sorted cells for progenitor populations or by conducting a resort analysis before the actual sorts for HSC. Data were analyzed with FACS DiVa (Becton Dickinson), CELLQuest Pro (Becton Dickinson) and WinMDI 2.8 ([www.facs.scribbs.edu](http://www.facs.scribbs.edu)) softwares.

#### **7.4. Cell Culture Conditions**

All cells were cultured at 37°C, 5% CO<sub>2</sub> and 95% relative air humidity in a standard tissue culture incubator (Microbiological Incubator CD210; Binder; Tuttlingen, Germany).

All centrifugation steps were carried out with 240 x g for 5 min if not indicated differently. Cells were washed using sterile PBS. To ensure good quality of the media, cell culture media were not stored for longer than 4 weeks after preparation.

##### **7.4.1. Colony Formation Assay**

For colony assays of virus infected cells, cells were infected in 96 well plates for 3 d in 100ng/ml SCF and 100ng/ml TPO in 100µl SFEM. VENUS positive cells were sorted into IMDM with 2% FCS. Cells were counted in Terasaki plates by adding 5µl of cell suspension per Terasaki well and centrifugation at 400xg for 5 min. 400 cells

were added in 100µl IMDM with FCS to 1.1ml semi solid media allowing formation of all myeloid lineages (Methocult, cat no 03434, Stem cell Technologies) and 1% Pencillin/Streptomycin (cat no 15070063, Invitrogen). The suspension was vortexed for 10 s and pipetted carefully, to avoid transferring of bubbles, into one 35mm plate. After 7 d (progenitors) or 10 d (stem cells) at 37°C, cell clusters containing a minimum of 30 cells were counted as colonies.

Colony types were identified as follows: Erythroid colonies contain at least 30 erythroid cells that are tiny and irregular in shape and appear as if they are fused together. Mature erythroid colonies turn red-brown at the center, as they produce hemoglobin. Megakaryocyte colonies contain at least 2 megakaryocytes. Megakaryocytes can be identified by their large size and their orange-skin appearing plasma membrane. They also have a segmented nucleus that can be easily identified when observing nuclear membrane localized fluorescent protein infected cells. Granulocyte colonies contain at least 30 small cells that are slightly bigger than erythrocytes. Granulocyte colonies can be small and dispersed or when they are larger become tightly packed and contain several clusters. Macrophage colonies contain at least 30 cells. Macrophages can be easily identified by their small nucleus and long spindle-like shape, which becomes especially apparent when they are able to attach to the bottom of the dish due to limited amount of methylcellulose. GM colonies are characterized by the presence of both granulocytes and macrophages. They can be identified by tightly packed centers and are more spread out around the edges. ME colonies contain megakaryocytes and erythrocytes and it is important to try to identify erythroid clusters among the large megakaryocytes. Large megakaryocyte only colonies also contain smaller cells which are megakaryocyte committed cells and not erythrocytes. GEMM colonies contain all four myeloid cell types and are consistent of 500 or more cells. To distinguish them from large GM colonies, it is easiest to identify the large megakaryocytes among them. Also erythrocyte clusters should be present on the colonies edges.

## 7.4.2. Cell Lines

### 7.4.2.1. PA6 Cell Culture

PA6 (MC3T3-G2/PA6) stroma cells were cultured as described previously (Kodama, Amagai et al. 1982). PA6 cells were kept in medium containing 10% of FCS (cat no P30-3302, PAN Biotech GmbH) in  $\alpha$ -minimal essential medium ( $\alpha$ -MEM).  $\alpha$ -MEM was prepared from powder (cat no 25080, Gibco/Invitrogen, Karlsruhe, Germany) which was solved in a sodium bicarbonate solution (cat no 11900-016, Gibco/Invitrogen) and sterile injection water (cat no 7202A161, Braun, Melsungen, Germany) according to manufacturer's instructions. PA6 cells were only kept for a maximum of 25 passages and only dissociated and diluted when 100% confluent as otherwise cells lost their supportive properties. In general, PA6 stroma was diluted every 4 days 1:4 by washing with PBS, trypsinizing with 0.05% Trypsin/EDTA (cat no 25300-054, Gibco/Invitrogen) for 2 min at 37°C. Dissociated PA6 cells were resuspended in culture medium and mixed gently to obtain a homogenous cell solution which was diluted with medium, seeded onto fresh tissue culture dishes and moved carefully to ensure equal distribution of cells on the culture plate.

### 7.4.2.2. Freezing and Thawing of Cells

To store PA6, cells were first trypsinized, resuspended in normal culture medium and centrifuged. The cell pellet was then resuspended in culture medium containing 10% dimethylsulfoxide (DMSO, cat no D2438, Sigma) and transferred to cryotubes and frozen in Cryo Freezing containers (cat no 5100-0001, Nalgene, Rochester, USA) at -80 °C. After one day, cells were transferred into the nitrogen tank. For thawing, PA6 cells were removed from the nitrogen tank and the lid of the cryotube was slightly opened to permit gas pressure release upon warming up. Cells were kept in a 37°C water bath for the time the cells needed to defrost completely. Cells were washed with 10ml of culture medium to remove DMSO and were transferred into a well of a 6-well cell culture dish. The medium was changed again on the next day.

#### 7.4.2.3. Transient transfections

All transient transfections were carried out using Lipofectamin2000 (cat no 11668-019, Gibco/Invitrogen, Karlsruhe, Germany) and Opti-MEM (cat no 51985, Gibco/Invitrogen). To check the fluorescence signal produced from ubiquitously expressed plasmid DNA, HEK cells were transfected. Cells were prepared in a 10cm<sup>2</sup> dish to be approximately 30% confluent at the day of transfection. For transfection 10µl Lipofectamin2000 were mixed with 90µl Opti-MEM and incubated 15 min at RT. 2µg of DNA was added and vortexed. After incubating another 15 min at RT the culture medium was removed and replaced with the Lipofectamin2000-DNA suspension. Cells were allowed to take up DNA and grow for at least 24 h before analysis.

To check specific localization of ubiquitously expressed tagged fluorescent proteins, PA6 cells were transiently transfected. 30% confluent PA6 grown in a 6-well dish were transfected as follows: 15µl Lipofectamin2000 were mixed with 85µl opti-MEM. Separately, 2µg DNA were mixed with Opti-MEM to a final volume of 100µl. Both were incubated for 20 min at RT, mixed and incubated for another 20 min at RT. Afterwards, the medium of PA6 cells was removed, replaced with the lipofectamin-DNA mixture and incubated for 2 d before analysis.

#### 7.4.3. Primary Cells

##### 7.4.3.1. HSC Cocultures on PA6

Confluent PA6 layers were utilized for cocultures with bone marrow stem and progenitor cells. Isolated bone marrow cells were cultured on PA6 layers in IMDM (Osmolarity: 315, cat no P04-20451S1, PAN Biotech GmbH) with 20% horse serum (HS, cat no 16050-122, Gibco/Invitrogen), 10<sup>-7</sup>M hydrocortisone (cat no H0888, Sigma) and 100ng/ml SCF (cat no 250-03, PeproTech, Hamburg, Germany). For in culture staining, CD48 Alexa647 was added to the media at 0.2µg/ml.

#### 7.4.3.2. Stroma Free Suspension Culture

For stroma free cultures of isolated hematopoietic stem and progenitor cells, cells were cultivated in serum free media (SFEM, no 09650, Stem Cell Technologies) with 100ng/ml SCF (cat no 250-03)), SCF and 100ng/ml TPO (cat no 315-14), SCF and 10ng/ml IL3 (cat no 213-13), or SCF and 100ng/ml IL6 (cat no 216-16, all PeproTech). As in PA6 cocultures, CD48 Alexa647 was added to the culture media at a dilution of 0.2µg/ml.

#### 7.4.3.3. Fibroblast Isolation from Mouse Tail Clips

Fibroblasts were isolated out of 5mm long tailclips from transgenic mice. The outer skin containing hair was removed and the remaining tissue chopped into small pieces with scissors. Tissue was suspended in 100µl of PBS containing 7mg/ml collagenase1 and 7mg/ml collagenase2 and transferred to a 96 well plate. The plate was incubated for 30 min in a 37°C shaker. Subsequently, enzymatic reaction was stopped by adding 150µl of DMEM with 10% FCS. After 7 days, cells were growing out of tissue and can then be infected by adding 10<sup>5</sup> virus particles per well of CRE virus (546 pRRL.PPT.SF.CRE-IRES-mito-tdTomato-pre) or control virus (544 pRRL.PPT.SF.IRES-mito tdTomato pre). Cells were checked daily for fluorescence expressing cells. Cells were trypsinized and resuspended in FACS buffer and analyzed on the FACS Calibur.

### 7.5. Virus Production

HEK 293T cells were kept in DMEM (cat no 41966, Gibco/Invitrogen) containing 10% FCS and split every 2 d at a ratio of 1:8. For virus production cells were seeded at a density of 5x10<sup>6</sup> cells per 60cm<sup>2</sup>. For each 60cm<sup>2</sup> dish the following plasmids were added to 450µl of water and 50µl of CaCl<sub>2</sub> solution (cat no CAPHOS-1KT, Sigma) 16 h after cell seeding: 5ng of transfer vector containing the candidate gene (derived from plasmid 390 pRRL.PPT.SF.GFPpre), 2ng envelop vector containing either ecotropic (plasmid 391 K73 pEcoEnv-IRES-puro) or VSVG

pseudotyped envelop protein (plasmid 495 pMD2.VSVG), 10ng plasmid containing RRE (Rev responsive element, plasmid 393 pMDLg\_pRRE), and 5ng plasmid containing Rev (regulator of expression of virion proteins, plasmid 392 pRSV\_Rev), 390 pRRL.PPT.SF.GFPpre, 391 K73 pEcoEnv-IRES-puro, 392 pRSV\_Rev, 393 pMDLg\_pRRE , and 495 pMD2.VSVG were all obtained from Dr. Christopher Baum and previously published in Schambach et al. 2006 (Schambach, Galla et al. 2006).

The latter two elements are needed for an increased expression efficiency of the viral RNA. The plasmid mix was then added to 500µl of HEPES buffered saline (HBS, from CAPHOS-1KT, Sigma) using air bubbling and subsequently the mixture was vortexed for 10s and incubated for 20min. This allowed formation of CaPO<sub>4</sub> crystals which enabled transfer of DNA into cells. Growth media was removed from HEK 293T cells and replaced by 10ml of transfer media (TF) containing DMEM, 10% FCS, 1% sodium pyruvate (cat no S8636, Sigma), 20nM HEPES (cat no 15630-856, Gibco/Invitrogen) and 15µM chloroquine (cat no C6628, Sigma). After incubation, the DNA-HBS mix was added slowly to HEK 293T cells in fresh TF medium and incubated for 8 h in a cell culture incubator allowing DNA uptake by the cells. After incubation, medium was replaced by fresh TF medium without chloroquine. Cells were allowed to produce virus for 36 h, after which the supernatant was removed, pooled and kept on ice. The virus containing media was then centrifuged at 240 x g for 5 min at 4°C and the supernatant filtered through a 0.2 µm filter (cat no Minisart 17597, Sartorius-Stedim, Göttingen, Germany) to remove cell debris. Cell culture dishes containing HEK 293T cells from the virus production were checked under the microscope for fluorescent signal produced by transfected expression plasmids. Viral supernatant was then transferred to polyallomer centrifugation tubes (cat no 326823, Beckman, Krefeld, Germany) and centrifuged at 10000 x g for 16 h at 4°C for ecotropic virus and at 50000 x g for 1 h at 4°C for VSVG pseudotyped virus. After centrifugation, the supernatant was removed from the ultra centrifugation tubes, the pellet resuspended in 200µl of SFEM and the virus aliquoted and frozen at -80°C.

### 7.5.1. Virus Titration

3T3 NIH cells were kept in DMEM with 10% FCS and seeded every 3d at  $10^5$  cells per  $25\text{cm}^2$ . For virus titration,  $5 \times 10^4$  cells per well were seeded into a 24 well plate. 16 h after cell plating, cells were counted and medium was changed and virus was thawed and added in triplicates at dilutions from  $10^{-1}$  to  $10^{-4}$ . After 48 h cells were checked for the presence of fluorescence signal in the microscope. Cells were then trypsinized, suspended in 300 $\mu\text{l}$  of fresh media per well and subsequently analyzed by FACS. The virus titer was calculated considering obtained percentages of VENUS<sup>+</sup> cells and dilution factors. Briefly, the number of counted cells from one well times the percentage of VENUS<sup>+</sup> cells and divided by 100 equals the amount of virus particles per well.

The virus titer equals the amount of virus per well times the dilution factor per 1ml media that the cells are contained in. The virus titers from 3 wells are averaged. The final titer is the average of all virus dilutions that yield percentages of VENUS<sup>+</sup> cells between 3% and 30%.

### 7.5.2. Virus Infection

Cells isolated by FACS sorting were added in 5 $\mu\text{l}$  volume in a Terasaki well and centrifuged. Cells that were at the bottom of the well were counted. For virus infection, cells were centrifuged in an eppendorf tube for 400xg for 10 min at 4°C and left in 100 $\mu\text{l}$  of SFEM containing 100ng/ml SCF and 100ng/ml TPO for each viral vector.

For infection of HSC by spin infection wells of a 96 well plate were coated with retronectin (cat no TAK T100, Takara, Madison, USA). Per well 50 $\mu\text{l}$  of retronectin in PBS at a concentration of 20 $\mu\text{g}/\text{ml}$  were added, incubated for 2 h, blocked with 2% BSA for 30 min and washed with PBS. Cells in SFEM were added to the well together with 10 $\mu\text{g}/\text{ml}$  protamine sulfate (cat no P4380, Sigma) and virus at a MOI of 600. The plate was spun at 37°C (or as indicated) for 1 h at 400 x g.

For standard infection procedure, the cell suspension was transferred to a 96 well plate and virus was added at MOI of 100. Not more than 1000 cells should be infected per one well to avoid accumulation of precipitate of virus as this can

interfere with infection efficiency. Adding of virus was done in the S2 lab and cells were incubated over night at 37°C in the S2 lab incubator to allow for infection. After infection, supernatant still contains active virus so it is important to handle it with care. Cells were resuspended in 1ml SFEM containing cytokines pertinent to the experiment and washed twice in 1ml in an 1.5ml eppendorf tube by centrifugation.

### 7.6. Transplantation Experiments

For all transplantation experiments, non irradiated  $W^{41}/W^{41}$  mice, generous gift from Dr. Norman Iscove, were used as recipient mice. Bl6 were utilized as donor mice. Differential expression of CD45 alleles distinguished donor (CD45.2) from recipient (CD45.1) blood cells in peripheral blood (PB).

For experiments analyzing reconstitution potential of cultured HSC, HSC were cultured on PA6 for 90 h, dissociated and stained with antibodies. Cells were stained with 50ng CD45 FITC (30-F11, eBioscience), 50ng self labeled CD48 Alexa647 per  $10^6$  cells as well as KSL antibodies (as in HSC isolation from bone marrow) and CD45<sup>+</sup>CD48<sup>-</sup> and CD45<sup>+</sup>CD48<sup>+</sup> cells were sorted. CD48<sup>-</sup> cells equivalent to 82 and 500 CD48<sup>-</sup>KSL cells respectively as well as CD48<sup>+</sup> cells equivalent to 271 CD48<sup>+</sup>KSL cells were transplanted in triplicates into recipient mice. For experiments analyzing the effect of candidate gene expression on HSC potential, 700 HSC per mouse and virus were cultured in triplicates in the presence of SCF and virus for 2 d and were transplanted into recipients.

For all transplantations, isolated cells were mixed with  $10^5$  mononucleated bone marrow cells and resuspended in 300µl of sterile PBS per mouse. The tail of the recipient mice was pretreated with a heating lamp to facilitate injection into the tail vein. Cell suspension was injected using a 28G needle.

For both experiments, the percentage of donor cells in the PB was assessed every 4 weeks for 16 weeks. Briefly, 5mm of mouse tail was cut and 3 drops of blood collected in tubes containing 30µl Sodium Salt (H4784, Sigma) dissolved in PBS. The following lysis was performed twice: 500µl PBS were added and the solution pelleted for 10 min. After removal of supernatant, 30µl of ACK lysing buffer (cat no 10-548E, Lonza, Basel, Switzerland) buffer were added to the pellet and vortexed for 1 min.

Cells were subsequently resuspended in FACS buffer and stained as follows. For analysis of peripheral blood (PB) from transplanted mice,  $10^6$  cells were stained with 50ng biotinylated CD45.1 (A20, cat no 17-0453), 40ng CD45.2 APC (104, cat no 17-0454, eBioscience), 40ng Mac-1 PECy7 (M1/70, cat no 552850, Pharmingen/BD Biosciences), 40ng Gr-1 PECy7 (RB6-8C5, cat no 552985, Pharmingen/BD Bioscience), 40ng B220 PE (RA3-6B2, cat no 12-0452, eBioscience), 40ng Ter119 APC Alexa780 (Ter119, cat no 475921, eBioscience), and 40ng Streptavidin Pacific Blue (cat no S11222, Molecular Probes/Invitrogen, Karlsruhe, Germany).

Ter119 negative cells were analyzed for the expression of CD45.1 (recipient cells) and CD45.2 (donor cells). CD45.2 cells were then analyzed for the presence of myeloid (Gr-1 and Mac-1 expressing) cells and lymphoid (B220 expressing) cells.

In mice transplanted with virus infected cells, VENUS expression of donor cells was assessed in addition. Mice transplanted with virus infected cells were sacrificed 18 weeks after transplant, bone marrow was isolated and separated by a Histopaque 1083 gradient. The percentage of VENUS<sup>+</sup> cells within the donor cells in HSC (CD150<sup>+</sup>CD48<sup>-</sup>CD34<sup>-</sup>KSL), KSL, CMP, GMP, MEP, CLP as well as myeloid and erythroid lineage cells was determined.

## **7.7. Plasmid Vector Cloning**

### **7.7.1. Purification of Plasmid DNA**

High copy plasmids were purified from competent bacteria using the Qiaprep Spin Miniprep Kit or the Qiagen Plasmid Maxi Kit (cat no 27104 and 12165, respectively, Qiagen, Hilden, Germany). All DNA was solved in sterile bi-distilled water.

### **7.7.2. Construction of Plasmid DNA**

DNA was constructed using the Clone Manager software 7, 8 and 9 Professional Editions.

### 7.7.3. Transformation of Bacteria

To transform bacteria with plasmids, heat-shock competent *Escherichia coli* (DH5 $\alpha$ ) were defrosted on ice for about 15 to 30 min. 25ng of plasmid DNA or the entire heat inactivated ligation cocktail were added to 50 $\mu$ l bacteria. After incubating for 0.5 h on ice, cells were heated to 42°C for 45 sec before cooling them in ice for 2 min. Cells were mixed with 0.5 ml LB (LB Broth Base, cat no 12780-029; Invitrogen, Karlsruhe, Germany) medium without any antibiotics and kept at 37°C while constantly shaking. 40 and 400  $\mu$ l bacteria were plated onto LB agar plates containing the required antibiotic, and cultured over night at 37°C.

### 7.7.4. Restriction Digestions and Ligations

Restriction digestions and ligations were carried out using enzymes and suitable buffers from NEB (New England Biolabs, Ipswich, USA) or Fermentas (St.Leon-Roth, Germany) according to the manufacturer's instructions.

### 7.7.5. Agarose Gels

After digestion DNA fragments were separated on 0.8 to 2% agarose gels prepared in TAE (Tris: cat no 5429.2, Roth, Karlsruhe, Germany; Acetate: cat no 1.00063.2511, Merck, Darmstadt, Germany; EDTA disodium salt dihydrate: cat no 8043.2, Roth, Karlsruhe, Germany), agarose (cat no 8700500, Biozym, Oldendorf, Germany) and Ethidium bromide (cat no 2218.2, Roth, Karlsruhe). DNA fragments were separated using voltages between 70 and 200 V in TAE-buffer depending on the size of gels.

### **7.7.6. Purification of DNA Fragments**

DNA fragments were cut out from agarose gels using a scalpel and purified from the agarose gel using the QIAEX II Gel Extraction Kit or the QIAQUICK Gel Extraction Kit (cat no 20021 and 28704, respectively, both Qiagen, Hilden, Germany). Purification of PCR products was performed using the QIAquick PCR Purification Kit (cat no 28104, Qiagen, Hilden, Germany).

### **7.7.7. Sequencing**

Sequencing was either performed in the GSF sequencing facility using BigDye® Terminator v3.1 Cycle Sequencing Kit (cat no 4337456, Applied Biosystems, Foster City, USA) and the following PCR conditions: 1 cycle at 96°C for 1 min, 35 cycles 96°C for 10 s, 50°C for 5 s, and 60°C for 4 min. Alternatively, DNA and primers were sent to MWG, Ebersberg, Germany.

## **7.8. Reverse Transcriptase-PCR of Stem and Progenitor Cells**

Reverse transcriptase (RT) polymerase chain reaction (PCR) was performed with primers detecting candidate genes (Table 1) in all mentioned bone marrow populations. For RT-PCR reactions, all steps were performed using previously untouched and autoclaved eppendorf tubes and pipette tips with filters. 500 cells of each bone marrow population were sorted into eppendorf tubes containing One Step RT-PCR (cat no 210210, Quiagen) master mix made up according to manufacturer's instructions. Sorted cell suspension in mastermix was vortexed and frozen. 50 cell equivalents in master mix were employed in individual RT-PCR reactions. After addition of enzyme and primers, reverse transcription was performed for 30 min at 50°C. Subsequently the PCR reaction was initiated by activation of polymerase for 15 min at 95°C. PCR condition constituted 40 cycles of denaturation for 1 min at 94°C, annealing for 1 min at 60°C and extension for 1 min at 72°C. A final extension step for 10 min at 72°C ensured complete formation of all PCR products. In each sort and

RT-PCR reaction all genes including  $\beta$ -actin and all populations were analyzed in one experiment. The complete PCR reaction was analyzed on a 2% agarose gel.

### **7.8.1. Primer design**

Primers were designed using the Clone Manager software 7, 8 and 9 Professional Editions. Primer sequences and binding locations are listed in Table 1. Design of specific primers to Quaking1 isoforms was not possible because most exons are shared by all three isoforms and additionally sequences are repeated within exons. Therefore primers detecting all three isoforms were designed for Quaking1.

## **7.9. Time Lapse Microscopy**

### **7.9.1. Preparation of Specimen**

Cells in culture need constant CO<sub>2</sub> levels of 5%. To allow for maintenance of CO<sub>2</sub> in the culture vessels during time lapse movies, medium and gas containing 5% CO<sub>2</sub> was contained without exchange for the duration of movies (up to 7 d). In detail, purified cells were plated in medium incubated in the cell culture incubator over night to allow for CO<sub>2</sub> saturation. After cell plating, cell culture flasks and dishes were kept in the incubator for at least another hour to allow for gas exchange. Immediately before the start of the movie, caps of cell culture flasks were tightly closed and multiwell plates were sealed with scotch tape to prevent gas exchange with surrounding air.

### **7.9.2. Acquisition of Time Lapse Images**

Time lapse movies were recorded using a Zeiss inverted fluorescence microscope (Axiovert 200 M, Zeiss, Hallbergmoos, Germany), a motorized stage (cat no 0431478, Märzhäuser, Wetzlar-Steindorf, Germany) and a PECON heating system

to heat a XL incubator (Erbach, Germany) at 37 °C. Images were acquired using Aviovision 4.5 software up-graded with a software developed in our laboratory by Timm Schroeder (Eilken, Nishikawa et al. 2009).

Phase contrast images were taken every 2 min with 10x EC-Plan-Neofluar Ph1 (cat no 440331-9902-000, Zeiss) objective, a 0.63x TV adaptor using a AxioCam HRm camera at 1388x1040 or 2776x2080 pixel resolution (Zeiss). Fluorescence images were acquired at regular intervals using a mercury (HBO 103 W/2) or a xenon (XBO 75 W/2 ORF, both Osram, Augsburg, Germany) lamp. Illumination to detect CD48 staining was performed every 50 to 100 minutes (800 ms excitation) using filtersets 26 (cat no 488026-0000-000, Zeiss), 50 (cat no 488050-0000-000, Zeiss), or Cy5 ET-filterset (cat no F46-006, AHF, Tübingen, Germany). VENUS signals from lentivirus overexpression of fusion genes were recorded every 12 to 18 min (500 to 1000 ms excitation) using filterset 46HE (cat no 489046-0000-000, Zeiss).

Acquired images were saved in jpg format compressed to 97% quality for phase contrast images and left at 100% quality for fluorescent images.

### **7.10. Data Analysis**

Data were analyzed using TTT (Timm's Tracking Tool, software developed in our laboratory, (Eilken, Nishikawa et al. 2009)) on Siemens Celsius R630 workstations with 4 to 32 GB of RAM and SUSE Linux operating systems with KDE desktop. Movies were analyzed using all recorded phase contrast and fluorescent images without further compression. Image contrast was manually enhanced for each wavelength channel separately to optimize recognition of relevant cellular features. Individual cells were observed and tracked manually evaluating every time point. Relevant properties and behaviour (division, death, position, adherence, fluorescence, morphology) of cells were stored and displayed in pedigrees. Fluorescence intensities were quantified with TTT software as well. All cells with questionable identity were excluded from relevant analyses.

**7.10.1. Image Processing**

Movies were annotated and assembled to Audio Video Interleave (AVI) files using Metamorph Offline 6.1r4. Still images were processed on Axiovision 4.5 software.

**7.10.2. Statistical Analysis**

The statistical significance of differences was determined using the student's t-test for unpaired data.



---

## 8. References

- Audet, J., C. L. Miller, et al. (2002). "Common and distinct features of cytokine effects on hematopoietic stem and progenitor cells revealed by dose-response surface analysis." Biotechnol Bioeng **80**(4): 393-404.
- Baker, N. E., M. Mlodzik, et al. (1990). "Spacing differentiation in the developing *Drosophila* eye: a fibrinogen-related lateral inhibitor encoded by *scabrous*." Science **250**(4986): 1370-7.
- Barker, D. D., C. Wang, et al. (1992). "Pumilio is essential for function but not for distribution of the *Drosophila* abdominal determinant *Nanos*." Genes Dev **6**(12A): 2312-26.
- Bauer, N., A. V. Fonseca, et al. (2008). "New insights into the cell biology of hematopoietic progenitors by studying prominin-1 (CD133)." Cells Tissues Organs **188**(1-2): 127-38.
- Beckmann, J., S. Scheitza, et al. (2007). "Asymmetric cell division within the human hematopoietic stem and progenitor cell compartment: identification of asymmetrically segregating proteins." Blood **109**(12): 5494-501.
- Bohnsack, B. L., L. Lai, et al. (2006). "Visceral endoderm function is regulated by *quaking* and required for vascular development." Genesis **44**(2): 93-104.
- Boswell, H. S., P. M. Wade, Jr., et al. (1984). "Thy-1 antigen expression by murine high-proliferative capacity hematopoietic progenitor cells. I. Relation between sensitivity to depletion by Thy-1 antibody and stem cell generation potential." J Immunol **133**(6): 2940-9.
- Bradley, T. R. and D. Metcalf (1966). "The growth of mouse bone marrow cells in vitro." Aust J Exp Biol Med Sci **44**(3): 287-99.

- Broadus, J., S. Fuerstenberg, et al. (1998). "Staufen-dependent localization of prospero mRNA contributes to neuroblast daughter-cell fate." Nature **391**(6669): 792-5.
- Brown, J., M. F. Greaves, et al. (1991). "The gene encoding the stem cell antigen, CD34, is conserved in mouse and expressed in haemopoietic progenitor cell lines, brain, and embryonic fibroblasts." Int Immunol **3**(2): 175-84.
- Brummendorf, T. H., W. Dragowska, et al. (1998). "Asymmetric cell divisions sustain long-term hematopoiesis from single-sorted human fetal liver cells." J Exp Med **188**(6): 1117-24.
- Calvi, L. M., G. B. Adams, et al. (2003). "Osteoblastic cells regulate the haematopoietic stem cell niche." Nature **425**(6960): 841-6.
- Chang, A. H. and M. Sadelain (2007). "The genetic engineering of hematopoietic stem cells: the rise of lentiviral vectors, the conundrum of the Itr, and the promise of lineage-restricted vectors." Mol Ther **15**(3): 445-56.
- Chang, J. T., V. R. Palanivel, et al. (2007). "Asymmetric T lymphocyte division in the initiation of adaptive immune responses." Science **315**(5819): 1687-91.
- Chang, L. J., V. Urlacher, et al. (1999). "Efficacy and safety analyses of a recombinant human immunodeficiency virus type 1 derived vector system." Gene Ther **6**(5): 715-28.
- Cramer, E. M. (1999). "Megakaryocyte structure and function." Curr Opin Hematol **6**(5): 354-61.
- Cramer, E. M. and J. Breton-Gorius (1987). "Ultrastructural localization of lysozyme in human neutrophils by immunogold." J Leukoc Biol **41**(3): 242-7.

- 
- Crittenden, S. L., D. S. Bernstein, et al. (2002). "A conserved RNA-binding protein controls germline stem cells in *Caenorhabditis elegans*." Nature **417**(6889): 660-3.
- de Felipe, P., V. Martin, et al. (1999). "Use of the 2A sequence from foot-and-mouth disease virus in the generation of retroviral vectors for gene therapy." Gene Ther **6**(2): 198-208.
- Dexter, T. M., E. G. Wright, et al. (1977). "Regulation of haemopoietic stem cell proliferation in long term bone marrow cultures." Biomedicine **27**(9-10): 344-9.
- Dubreuil, V., A. M. Marzesco, et al. (2007). "Midbody and primary cilium of neural progenitors release extracellular membrane particles enriched in the stem cell marker prominin-1." J Cell Biol **176**(4): 483-95.
- Duchaine, T., H. J. Wang, et al. (2000). "A novel murine Staufen isoform modulates the RNA content of Staufen complexes." Mol Cell Biol **20**(15): 5592-601.
- Duchaine, T. F., I. Hemraj, et al. (2002). "Staufen2 isoforms localize to the somatodendritic domain of neurons and interact with different organelles." J Cell Sci **115**(Pt 16): 3285-95.
- Dugre-Brisson, S., G. Elvira, et al. (2005). "Interaction of Staufen1 with the 5' end of mRNA facilitates translation of these RNAs." Nucleic Acids Res **33**(15): 4797-812.
- Dull, T., R. Zufferey, et al. (1998). "A third-generation lentivirus vector with a conditional packaging system." J Virol **72**(11): 8463-71.
- Dykstra, B., J. Ramunas, et al. (2006). "High-resolution video monitoring of hematopoietic stem cells cultured in single-cell arrays identifies new features of self-renewal." Proc Natl Acad Sci U S A **103**(21): 8185-90.

- Ebersole, T. A., Q. Chen, et al. (1996). "The quaking gene product necessary in embryogenesis and myelination combines features of RNA binding and signal transduction proteins." Nat Genet **12**(3): 260-5.
- Eckmann, C. R., B. Kraemer, et al. (2002). "GLD-3, a bicaudal-C homolog that inhibits FBF to control germline sex determination in *C. elegans*." Dev Cell **3**(5): 697-710.
- Eilken, H. M., S. Nishikawa, et al. (2009). "Continuous single-cell imaging of blood generation from haemogenic endothelium." Nature **457**(7231): 896-900.
- Ema, H., H. Takano, et al. (2000). "In vitro self-renewal division of hematopoietic stem cells." J Exp Med **192**(9): 1281-8.
- Ephrussi, A., L. K. Dickinson, et al. (1991). "Oskar organizes the germ plasm and directs localization of the posterior determinant nanos." Cell **66**(1): 37-50.
- Fargeas, C. A., A.-V. Fonseca, et al. (2006). "Prominin-1 (CD133): from progenitor cells to human diseases." Future Lipidology **1**(2): 213-225.
- Faubert, A., J. Lessard, et al. (2004). "Are genetic determinants of asymmetric stem cell division active in hematopoietic stem cells?" Oncogene **23**(43): 7247-55.
- Faust, N., F. Varas, et al. (2000). "Insertion of enhanced green fluorescent protein into the lysozyme gene creates mice with green fluorescent granulocytes and macrophages." Blood **96**(2): 719-26.
- Ferrandon, D., L. Elphick, et al. (1994). "Staufen protein associates with the 3'UTR of bicoid mRNA to form particles that move in a microtubule-dependent manner." Cell **79**(7): 1221-32.

- 
- Fleming, T. J., M. L. Fleming, et al. (1993). "Selective expression of Ly-6G on myeloid lineage cells in mouse bone marrow. RB6-8C5 mAb to granulocyte-differentiation antigen (Gr-1) detects members of the Ly-6 family." J Immunol **151**(5): 2399-408.
- Forbes, A. and R. Lehmann (1998). "Nanos and Pumilio have critical roles in the development and function of Drosophila germline stem cells." Development **125**(4): 679-90.
- Francis, R., M. K. Barton, et al. (1995). "gld-1, a tumor suppressor gene required for oocyte development in Caenorhabditis elegans." Genetics **139**(2): 579-606.
- Francis, R., E. Maine, et al. (1995). "Analysis of the multiple roles of gld-1 in germline development: interactions with the sex determination cascade and the glp-1 signaling pathway." Genetics **139**(2): 607-30.
- Fuxa, M. and M. Busslinger (2007). "Reporter gene insertions reveal a strictly B lymphoid-specific expression pattern of Pax5 in support of its B cell identity function." J Immunol **178**(5): 3031-7.
- Gerber, A. P., S. Luschig, et al. (2006). "Genome-wide identification of mRNAs associated with the translational regulator PUMILIO in Drosophila melanogaster." Proc Natl Acad Sci U S A **103**(12): 4487-92.
- Giebel, B., D. Corbeil, et al. (2004). "Segregation of lipid raft markers including CD133 in polarized human hematopoietic stem and progenitor cells." Blood **104**(8): 2332-8.
- Giebel, B., T. Zhang, et al. (2006). "Primitive human hematopoietic cells give rise to differentially specified daughter cells upon their initial cell division." Blood **107**(5): 2146-52.

- Giesert, C., G. Almeida-Porada, et al. (2001). "The monoclonal antibody W7C5 defines a novel surface antigen on hematopoietic stem cells." Ann N Y Acad Sci **938**: 175-83.
- Gordon, S., J. Todd, et al. (1974). "In vitro synthesis and secretion of lysozyme by mononuclear phagocytes." J Exp Med **139**(5): 1228-48.
- Hardy, R. J., C. L. Loushin, et al. (1996). "Neural cell type-specific expression of OKI proteins is altered in quakingviable mutant mice." J Neurosci **16**(24): 7941-9.
- Hardy, R. R. and K. Hayakawa (2001). "B cell development pathways." Annu Rev Immunol **19**: 595-621.
- Heck, S., O. Ermakova, et al. (2003). "Distinguishable live erythroid and myeloid cells in beta-globin ECFP x lysozyme EGFP mice." Blood **101**(3): 903-6.
- Heissig, B., K. Hattori, et al. (2002). "Recruitment of stem and progenitor cells from the bone marrow niche requires MMP-9 mediated release of kit-ligand." Cell **109**(5): 625-37.
- Huang, S., P. Law, et al. (1999). "Symmetry of initial cell divisions among primitive hematopoietic progenitors is independent of ontogenic age and regulatory molecules." Blood **94**(8): 2595-604.
- Imamoto, N., T. Shimamoto, et al. (1995). "In vivo evidence for involvement of a 58 kDa component of nuclear pore-targeting complex in nuclear protein import." Embo J **14**(15): 3617-26.
- Jobim, M. and L. F. Jobim (2008). "Natural killer cells and immune surveillance." J Pediatr (Rio J) **84**(4 Suppl): S58-67.

- 
- Jones, A. R. and T. Schedl (1995). "Mutations in *gld-1*, a female germ cell-specific tumor suppressor gene in *Caenorhabditis elegans*, affect a conserved domain also found in Src-associated protein Sam68." Genes Dev **9**(12): 1491-504.
- Karpowicz, P., C. Morshead, et al. (2005). "Support for the immortal strand hypothesis: neural stem cells partition DNA asymmetrically in vitro." J Cell Biol **170**(5): 721-32.
- Kato, Y., A. Iwama, et al. (2005). "Selective activation of STAT5 unveils its role in stem cell self-renewal in normal and leukemic hematopoiesis." J Exp Med **202**(1): 169-79.
- Kaushansky, K. (2008). "Historical review: megakaryopoiesis and thrombopoiesis." Blood **111**(3): 981-6.
- Kiebler, M. A., I. Hemraj, et al. (1999). "The mammalian stau6 protein localizes to the somatodendritic domain of cultured hippocampal neurons: implications for its involvement in mRNA transport." J Neurosci **19**(1): 288-97.
- Kiel, M. J., S. He, et al. (2007). "Haematopoietic stem cells do not asymmetrically segregate chromosomes or retain BrdU." Nature **449**(7159): 238-42.
- Kiel, M. J., O. H. Yilmaz, et al. (2005). "SLAM family receptors distinguish hematopoietic stem and progenitor cells and reveal endothelial niches for stem cells." Cell **121**(7): 1109-21.
- Kim-Ha, J., K. Kerr, et al. (1995). "Translational regulation of *oskar* mRNA by *bruno*, an ovarian RNA-binding protein, is essential." Cell **81**(3): 403-12.
- Kim-Ha, J., J. L. Smith, et al. (1991). "*oskar* mRNA is localized to the posterior pole of the *Drosophila* oocyte." Cell **66**(1): 23-35.

- Kim, I., S. He, et al. (2006). "Enhanced purification of fetal liver hematopoietic stem cells using SLAM family receptors." Blood **108**(2): 737-44.
- Kim, Y. K., L. Furic, et al. (2005). "Mammalian Staufen1 recruits Upf1 to specific mRNA 3'UTRs so as to elicit mRNA decay." Cell **120**(2): 195-208.
- Kimble, J. and S. L. Crittenden (2007). "Controls of germline stem cells, entry into meiosis, and the sperm/oocyte decision in *Caenorhabditis elegans*." Annu Rev Cell Dev Biol **23**: 405-33.
- Knoblich, J. A., L. Y. Jan, et al. (1995). "Asymmetric segregation of Numb and Prospero during cell division." Nature **377**(6550): 624-7.
- Kodama, H., M. Nose, et al. (1994). "Involvement of the c-kit receptor in the adhesion of hematopoietic stem cells to stromal cells." Exp Hematol **22**(10): 979-84.
- Kodama, H., M. Nose, et al. (1992). "In vitro proliferation of primitive hemopoietic stem cells supported by stromal cells: evidence for the presence of a mechanism(s) other than that involving c-kit receptor and its ligand." J Exp Med **176**(2): 351-61.
- Kodama, H., H. Sudo, et al. (1984). "In vitro hemopoiesis within a microenvironment created by MC3T3-G2/PA6 preadipocytes." J Cell Physiol **118**(3): 233-40.
- Kodama, H. A., Y. Amagai, et al. (1982). "A new preadipose cell line derived from newborn mouse calvaria can promote the proliferation of pluripotent hemopoietic stem cells in vitro." J Cell Physiol **112**(1): 89-95.
- Kohrmann, M., M. Luo, et al. (1999). "Microtubule-dependent recruitment of Staufen-green fluorescent protein into large RNA-containing granules and subsequent dendritic transport in living hippocampal neurons." Mol Biol Cell **10**(9): 2945-53.

- 
- Kondo, M., I. L. Weissman, et al. (1997). "Identification of clonogenic common lymphoid progenitors in mouse bone marrow." Cell **91**(5): 661-72.
- Kuby, J. (1997). Immunology. New York, W.H. Freeman and Company.
- Kuwata, N., H. Igarashi, et al. (1999). "Cutting edge: absence of expression of RAG1 in peritoneal B-1 cells detected by knocking into RAG1 locus with green fluorescent protein gene." J Immunol **163**(12): 6355-9.
- Lamont, L. B., S. L. Crittenden, et al. (2004). "FBF-1 and FBF-2 regulate the size of the mitotic region in the *C. elegans* germline." Dev Cell **7**(5): 697-707.
- Le, S., R. Sternglanz, et al. (2000). "Identification of two RNA-binding proteins associated with human telomerase RNA." Mol Biol Cell **11**(3): 999-1010.
- Leary, A. G., L. C. Strauss, et al. (1985). "Disparate differentiation in hemopoietic colonies derived from human paired progenitors." Blood **66**(2): 327-32.
- Lee, A., J. D. Kessler, et al. (2005). "Isolation of neural stem cells from the postnatal cerebellum." Nat Neurosci **8**(6): 723-9.
- Lee, M. H., B. Hook, et al. (2007). "Conserved regulation of MAP kinase expression by PUF RNA-binding proteins." PLoS Genet **3**(12): e233.
- Lehmann, R. and C. Nusslein-Volhard (1991). "The maternal gene nanos has a central role in posterior pattern formation of the *Drosophila* embryo." Development **112**(3): 679-91.
- Li, P., X. Yang, et al. (1997). "Inscuteable and Staufen mediate asymmetric localization and segregation of prospero RNA during *Drosophila* neuroblast cell divisions." Cell **90**(3): 437-47.

- Li, Z., Y. Zhang, et al. (2000). "Destabilization and mislocalization of myelin basic protein mRNAs in quaking dysmyelination lacking the QKI RNA-binding proteins." J Neurosci **20**(13): 4944-53.
- Lin, H. and A. C. Spradling (1997). "A novel group of pumilio mutations affects the asymmetric division of germline stem cells in the Drosophila ovary." Development **124**(12): 2463-76.
- Macdonald, P. M. (1992). "The Drosophila pumilio gene: an unusually long transcription unit and an unusual protein." Development **114**(1): 221-32.
- Marin, V. A. and T. C. Evans (2003). "Translational repression of a C. elegans Notch mRNA by the STAR/KH domain protein GLD-1." Development **130**(12): 2623-32.
- Marzesco, A. M., P. Janich, et al. (2005). "Release of extracellular membrane particles carrying the stem cell marker prominin-1 (CD133) from neural progenitors and other epithelial cells." J Cell Sci **118**(Pt 13): 2849-58.
- Mayani, H., W. Dragowska, et al. (1993). "Lineage commitment in human hemopoiesis involves asymmetric cell division of multipotent progenitors and does not appear to be influenced by cytokines." J Cell Physiol **157**(3): 579-86.
- Mazzone, A. and G. Ricevuti (1995). "Leukocyte CD11/CD18 integrins: biological and clinical relevance." Haematologica **80**(2): 161-75.
- McKenzie, J. L., K. Takenaka, et al. (2007). "Low rhodamine 123 retention identifies long-term human hematopoietic stem cells within the Lin-CD34+CD38- population." Blood **109**(2): 543-5.
- Mee, C. J., E. C. Pym, et al. (2004). "Regulation of neuronal excitability through pumilio-dependent control of a sodium channel gene." J Neurosci **24**(40): 8695-703.

- Menon, K. P., S. Sanyal, et al. (2004). "The translational repressor Pumilio regulates presynaptic morphology and controls postsynaptic accumulation of translation factor eIF-4E." Neuron **44**(4): 663-76.
- Metcalf, D. (2005). *Blood Lines - An Introduction to Characterizing Blood Disease of the Post-Genomic Mouse*, AlphaMed Press.
- Metcalf, D., G. J. Nossal, et al. (1975). "Growth of B-lymphocyte colonies in vitro." J Exp Med **142**(6): 1534-49.
- Mezquita, J., M. Pau, et al. (1998). "Four isoforms of the signal-transduction and RNA-binding protein QKI expressed during chicken spermatogenesis." Mol Reprod Dev **50**(1): 70-8.
- Micklem, D. R., J. Adams, et al. (2000). "Distinct roles of two conserved Stauf domains in oskar mRNA localization and translation." EMBO J **19**(6): 1366-77.
- Miller, C. L. and C. J. Eaves (1997). "Expansion in vitro of adult murine hematopoietic stem cells with transplantable lympho-myeloid reconstituting ability." Proc Natl Acad Sci U S A **94**(25): 13648-53.
- Moore, F. L., J. Jaruzelska, et al. (2003). "Human Pumilio-2 is expressed in embryonic stem cells and germ cells and interacts with DAZ (Deleted in AZoospermia) and DAZ-like proteins." Proc Natl Acad Sci U S A **100**(2): 538-43.
- Moore, K. A., H. Ema, et al. (1997). "In vitro maintenance of highly purified, transplantable hematopoietic stem cells." Blood **89**(12): 4337-47.
- Moore, K. A. and I. R. Lemischka (2006). "Stem cells and their niches." Science **311**(5769): 1880-5.

- Mouland, A. J., J. Mercier, et al. (2000). "The double-stranded RNA-binding protein Staufen is incorporated in human immunodeficiency virus type 1: evidence for a role in genomic RNA encapsidation." J Virol **74**(12): 5441-51.
- Muraro, N. I., A. J. Weston, et al. (2008). "Pumilio binds para mRNA and requires Nanos and Brat to regulate sodium current in Drosophila motoneurons." J Neurosci **28**(9): 2099-109.
- Murata, Y. and R. P. Wharton (1995). "Binding of pumilio to maternal hunchback mRNA is required for posterior patterning in Drosophila embryos." Cell **80**(5): 747-56.
- Nakano, T., H. Kodama, et al. (1994). "Generation of lymphohematopoietic cells from embryonic stem cells in culture." Science **265**(5175): 1098-101.
- Nakano, T., H. Kodama, et al. (1996). "In vitro development of primitive and definitive erythrocytes from different precursors." Science **272**(5262): 722-4.
- Naldini, L., U. Blomer, et al. (1996). "In vivo gene delivery and stable transduction of nondividing cells by a lentiviral vector." Science **272**(5259): 263-7.
- Noda, S., K. Horiguchi, et al. (2008). "Repopulating activity of ex vivo-expanded murine hematopoietic stem cells resides in the CD48-c-Kit+Sca-1+lineage marker- cell population." Stem Cells **26**(3): 646-55.
- Noveroske, J. K., L. Lai, et al. (2002). "Quaking is essential for blood vessel development." Genesis **32**(3): 218-30.
- Nygren, J. M., D. Bryder, et al. (2006). "Prolonged cell cycle transit is a defining and developmentally conserved hemopoietic stem cell property." J Immunol **177**(1): 201-8.

- 
- Ogawa, M., T. Suda, et al. (1984). "Differentiation and proliferative kinetics of hemopoietic stem cells in culture." Prog Clin Biol Res **148**: 35-43.
- Osawa, M., K. Hanada, et al. (1996). "Long-term lymphohematopoietic reconstitution by a single CD34-low/negative hematopoietic stem cell." Science **273**(5272): 242-5.
- Passegue, E., A. J. Wagers, et al. (2005). "Global analysis of proliferation and cell cycle gene expression in the regulation of hematopoietic stem and progenitor cell fates." J Exp Med **202**(11): 1599-611.
- Pronk, C. J., D. J. Rossi, et al. (2007). "Elucidation of the phenotypic, functional, and molecular topography of a myeloerythroid progenitor cell hierarchy." Cell Stem Cell **1**(4): 428-42.
- Punzel, M., D. Liu, et al. (2003). "The symmetry of initial divisions of human hematopoietic progenitors is altered only by the cellular microenvironment." Exp Hematol **31**(4): 339-47.
- Punzel, M., T. Zhang, et al. (2002). "Functional analysis of initial cell divisions defines the subsequent fate of individual human CD34(+)CD38(-) cells." Exp Hematol **30**(5): 464-72.
- Richardson, G. D., C. N. Robson, et al. (2004). "CD133, a novel marker for human prostatic epithelial stem cells." J Cell Sci **117**(Pt 16): 3539-45.
- Rieger, M. A., P. S. Hoppe, et al. (2009). "Hematopoietic cytokines can instruct lineage choice." Science.
- Rieger, M. A. and T. Schroeder (2008). "Exploring hematopoiesis at single cell resolution." Cells Tissues Organs **188**(1-2): 139-49.

- Rieger, M. A., B. M. Smejkal, et al. (2009). "Improved prospective identification of megakaryocyte-erythrocyte progenitor cells." Br J Haematol **144**(3): 448-51.
- Roper, K., D. Corbeil, et al. (2000). "Retention of prominin in microvilli reveals distinct cholesterol-based lipid micro-domains in the apical plasma membrane." Nat Cell Biol **2**(9): 582-92.
- Sato, T., J. H. Laver, et al. (1999). "Reversible expression of CD34 by murine hematopoietic stem cells." Blood **94**(8): 2548-54.
- Schambach, A., M. Galla, et al. (2006). "Lentiviral vectors pseudotyped with murine ecotropic envelope: increased biosafety and convenience in preclinical research." Exp Hematol **34**(5): 588-92.
- Schroeder, T. (2007). "Asymmetric Cell Division in Normal and Malignant Hematopoietic Precursor Cells." Cell Stem Cell **1**(5): 479-481.
- Schupbach, T. and E. Wieschaus (1986). "Germline autonomy of maternal-effect mutations altering the embryonic body pattern of *Drosophila*." Dev Biol **113**(2): 443-8.
- Schweers, B. A., K. J. Walters, et al. (2002). "The *Drosophila melanogaster* translational repressor pumilio regulates neuronal excitability." Genetics **161**(3): 1177-85.
- Seita, J., H. Ema, et al. (2007). "Lnk negatively regulates self-renewal of hematopoietic stem cells by modifying thrombopoietin-mediated signal transduction." Proc Natl Acad Sci U S A **104**(7): 2349-54.
- Shen, Q., W. Zhong, et al. (2002). "Asymmetric Numb distribution is critical for asymmetric cell division of mouse cerebral cortical stem cells and neuroblasts." Development **129**(20): 4843-53.

- 
- Shimizu, N., S. Noda, et al. (2008). "Identification of genes potentially involved in supporting hematopoietic stem cell activity of stromal cell line MC3T3-G2/PA6." Int J Hematol **87**(3): 239-45.
- Shinin, V., B. Gayraud-Morel, et al. (2006). "Asymmetric division and cosegregation of template DNA strands in adult muscle satellite cells." Nat Cell Biol **8**(7): 677-87.
- Sidman, R. L., M. M. Dickie, et al. (1964). "Mutant Mice (Quaking and Jimpy) with Deficient Myelination in the Central Nervous System." Science **144**: 309-11.
- Smith, G. H. (2005). "Label-retaining epithelial cells in mouse mammary gland divide asymmetrically and retain their template DNA strands." Development **132**(4): 681-7.
- Spasov, D. S. and R. Jurecic (2003). "Mouse Pum1 and Pum2 genes, members of the Pumilio family of RNA-binding proteins, show differential expression in fetal and adult hematopoietic stem cells and progenitors." Blood Cells Mol Dis **30**(1): 55-69.
- Spik, A., S. Oczkowski, et al. (2006). "Human fertility protein PUMILIO2 interacts in vitro with testis mRNA encoding Cdc42 effector 3 (CEP3)." Reprod Biol **6**(2): 103-13.
- St Johnston, D., D. Beuchle, et al. (1991). "Staufen, a gene required to localize maternal RNAs in the Drosophila egg." Cell **66**(1): 51-63.
- St Johnston, D., N. H. Brown, et al. (1992). "A conserved double-stranded RNA-binding domain." Proc Natl Acad Sci U S A **89**(22): 10979-83.
- St Johnston, D., W. Driever, et al. (1989). "Multiple steps in the localization of bicoid RNA to the anterior pole of the Drosophila oocyte." Development **107** **Suppl**: 13-9.

- Suda, T., J. Suda, et al. (1983). "Single-cell origin of mouse hemopoietic colonies expressing multiple lineages in variable combinations." Proc Natl Acad Sci U S A **80**(21): 6689-93.
- Suda, T., J. Suda, et al. (1984). "Disparate differentiation in mouse hemopoietic colonies derived from paired progenitors." Proc Natl Acad Sci U S A **81**(8): 2520-4.
- Sudo, T., M. Ito, et al. (1989). "Interleukin 7 production and function in stromal cell-dependent B cell development." J Exp Med **170**(1): 333-8.
- Suh, N., B. Jedamzik, et al. (2006). "The GLD-2 poly(A) polymerase activates gld-1 mRNA in the *Caenorhabditis elegans* germ line." Proc Natl Acad Sci U S A **103**(41): 15108-12.
- Szilvassy, S. J., R. K. Humphries, et al. (1990). "Quantitative assay for totipotent reconstituting hematopoietic stem cells by a competitive repopulation strategy." Proc Natl Acad Sci U S A **87**(22): 8736-40.
- Szilvassy, S. J., K. P. Weller, et al. (1996). "Leukemia inhibitory factor upregulates cytokine expression by a murine stromal cell line enabling the maintenance of highly enriched competitive repopulating stem cells." Blood **87**(11): 4618-28.
- Takano, H., H. Ema, et al. (2004). "Asymmetric division and lineage commitment at the level of hematopoietic stem cells: inference from differentiation in daughter cell and granddaughter cell pairs." J Exp Med **199**(3): 295-302.
- Tang, S. J., D. Meulemans, et al. (2001). "A role for a rat homolog of staufen in the transport of RNA to neuronal dendrites." Neuron **32**(3): 463-75.
- Testa, U. (2004). "Apoptotic mechanisms in the control of erythropoiesis." Leukemia **18**(7): 1176-99.

- 
- Thomas, M. G., L. J. Tosar, et al. (2009). "Mammalian Staufen 1 is recruited to stress granules and impairs their assembly." J Cell Sci **122**(Pt 4): 563-73.
- Uchida, N., D. W. Buck, et al. (2000). "Direct isolation of human central nervous system stem cells." Proc Natl Acad Sci U S A **97**(26): 14720-5.
- Uchida, N., R. E. Sutton, et al. (1998). "HIV, but not murine leukemia virus, vectors mediate high efficiency gene transfer into freshly isolated G0/G1 human hematopoietic stem cells." Proc Natl Acad Sci U S A **95**(20): 11939-44.
- Uchida, N. and I. L. Weissman (1992). "Searching for hematopoietic stem cells: evidence that Thy-1.1<sup>lo</sup> Lin<sup>-</sup> Sca-1<sup>+</sup> cells are the only stem cells in C57BL/Ka-Thy-1.1 bone marrow." J Exp Med **175**(1): 175-84.
- Ueno, H., M. Sakita-Ishikawa, et al. (2003). "A stromal cell-derived membrane protein that supports hematopoietic stem cells." Nat Immunol **4**(5): 457-63.
- Vercauteren, S. M. and H. J. Sutherland (2001). "CD133 (AC133) expression on AML cells and progenitors." Cytotherapy **3**(6): 449-59.
- Vernet, C. and K. Artzt (1997). "STAR, a gene family involved in signal transduction and activation of RNA." Trends Genet **13**(12): 479-84.
- Vessey, J. P., A. Vaccani, et al. (2006). "Dendritic localization of the translational repressor Pumilio 2 and its contribution to dendritic stress granules." J Neurosci **26**(24): 6496-508.
- Wandzioch, E., C. E. Edling, et al. (2004). "Activation of the MAP kinase pathway by c-Kit is PI-3 kinase dependent in hematopoietic progenitor/stem cell lines." Blood **104**(1): 51-7.

- Wang, H., L. J. Pierce, et al. (2005). "Lymphoid potential of primitive bone marrow progenitors evaluated in vitro." Ann N Y Acad Sci **1044**: 210-9.
- Wang, H., L. J. Pierce, et al. (2006). "Distinct roles of IL-7 and stem cell factor in the OP9-DL1 T-cell differentiation culture system." Exp Hematol **34**(12): 1730-40.
- Weigmann, A., D. Corbeil, et al. (1997). "Prominin, a novel microvilli-specific polytopic membrane protein of the apical surface of epithelial cells, is targeted to plasmalemmal protrusions of non-epithelial cells." Proc Natl Acad Sci U S A **94**(23): 12425-30.
- Wickham, L., T. Duchaine, et al. (1999). "Mammalian staufen is a double-stranded-RNA- and tubulin-binding protein which localizes to the rough endoplasmic reticulum." Mol Cell Biol **19**(3): 2220-30.
- Wilson, A., E. Laurenti, et al. (2008). "Hematopoietic stem cells reversibly switch from dormancy to self-renewal during homeostasis and repair." Cell **135**(6): 1118-29.
- Wu, M., H. Y. Kwon, et al. (2007). "Imaging hematopoietic precursor division in real time." Cell Stem Cell **1**(5): 541-54.
- Xie, T. and A. C. Spradling (2000). "A niche maintaining germ line stem cells in the *Drosophila* ovary." Science **290**(5490): 328-30.
- Yamazaki, S., A. Iwama, et al. (2006). "Cytokine signals modulated via lipid rafts mimic niche signals and induce hibernation in hematopoietic stem cells." EMBO J **25**(15): 3515-23.
- Yang, L., D. Bryder, et al. (2005). "Identification of Lin(-)Sca1(+)kit(+)CD34(+)Flt3-short-term hematopoietic stem cells capable of rapidly reconstituting and rescuing myeloablated transplant recipients." Blood **105**(7): 2717-23.

- 
- Ye, B., C. Petritsch, et al. (2004). "Nanos and Pumilio are essential for dendrite morphogenesis in *Drosophila* peripheral neurons." Curr Biol **14**(4): 314-21.
- Yilmaz, O. H., M. J. Kiel, et al. (2006). "SLAM family markers are conserved among hematopoietic stem cells from old and reconstituted mice and markedly increase their purity." Blood **107**(3): 924-30.
- Yin, A. H., S. Miraglia, et al. (1997). "AC133, a novel marker for human hematopoietic stem and progenitor cells." Blood **90**(12): 5002-12.
- Zhang, C. C. and H. F. Lodish (2005). "Murine hematopoietic stem cells change their surface phenotype during ex vivo expansion." Blood **105**(11): 4314-20.
- Zhang, J., F. Varas, et al. (2007). "CD41-YFP mice allow in vivo labeling of megakaryocytic cells and reveal a subset of platelets hyperreactive to thrombin stimulation." Exp Hematol **35**(3): 490-499.
- Zhong, W., M. M. Jiang, et al. (2000). "Mouse numb is an essential gene involved in cortical neurogenesis." Proc Natl Acad Sci U S A **97**(12): 6844-9.
- Zhu, L., P. Gibson, et al. (2009). "Prominin 1 marks intestinal stem cells that are susceptible to neoplastic transformation." Nature **457**(7229): 603-7.
- Zorn, A. M. and P. A. Krieg (1997). "The KH domain protein encoded by quaking functions as a dimer and is essential for notochord development in *Xenopus* embryos." Genes Dev **11**(17): 2176-90.



## 9. Legends to Time Lapse Movies

### **Supplemental Movie 5.1A:**

Time lapse movie shows second division of corresponding pedigree in Figure 5.2. The original time lapse video was recorded and analyzed with the same temporal resolution as shown in this movie. All time lapse movies were recorded and analyzed with this resolution (2 min intervals). Red dots are tracking marks and indicate the cells in the pedigree in Figure 5.2A.

Time scale: days – hours:minutes:seconds

### **Supplemental Movie 5.1B:**

Time lapse movie corresponding to Figure 5.2 shows colony formation of a single isolated HSC on PA6. The first three divisions of the initially plated cell are shown. Red circles are tracking marks and indicate the cells displayed in the pedigree in Figure 5.2A. Temporal resolution is compressed for displaying purposes.

Time scale: days – hours:minutes:seconds

### **Supplemental Movie 5.2:**

Time lapse movie corresponding to Figure 5.5 shows asymmetric generation times of progeny of a single isolated HSC on PA6. The first two divisions are shown. Arrows and pauses in the movie correspond to panels B, C, and D in Figure 5.5 and indicate asymmetric timing of divisions of HSC daughter cells. Temporal resolution is compressed for displaying purposes.

Time scale: days – hours:minutes:seconds

### **Supplemental Movie 5.3:**

Time lapse movie corresponding to Figure 5.8 shows generation of Megakaryocytes from isolated MPP on PA6. Cell size increases and cells undergo endomitosis as cells differentiate into Megakaryocytes. Blue and red arrows correspond to arrows in pedigree and panels of Figure 5.8. Pauses in movie correspond to panels 5.8B, C, and D. Temporal resolution is compressed for displaying purposes.

Time scale: days – hours:minutes:seconds

**Supplemental Movie 5.4:**

Time lapse movie corresponding to Figure 5.14 shows mother cell onset of CD48 expression in colony derived from an isolated MPP on PA6. Left panel displays phase contrast images, while right panel displays CD48 Alexa647 fluorescent signals. All cells within the colony show CD48 fluorescence. Red circles indicate track marks that highlight cell location. Pause in movie corresponds to Figure 5.14B. Temporal resolution is compressed for displaying purposes.

Time scale: days – hours:minutes:seconds

**Supplemental Movie 5.5:**

Time lapse movie corresponding to Figure 5.15 shows symmetric onset of CD48 expression in HSC progeny cells cultured in stroma free suspension culture containing SCF and TPO. Left panel displays phase contrast images, while right panel displays CD48 Alexa647 fluorescent images. Red circles indicate track marks that highlight cell location. Pause corresponds to panel C in Figure 5.15 and indicates weak onset of CD48 expression in marked cells. Temporal resolution is compressed for displaying purposes.

Time scale: days – hours:minutes:seconds

**Supplemental Movie 5.6:**

Time lapse movie corresponding to Figure 5.19 shows asymmetric onset of CD48 expression in HSC progeny cells cultured in stroma free suspension culture containing SCF and TPO. Left panel displays phase contrast images, while right panel displays CD48 Alexa647 fluorescent images. Red circles indicate track marks that highlight cell location. Arrows and pauses in movie correspond to cells in panels B, C, and D in Figure 5.19. Blue arrows indicate CD48 positive cells, while white arrows indicate CD48 negative cells. Temporal resolution is compressed for displaying purposes.

Time scale: days – hours:minutes:seconds

**Supplemental Movie 5.7:**

Time lapse movie corresponding to Figure 5.20 shows asymmetric onset of CD48 expression in HSC progeny cells cultured in stroma free suspension culture

containing SCF and IL3. Left panel displays phase contrast images, while right panel displays CD48 Alexa647 fluorescent images. Red circles indicate track marks that highlight cell location. Arrows and pauses in movie correspond to cells in panels B, C, and D in Figure 5.20. Blue arrows indicated CD48 positive cells, while white and black arrows indicate CD48 negative cells. Initial viewing field encompassed the whole colony, but is shown here in two viewing fields to show cells in detail.

Temporal resolution is compressed for displaying purposes.

Time scale: days – hours:minutes:seconds

#### **Supplemental Movies 5.8A-D:**

Time lapse movies corresponding to data points of sister cell pairs of Staufen1 expressing cells in Figure 5.26A show protein segregation during division. Left panel displays phase contrast images, while right panel displays VENUS expression in fluorescent images. Orange arrow indicates mother cell, blue arrows indicate daughter cells. Temporal resolution is compressed for displaying purposes.

Time scale: days – hours:minutes:seconds

#### **Supplemental Movies 5.9A-D:**

Time lapse movies corresponding to data points of sister cell pairs of Staufen<sup>i</sup> expressing cells in Figure 5.26B show protein segregation during division. Left panel displays phase contrast images, while right panel displays VENUS expression in fluorescent images. Orange arrow indicates mother cell, blue arrows indicate daughter cells. Temporal resolution is compressed for displaying purposes.

Time scale: days – hours:minutes:seconds

#### **Supplemental Movies 5.10A-D:**

Time lapse movies corresponding to data points of sister cell pairs of Pumilio1 expressing cells in Figure 5.27 show protein segregation during division. Left panel displays phase contrast images, while right panel displays VENUS expression in fluorescent images. Orange arrow indicates mother cell, blue arrows indicate daughter cells. Temporal resolution is compressed for displaying purposes.

Time scale: days – hours:minutes:seconds



## 10. Abbreviations

°C	Degree Celsius
μ	Micro
ACD	Asymmetric cell division
AML	Acute myeloid leukaemia
Amp	Ampicillin
APC	Allophycocyanine
bp	Base pair
BSA	Bovine serum albumin
CAG	Chicken beta actin
cat no	Catalogue number
CLP	Common lymphoid progenitor
CMP	Common myeloid progenitor
CRU	Competitive repopulation unit
d	Day
D	Diffusion coefficient
DMSO	Dimethyl-sulfoxide
DNA	Desoxiribonucleic acid
dsRBD	dsRNA binding domain
EDTA	Ethylene-diamin-tetraacetic acid
Ery	Erythrocyte colony
FACS	Fluorescence activated cell sorting
FCS	Fetal calf serum
FITC	Fluorescein-isothiocyanate
Flt3	Fms-related tyrosine kinase 3
FCS	Fetal calf serum
FSC	Forward scatter
FOB	Fluorescence over background
g	Gram
G	Granulocyte colonies
GB	Giga byte

GEMM	Granulocyte erythrocyte macrophage megakaryocyte colony
GFP	Green fluorescent protein
GM	Granulocyte macrophage colony
GMP	Granulocyte monocyte progenitor
GT	Generation time
h	Hour
HBSS	Hank's buffered saline solution
HS	Horse serum
HSC	Hematopoietic stem cell(s)
IL	Interleukin
IRES	Internal ribosomal entry site
L	Liter
LB	LB broth base
M	Macrophage colony
ME	Megakaryocyte erythroid colony
Mega	Megakaryocyte colony
MEM	Minimal essential medium
MEP	Megakaryocyte erythrocyte progenitor
min	Minutes
ml	Milliliter
MPP	Multipotent progenitor
MOI	Moiety of infection
nucmem	Nuclear membrane
nm	Nanometer
ng	Nanogram
PB	Peripheral blood
PBS	Phosphate buffered saline
PE	Phycoerythrine
PI	Propidium iodide
RCF	Radial central force
RT	Room temperature
RT-PCR	Reverse transcriptase polymerase chain reaction

---

Sca-1	Stem cell antigen 1
SCF	Stem cell factor
SCID	Severe combined immune deficiency
SDS	Sodium dodecyl sulfate
s	Seconds
SSC	Side scatter
STAR	Signal transducer and activator of RNA
TAE	Tris acetate EDTA
TCR	T-cell receptor
TPO	Thrombopoietin
TTT	Timm's Tracking Tool
V	Volt
VSVG	Vesicular stomatitis virus G protein
wt	Wildtype



Ehrenwörtliche Erklärung:

Hiermit erkläre ich, dass ich die vorliegende Dissertation selbstständig und ohne unerlaubte Hilfe angefertigt habe. Ferner habe ich weder versucht eine Dissertation einzureichen oder eine Doktorprüfung durchzuführen, noch wurde die Dissertation oder Teile derselben einer anderen Prüfungskommission vorgelegt.

München, am 23. July, 2009

Andrea Hermann



## Acknowledgements

**I would like to thank Timm Schroeder for teaching me so many things about scientific work and for motivating me during frustrating times.**

**Thanks to Benedikt Grothe for officially supervising me.**

**I'm indebted to my labmembers for the excellent working atmosphere in the lab, for technical help and for the exciting discussions in labmeeting. Thank you all for making daily lablife so much more fun!**

**Thank you, Michael for your support with time lapse imaging. Thank you, Angi for numerous mouse preps and all the transplants. Thank you, Christian for support with virus production and being helpful with many so many things. Thanks to Bernhard, for programming all the TTT things I needed. Thank you, Phillip for Schnitzel support and five minutes hand-on time. Special thanks to Erin, Annemieke and Hanna for critically reading parts of this manuscript.**

**Hanna I want to thank you very much for all those intense discussion about life during many tea breaks and lunches.**

**I could not have done this work without the constant support of my family and friends. I want to thank my mother, father, sister and Nadine, Birgit, Barbara and Michelle for always being there.**



## Curriculum Vitae

Name: Andrea Hermann  
Date of birth: 19.2.1979  
Place of birth: Salzburg, Austria  
Nationality: Austrian  
Marital status: single

### **Education:**

**1997**                      **High school diploma** (Abitur)

**1997-2000**                **Vordiplom Genetik,**  
Universität Salzburg, Austria

**2000-2001**                **Joint Study Exchange**  
University of Maine, Orono, ME, USA

**2001-2004**                **Master of Science in Microbiology**  
University of Maine, Orono, ME, USA

**Since 02-2005**            **PhD Thesis**  
At the Institute of Stem Cell Research, Helmholtz  
Zentrum München. Supervisor is Prof. Benedikt  
Grothe, Faculty of Biology of the Ludwig-  
Maximilians-Universität, München

